Norwegian School of Economics
Bergen, Fall 2023

# Flexible Production of Green Ammonia

*An Optimisation Approach to Cost-Efficient and Adaptable Power to Ammonia Production in Denmark*

**John Kristian Ellertsen & Sondre Gunnar Haugen**

**Supervisor: Endre Bjørndal & Mette Bjørndal**

Master thesis, Economics and Business Administration

Major: Business Analytics

NORWEGIAN SCHOOL OF ECONOMICS

# Acknowledgements

This thesis serves as the concluding research for our master's program in Business Analytics at the Norwegian School of Economics (NHH). It has been deeply rewarding to be given the privilege to delve into such an important and interesting component of tomorrow's energy ecosystem. We would like to take this moment to extend our heartfelt gratitude to all those who have assisted us throughout this journey.

Firstly, we want to express our sincere gratitude to our supervisors, Mette Bjørndal and Endre Bjørndal, for their valuable guidance over the course of writing this thesis. For directing our thoughts in the process of organising the thesis, proof-checking the model, and sharing their knowledge in energy and methodology. Lastly, we want to thank them for many engaging and noteworthy discussions throughout this period.

Additionally, we wish to express our appreciation to Daniel Janzen from Grennsight AS who provided us with the idea of writing about ammonia, a forthcoming energy carrier with significant potential. An idea that seemed to have endless opportunities for research. We also want to express our gratitude to Kjetil T. Midthun, for valuable inputs. Finally, we would like to thank NordPool for their assistance throughout the electricity data gathering phase.

Thank you so much!

Norwegian School of Economics

Bergen, September 2023

John Kristian Ellertsen

Sondre Gunnar Haugen

# Abstract

The majority of global ammonia production relies on non-renewable energy, as green ammonia is substantially more expensive. However, the energy landscape is changing, and countries like Denmark are expanding their capacity in renewable energy. Given this increase in renewable capacity, demand for ammonia, and net-zero solutions, it is essential to reduce the total cost of ammonia and increase its competitiveness.

The primary objective of this thesis is to study the feasibility of decreasing the overall cost of ammonia in the established renewable market of Denmark. The ammonia production configuration considered in this thesis consists of alkaline water electrolysis and Haber-Bosch synthesis. We employed a multi-period, mixed integer optimisation model over the three coming decades and adjusted key elements to see their effect on cost. The ammonia system considered is grid-connected to the west Denmark electricity grid DK1 and utilise historical NordPool data from the same electricity grid for our optimization model.

The findings indicates that savings of up to 1,5 percent are possible for ammonia production, when utilising excess production capacity and the capabilities are improved to satisfy annual demand. The savings occur as a result of more production during advantageous time periods. However, excessive production capacity increases costs as a result of the systems capabilities. Furthermore, we find intermediate hydrogen storage to not be beneficial, except for long-term periods of extreme electricity price volatility with no excess production capacity. Additionally, the alkaline electrolysis should be minimized in relations to the appropriate excess production capacity of the Haber-Bosch synthesis given its high degradation.

***Keywords*** – Ammonia production, Power-to-X (PtX), Power-to-Ammonia (PtA), Renewable Energy, Energy Carrier, Energy Transition, Alkaline Electrolysis, Haber-Bosch Process (HB), Mixed Integer Linear Optimisation (MILP)

# Nomenclature

**Acronyms**

| | |
|---|---|
| $AE$ | Alkaline Electrolysis |
| $AES$ | Ammonia Energy Storage |
| $AMPL$ | A Mathematical Programming Language |
| $ASU$ | Air Separator Unit |
| $CAPEX$ | Capital Expenditure |
| $CCS$ | Carbon Capture and Storage |
| $DKK$ | Danish Krone |
| $ETS$ | Emissions Trading System |
| $EUR$ | European Monetary Unit |
| $GHG$ | Green House Gasses |
| $HB$ | Haber-Bosch process |
| $HHV$ | High Heating Value |
| $LCOA$ | Levelized cost of ammonia |
| $LCOH$ | Levelized Cost of Hydrogen |
| $LHV$ | Low Heating Value |
| $MILP$ | Multi-Period, Mixed-Integer Linear Programming |
| $OPEX$ | Operational Expenditure |
| $PEM$ | Polymer Electrolyte Membrane |
| $PtA$ | Power to Ammonia |
| $PtH$ | Power to Hydrogen |
| $PtX$ | Power to X / Power to Fuels |
| $RE$ | Renewable Energy |

| | |
|---|---|
| $USD$ | American Dollar |
| $WACC$ | Weighted average cost of capital |

**Physics elements**

| | |
|---|---|
| $CO_2$ | Carbon dioxide |
| $H_2O$ | Water in liquid state |
| $N_2$ | Nitrogen |
| $NH_3$ | Ammonia |
| $e^-$ | Electron |
| $H^+$ | Proton |
| $H_2$ | Hydrogen |
| $O_2$ | Oxygen |
| $T$ | Temperature (K) |

**Physical Quantity**

| | |
|---|---|
| $GW$ | Gigawatt |
| $kW$ | Kilowatt |
| $kWh/kg$ | Kilowatt-hour per Kilogram |
| $kWh$ | Kilowatt-hour |
| $MJ$ | Mega-joule |
| $MW$ | Megawatt |
| $MWh/kg$ | Megawatt-hour per Kilogram |
| $MWh$ | Megawatt-hour |
| $Wh/L$ | Volumetric energy density |

# Contents

# List of Figures

# List of Tables

# 1 Introduction

Annually, global energy consumption is increasing. In connection with this increase, we observe a rise in global warming due to the use of non-renewable energy sources (Shiva Kumar & Himabindu, 2019). To combat this development, nations are pushing regulations towards non-polluting and low-carbon alternatives. This development can be observed on a global scale. Offshore and onshore wind power are progressively being integrated into the electricity grid, and in 2021 the world produced 273 TWh more electricity from wind, a 17 percent increase from 2020 (IEA, 2022b). This is an essential step towards achieving the Paris Agreement's Net Zero Emission NZE by 2050.

With this renewable transition, new challenges and opportunities have emerged. One of the prominent challenges with wind and solar is their high production volatility compared to fossil fuels and hydro power. With this increased volatility, it is important to avoid curtailment on the production side during periods where there is excess energy on the grid. To counter this, large energy storage over a longer period is needed (Verleysen et al., 2021). In accomplishing this, the production of clean hydrogen has been discovered to be an important component, as it is the first step in the production of different alternative energy carriers, like ammonia (Chehade et al., 2019). As ammonia has a higher volumetric energy density [1] and holds more hydrogen per molecule, it is more suitable for long term storage and transportation. The value chain, from renewable energy(RE) to energy carriers like ammonia, is known as Power-to-x (PtX) or power-to-fuels (Chehade et al., 2019).

## 1.1 Research Question

While ammonia is mainly used as a fertiliser in agriculture production, more use cases are being explored. In the marine world, ammonia is considered one of the most promising future fuels (Brinks & Chryssakis, 2022). Ammonia is further being tested as a carbon-free alternative for airplanes as opposed to today's jet fuel (Givens, 2022). With a high potential as the future fuel for both deep sea shipping and long-haul aviation, ammonia is becoming an increasingly important part of the net-zero future. Beyond its use case as a fuel, ammonia is also considered as one of the most promising energy storage options for

[1] Ammonia has a volumetric energy density of 11.5 MJ/L over hydrogen's 8.5 MJ/L. (Lan & Tao, 2014).

long-term energy storage (Varney, 2017). Its capability to function as an energy storage option to hinder curtailment of energy when the production is high (peak shaving), makes it a crucial component in the increasingly volatile renewable energy ecosystems. Ammonia is emerging as an important component as both an energy storage and energy carrier option, and the International Energy Association IEA has further projected that ammonia production will increase by nearly 110 percent by 2050 [2] (IEA, 2021a).

With growing interest in ammonia and its increasing significance, the need to reduce production costs is more relevant than ever. As of today, approximately 70 percent of ammonia is produced using natural gas instead of renewable resources (IEA, 2021a). The main driver for this development has been cost, as green ammonia is more expensive due to its high electricity consumption. To reach ammonia's net-zero-emission scenario by 2050, all ammonia needs to be produced in a sustainable manner (green ammonia).

Back in 2021, IEA published a report on ammonia in which they, among others, found a realistic near-net-zero scenario for 2050. This scenario finds that 40 percent of ammonia production will be based on electrolysis, with natural-gas-based CCS accounting for around 20 percent (IEA, 2021a). If this prediction proves accurate, the electricity demand to produce green ammonia will increase considerably, making it essential to find ways to either reduce energy consumption or cut energy costs associated with green ammonia production. The transition to renewable energy will further require a more flexible ammonia production to be resilient towards increased volatility from increased wind energy. Therefore, this paper aims to analyse and research if employing a more flexible electrolysis, synthesis, and utilization of the fluctuations on the energy grid can reduce the production cost of ammonia.

*How can an increase in the production flexibility of ammonia utilize energy price fluctuations to reduce the levelized cost of ammonia?*

The objective of this study is to test the hypothesis that the total levelized cost of ammonia (LCOA) may be reduced through utilizing energy price fluctuations by increasing the flexibility in the ammonia production process. Flexibility, in this context refers to alterations in the production capacity of the production units and its production

[2] IEA's Net Zero Emissions scenario (IEA, 2021a)

capabilities. Additionally, this include an intermediate storage capacity of hydrogen. The topic is studied using a mathematical linear optimization model, which determines the minimized cost of ammonia. The model applies relevant data from scientific articles and research. Additionally, it incorporates day-ahead data obtained from NordPool for the ODE [3] region in Denmark, covering the period from 2015 to 2020. Using historical day-ahead data, we forecast future pricing inside the Danish electrical system for the subsequent three decades. Representative time series are further utilized in order to decrease the computational resources needed. In accordance with the net-zero-emission production pathway projected for 2050 (IEA, 2021a), we intend to utilize electrolysis-based ammonia production as our method for hydrogen generation in the ammonia process. The technology under consideration has had a resurgence in interest in recent years due to its sustainability aspects. It is noteworthy that multiple projects with a total capacity of 3 metric tons (Mt), are anticipated to become operational by the year 2030 (IEA, 2021a).

## 1.2 Background

The Nordic countries have long been considered frontrunners in the field of renewable energy. Presently, they are further expanding their capacity in renewables with the aim of establishing a prominent position in Europe's energy sector (Bjørnflaten, 2022). According to a report by Rystad Energy, Finland, Sweden, and Denmark has been identified as the leading countries in the field of green energy (Bjørnflaten, 2022).

Denmark was the leading country globally in the field of wind energy in 2021. Among the IEA nations, Denmark had the greatest proportion of wind energy for both total primary energy consumption and electricity production (IEA, 2021c). Despite their position, Denmark continues to pursue ambitious development objectives. The nation has set a target to achieve a 70 percent reduction in greenhouse gas emissions (GHG) by the year 2030, relative to the emission level recorded in year 1990 (IEA, 2021c). This will be achieved, in part, by implementing a ban on sales of petrol-powered vehicles and the cessation of operations of all coal-fired power plants by the same year (IEA, 2021c). Denmark aims to further increase its renewable energy sources in order to cover 50 percent of the nation's total energy consumption[4]. Lastly, Denmark has committed to the Paris

[3] Odense, Southern Denmark Region, Denmark DK. code: ODE, Collected from NordPool PHP.

[4] Operating on 100 percent renewable electricity, 80 percent coming from wind power (IEA, 2021c).

Agreement to achieve carbon neutrality by the year 2050 (IEA, 2021c).

In 2021, Denmark embarked on its most extensive industrial development in history [5] (Energistyrelsen, 2021). The proposal involved the construction of an energy island in the North Sea, with two offshore wind farms holding a combined capacity of 10 Gw (State of Green, 2023). According to Pedersen (2021), Denmark is set to emerge as a major exporter of green electricity to the entire Northern European with this and similar initiatives.

Denmark's significant advancements in the field of renewable energy, along with its strong political will to establish a future-oriented energy system and its unrelenting commitment to meet its net-zero objective, position the country at the forefront of the transition towards sustainable energy (IEA, 2021c). Their push to establish a sustainable ecosystem, tackle obstacles, and innovate can all be observed in their development and research in *Power-to-X*. In conjunction with bordering nations, Denmark is engaged in the development and construction of an expanded energy infrastructure project referred to as *Power to X*[6] (Danish Ministry of Climate, Energy and Utilities, 2021). Power-to-X (PtX) is an umbrella term for technologies that utilise power in the form of electricity to produce fuels, materials, multiple types of energy carriers (e.g., power-to-ammonia PtA, power-to-hydrogen PtH, power-to-fuel), and more (Eurowind Energy, n.d.). While PtX possesses several applications, it plays a crucial and indispensable role in facilitating the shift of industries towards sustainable energy sources. This is particularly relevant in cases where electrification may be impractical or excessively costly. In Denmark's PtX system, the aim of the first stage is to produce green hydrogen through electrolysis (Energistyrelsen, n.d.-b). Then further on, focusing on the production of ammonia PtA. It has further implemented a PtX system characterised by a diverse array of offshore installations encompassing, wind turbines, platform installations, energy islands, and an interconnected network of cables and pipelines for the transmission of energy to both Denmark and surrounding nations. Denmark is now progressing towards the complete integration of renewable energy sources into its energy sector through the implementation and interconnection of a novel energy system with the national grid.

For the purpose of this thesis, Denmark stood out as a prime case study with its unique

[5] Energiø Nordøst and Bornholm Energy Island, a 10 GW and 3 GW energy island of the coast of Denmark. Bornholm has an estimated cost EUR 7.93 billion (State of Green, 2023).

[6] The EU Power-to-X ambitions includes the aim of installing 40 GW of renewable hydrogen electrolysis by 2030 (Ministry of Foreign Affairs of Denmark, n.d.-a).

renewable ecosystem. An ecosystem consisting to a high degree of wind energy, where PtX solutions are already being implemented in the form of PtH (Energistyrelsen, n.d.-b). Denmark's deep engagement in this field, along with its strong political will and decisive measures for continued development, positions it as a significant player in shaping the trajectory towards a net-zero future. Denmark is one of the most promising markets for exploring the potential of ammonia as an energy carrier and energy storage system for future energy systems. Hence, we find it suitable to study the impacts of incorporating renewable energy from the grid into green ammonia production.

With Denmark as a base for this thesis, we established a representative foundation for further integration of a PtA system in a renewable energy ecosystem. This integration seeks to provide a solution for a component in the net-zero future. The component of this future that has been studied in this research is ammonia.

Ammonia is becoming an essential part of resolving long-term energy storage and the net-zero fuel challenge (Varela et al., 2021). With a future based around green energy, we need the ability to store and transport energy efficiently and safely. Hydrogen is today viewed as an energy carrier option, but its chemical structure has many challenges. While hydrogen has many applications, ammonia has the potential to revolutionise deep sea shipping, marine transportation, and long-haul flights, among others. This as ammonia has a superior energy density [7], is easier to transport, and has a lower cost of storage (Lan & Tao, 2014).

In 2021 Strømholm and Rolfsen (2021) published a research paper on the possibility of utilizing the fluctuations in the Norwegian power grid to reduce the costs of producing green hydrogen. This research found, among others, that it is challenging to capitalise on electricity price fluctuations due to the cost of added production and the high cost of increased hydrogen storage. Today, both green ammonia and green hydrogen struggle with high cost, and both are important energy carriers for reaching a net-zero future. With increased volatility in the power market, due to increased reliance on wind power (Strømholm & Rolfsen, 2021), it is important to find ways to reduce this volatility. Utilising it to bring down the cost of hydrogen and ammonia might be one solution. Since ammonia has the lowest cost of storage, we want to investigate if the price fluctuations in a highly

[7] Ammonia has a volumetric energy density of 11.5 MJ/L over hydrogen's 8.5 MJ/L. (Lan & Tao, 2014)

wind-dependent market such as Denmark can help to decrease the total cost of ammonia.

Today, ammonia is mainly utilised in the production of fertilisers, accounting for 88 percent of total production (Pattabathhula & Richardson, 2016). While ammonia is a crucial chemical element in the production of fertilizers, it has a vast variety of use cases (e.g., working medium in heat pumps, energy vector, and more). Ammonia contains 17wt% hydrogen [8] by weight, which can be used directly in fuel cells or extracted through electro-oxidation or thermal decomposition (Cheddie, 2012). This makes ammonia a highly capable energy carrier for hydrogen, as it contains three hydrogen atoms and one nitrogen atom per molecule. In other words, ammonia contains more hydrogen atoms per molecule than hydrogen itself. Hydrogen is further an explosive substance, that needs a lower temperature and higher pressure than ammonia[9] when stored (Juangsa et al., 2021)(Okonkwo et al., 2023). The high energy density of ammonia, its low explosion hazard and less complicated storage management make it a viable energy vector for hydrogen and an energy carrier for long-term storage and transportation. In essence, ammonia is a preferable choice in situations where hydrogen storage or operations is impractical, and where electrification is either too expensive or unfeasible.

Ammonia is increasingly becoming an attractive investment, and Denmark is currently developing Europe's largest green ammonia plant, HØST, with a capex of 1.4 billion EUR (HØST PtX Esbjerg, n.d.). HØST PtX Esbjerg will be installed with a 1GW electrolyser and deploy the conventional Haber-Bosh process (HØST PtX Esbjerg, n.d.). The plant will produce green ammonia by 2028/29. The agriculture sector will utilise this green ammonia in their fertiliser production, positively contributing to decarbonizing the agriculture sector. Major shipping companies like DFDA and Maersk are looking into green ammonia as a sustainable fuel for their vessels (HØST PtX Esbjerg, n.d.).

Ammonia will become increasingly relevant in the future, both as a stabiliser for the renewable power market and as an energy carrier. Our objective is to research the feasibility of cost-efficient production of green ammonia in order to enhance its competitiveness.

[8] 17wt% indicates that per kg NH3 there contains 17% $H_2$ (Cheddie, 2012).

[9] Hydrogen needs higher pressure and lower temperature to gain satisfactory energy density, avoid leakage due to its small atom size and avoid material embrittlement (Dawood et al., 2020)(Okonkwo et al., 2023).

## 1.3 Literature review

Considerable amount of research has been conducted on all components of the ammonia production process. However, inside the field of ammonia production there is a greater abundance of research pertaining to the hydrogen production part. Although in recent years, there has been a significant surge in the number of academic papers focusing on green ammonia. This development in research can be attributed to the growing significance and interest in green ammonia as a relevant energy carrier and a net-zero component.

Armijo and Philibert (2020) have through their research paper *"Flexible Production of Green Hydrogen and Ammonia from Variable Solar and Wind Energy: Case Study of Chile and Argentina"*(Armijo & Philibert, 2020), studied the effects of implementing a more flexible ammonia synthesis compared to what's commercially available today. The primary objective was to achieve cost reduction through the integration of solar and wind power, while also prioritising the enhancement of ammonia synthesis flexibility. The production process involved the integration of water electrolysis technology for hydrogen and Haber-Bosh (HB) for the ammonia synthesis. They successfully achieved to decrease costs by minimising their dependence on intermediate hydrogen storage as a means to mitigate the fluctuations in renewable energy production. This research considers the volatility in the quantity of renewable power available but does not directly consider the electricity price fluctuations. The limitations of their work stem from the use of a given wind and solar energy infrastructure, which intermittently relies on grid electricity for start-up. This constraint imposes limitations on their ability to scale, since they are obligated to store all energy generated during periods of high output. While this paper may not have immediate relevance for Denmark's future net-zero ecosystem, it is important to highlight the enhanced flexibility included in the HB process, as it addresses one of the big obstacles associated with this method. Given that this flexibility is not theoretically implausible, it is crucial to examine the potential ramifications of this flexibility on the cost of production. Finally, the study provides a comprehensive overview of the components included in the production process of green ammonia (Armijo & Philibert, 2020).

Another study conducted by Strømholm and Rolfsen, 2021 looks at the possibility of utilising a more flexible hydrogen production process in order to decrease the levelized cost of hydrogen LCOH. This through the use of electricity price fluctuations in the Norwegian

electricity market. This paper, while looking at hydrogen and using Norway as region, has many relevant components as it uses electricity price fluctuations as the foundation. The research findings show that, under some conditions, it is possible to achieve reduced levelized cost of hydrogen (LCOH). However, due to the continued fixed demand for hydrogen and the significant expenses associated with storing additional hydrogen, this approach proved mostly unfeasible (Strømholm & Rolfsen, 2021). Given the comparatively low cost of storing ammonia and the use of a hydrogen buffer in the ammonia production process, we find it relevant to investigate if the price fluctuations for ammonia production holds financial significance. Based on our research, the objective of this paper is to combine the concept of employing a more flexible HB ammonia production compared to the commercially available option, while also optimising production in accordance with the volatility of Denmark's electricity grid. Furthermore, it is essential to assess if this would result in a more economically feasible levelized cost of ammonia LCOA.

The literature reviewed in relation to this research consistently endorse or employs the Haber-Bosch HB procedure for the NH3 synthesis, as it is widely recognised as the prevailing method. Additionally, there are other conversion technologies available, such as electrochemical, photochemical, and plasma. The electrochemical approach has the potential to achieve a higher energy output compared to HB, but it is currently characterised by significant underdevelopment (Juangsa et al., 2021). While the typical configuration of the synthesis is designed for continuous mass production, research published by Ikäheimo et al. (2018) states that reconfiguring the synthesis for dynamic production does not appear out of reach. Armijo and Philibert (2020) went deeper into this idea of a more flexible HB process. As further demonstrated through a R&D test with 25 percent ramp-up within one minute of the HB (Armijo & Philibert, 2020). This concept is still in the exploratory phase and in a small scale. Kuckshinrichs et al. (2017) provided the formula that are commonly used when scaling chemical process facilities.

Data from Cesaro et al. (2021) have been the centre for the data gathering process as they outline the important technical and economic factors of ammonia production, together with Armijo and Philibert (2020), Ikäheimo et al., 2018, Verleysen et al. (2023) and Verleysen et al. (2021). All these articles' data have further been compared to other articles in order to understand their validity. As a high number of data-points have been

collected from research papers. For technical data relating to the different components and their limitations Wang et al. (2023) and Ikäheimo et al. (2018) have provided a comprehensive in-depth overview. For the electrolyser in the hydrogen production process, Matute et al. (2019) have provided a comprehensive in-depth overview of the economic data. The day ahead electricity prices data for Denmark DK1 have been collected directly fromNord Pool, 2023 through their PHP server. The way this data is handled follows Strømholm and Rolfsen, 2021 approach to aggregate and sampling of the price data. Cesaro et al. (2021) has through their comprehensive review identified the economic data needed to analyse the cost of ammonia production. This article provides a thoroughly indication of the energy level required for the different components within the ammonia production process, along with financial data-points used in this thesis. Lastly, Cesaro et al. (2021), Armijo and Philibert (2020), and Bose et al. (2022) has combined provided the research base for the LCOA calculations.

The objective of this study is to examine if increased flexibility in ammonia production could contribute to cost reduction, considering the fluctuations in the electricity market. Many fundamental aspects of this paper builds on the research conducted by Armijo and Philibert (2020) and Strømholm and Rolfsen (2021). The flexible ammonia model proposed by Armijo and Philibert (2020) served as a valuable reference in developing the ammonia production model for our specific case-study. In addition to incorporating insights from Armijo and Philibert (2020), supplementary data from several other research papers was utilised. Building and expanding upon their research, we want to assess the potential of using intermediate hydrogen storage as a component to alleviate costs opposed to reducing its dependence. Given the presence of a reliable energy supply in our case, the necessity for flexibility is comparatively lower in comparison to an off-grid alternative. Hence our approach seeks to investigate if intermediate storage can mitigate the cost. Their cost measure approach through LCOA is in line with our objectives and have been utilised as a base for cost calculations. The mathematical model developed in this paper is inspired by Strømholm and Rolfsen (2021). Based on their approach this thesis builds further and goes beyond the electrolyser and hydrogen. The model presented in this paper widens the scope of the model to include the ASU and the HB. This facilitates for understanding the biggest cost drivers and the reasoning behind them.

## 1.4 Computer programs and thesis outlining

In the development of this thesis, we have utilised multiple computer applications. The data and optimisation model presented in chapters 3 and 4 are implemented in AMPL (A Mathematical Programming Language), an optimization software, and solved using the Gurobi solver. The programming language for statistical analysis R was used to conduct our analysis.

This thesis is outlined in the following manner. The second chapter provides a comprehensive understanding of the various forms of hydrogen and ammonia production, their production processes, as well as the advantages and drawbacks of the selected technology. Chapter 3 provides an overview of the technical and financial data, including NordPool elspot price data for Denmark west DK1. Lastly it states the cost of operation, grid fees, and functional parameters. In chapter 4, the linear optimisation model is expounded upon, and the objective function is presented. Chapter 5 investigates different scenarios and their effect on the total production cost. It further analyse the different cost drivers for ammonia production within the context of the Danish power system. Lastly, it conducts a sensitivity analysis of the assumptions underlying the model and of the biggest limitations of the thesis. Chapter 6 discuss the model limitations and factors beyond the sensitivity analysis. It compares the results with comparative literature and presents further research. Lastly, chapter 7 consists of the conclusion.

# 2 Ammonia Production Process

This chapter covers the different theoretical elements of ammonia production and utilisation. As the production of ammonia can be divided into three main steps, section 2.1 provides an introductory overview of the entire ammonia production process. Section 2.2 articulates the relevant theories behind hydrogen as the first stage in ammonia production. Additionally, it provides a comprehensive overview of the various electrolysis technologies used for hydrogen production. Section 2.3 elaborates on the air separator unit, with section 2.4 describing the theoretical aspects of ammonia production along with the most recent advancements.

## 2.1 Ammonia Production: An Overview

Ammonia is ranked as the second most manufactured inorganic compound globally, surpassed only by sulfuric acid (Econnect Energy, n.d.). This statement illustrates the proportional magnitude of yearly worldwide ammonia production[10], with China, US, Russia, India, and Indonesia accounting for around 60 percent of global output (Olabi et al., 2023). Today the majority of ammonia is produced using fossil fuels, with China being the biggest producer at 30 percent (IEA, 2021b). China mostly relies on coal-based production (Ghavam Seyedehhoma & Peter, 2021) making them the biggest emitter at 45 percent globally (IEA, 2021a). With ammonia production worldwide accounting for more than one percent of total global emissions yearly (Armijo & Philibert, 2020).

Given the need for green ammonia to satisfy current demand, reach net-zero production, and adapt to future growth, it is important to explore approaches that ensure sustainable green ammonia production. Hence, this paper focuses primarily on net-zero production approaches for both hydrogen and ammonia. Hydrogen is an essential part of the ammonia production, and it is therefore essential to include it when examining the ammonia production process. The hydrogen production process is further associated with having the largest energy consumption of all sections of the ammonia production process (Verleysen et al., 2023).

[10]The production of ammonia globally in 2022 was calculated to be approximately 150 million metric tons (Statista, 2023)

The ammonia production process can be conceptualized as a three-step process, Figure 2.1. Where the first and second step is the production of hydrogen and nitrogen. The merging of these two molecules in the third step, known as the ammonia synthesis, forms ammonia. The flowchart in Figure 2.1 illustrates these three steps. In this process hydrogen is produced through electrolysis, and nitrogen through the air separator unit (ASU). Both components can be viewed as input factors for the ammonia synthesis. As ammonia is comprised of hydrogen and nitrogen, hence its atomic symbol $NH_3$. Indicating that ammonia is compound of one nitrogen (N) and three hydrogen (H) atoms. In the production flowchart, Figure 2.1, the ASU is placed as a separate unit. Ordinarily the ASU would be included in the ammonia production unit, with hydrogen being the only additional process. The reasoning for excluding the ASU from the ammonia production unit in this figure is to enhance the visualization of the ammonia production process.

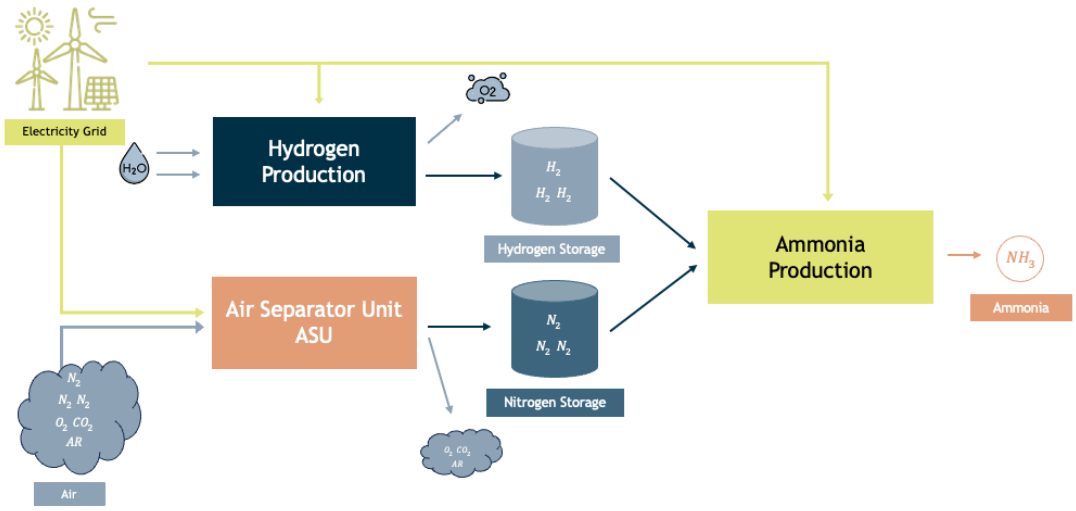


**Figure 2.1:** Ammonia production flow chart

The input factor hydrogen is made from splitting two water molecules ($2H_2O$) into one oxygen ($O_2$) and two hydrogen ($2H_2$) molecules. This process takes place in the electrolysis, entitled hydrogen production in Figure 2.1. For nitrogen, this is achieved through a process where nitrogen is isolated from atmospheric air. This process happens in the air separator unit (ASU). At this stage, the core components for ammonia production are introduced. The ammonia synthesis begins after the hydrogen buffer and ends in storage, where ammonia can either be stored or transported for use in other applications. Based on the flowchart, sections 2.2 and 2.3 provide an overview of hydrogen and various production methods. With sections 2.4 and 2.5 examining ammonia and its production process.

## 2.2 Hydrogen production

The first step in the ammonia production process is the production of hydrogen. Hydrogen is today one of the most promising sustainable fuels, as it is a non-polluting energy source where its electron only forms water upon oxidation (Lubitz & Tumas, 2007). Hydrogen ($H_2$) is the most prevalent element found in our universe. It is mostly found in water and organic compounds (Dawood et al., 2020). Hydrogen has an energy density that is two times that of other types of solid fuels (50 MJ/kg) at 140 MJ/kg (Shiva Kumar & Himabindu, 2019), but has a low energy level relative to volume. $H_2$ is the simplest and lightest element, composed of only one proton and one electron with an atomic mass of 1.00794 mass unit, making it highly flammable (Dawood et al., 2020). In 2021, the global production of hydrogen was approximately 94 million tonnes (Mt $H_2$) (IEA, 2021b). Although some of this was produced using green energy, the majority was produced using fossil fuels and biomass. Natural gas was the primary fuel source, accounting for 62 percent of the total, followed by coal, which represented 19 percent (Tang et al., 2023). There are three primary methods for producing hydrogen, illustrated in Figure 2.2. This is either through biomasses, fossil fuels, or water electrolysis, or in combination (IEA, 2022a). In 2019 about 96 percent of all hydrogen production stems from non-renewable sources (Shiva Kumar & Himabindu, 2019).

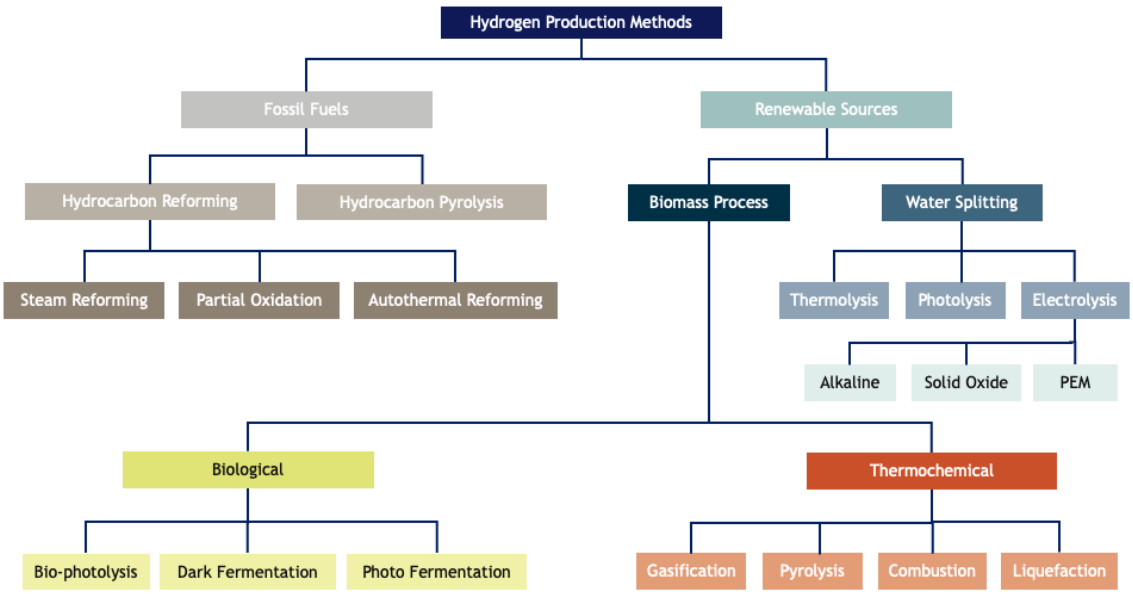


**Figure 2.2:** Overview of various hydrogen production approaches (Shiva Kumar & Himabindu, 2019).

This paper focuses on the production of hydrogen and ammonia derived from renewable sources, as renewables are projected to dominate the Danish energy market in the foreseeable future. There are a total of sixteen distinct methods for producing hydrogen as of today, illustrated in Figure 2.2. We observe that a total of twelve of these are related to renewable sources, with five utilizing water (also known as water splitting). These methods that utilise water are categorised as green hydrogen. This implies that they are free from $CO_2$ emissions when water and hydrogen are separated in the electrolysis. Additionally, the electricity utilised for this process is sourced from renewable energy sources such as wind, solar, and hydro power (Green Hydrogen Webinars, n.d.). Electrolysis as a method of water splitting, is the most used method for producing green ammonia (Dincer, 2012).

Water electrolysis as a method for hydrogen production is further essential for sustainable PtH and PtA projects. It also serves as a key component in achieving net-zero (Verleysen et al., 2021). Given that this thesis focuses on PtX development in Denmark, it will solely focus on water electrolysis (a hydrogen production method under water splitting). The water electrolysis process is predicted to be the most scalable and economically efficient when powered by renewable energy sources (such as wind and solar in Denmark) in the long term (Wang et al., 2023).

Water electrolysis (WE) is a method for producing hydrogen that provides a high concentration of purified water and hydrogen at 99.99% (Shiva Kumar & Himabindu, 2019). The equation for this reaction is given by (Shiva Kumar & Himabindu, 2019):

$$1H_2O + Electricity(237.2kJ.mol^{-1}) + Heat(48.6kj.mol^{-1}) \rightarrow H_2 + 1/2O_2 \tag{2.1}$$

According to the chemical formula, when two water molecules are subjected to a given quantity of electricity in combination with a given temperature, they will react and form two hydrogen atoms and one oxygen atom. In other words, the by-product from this chemical reaction is pure oxygen. Using a fuel cell, the hydrogen atoms can be converted into electrical energy. This application further exemplifies the versatility of hydrogen.

### 2.2.1 Electrolysis technologies

There are two approaches that are widely used and regarded as feasible in the literature of water splitting electrolysis. These two approaches are alkaline electrolysis (AE) and polymer electrolyte membrane electrolysis (PEM) (Matute et al., 2019). The primary distinction between these two technologies is the type of electrolyte utilised. While alkaline use a liquid membrane, PEM uses a solid membrane (Matute et al., 2019).

Water electrolysis (WE) offers several benefits in comparison to other production methods. Its most important benefits include outstanding cell efficiency and production purity, all while maintaining a sustainable process (Verleysen et al., 2021). Although WE have many apparent advantages, it is not the preferred choice for the majority of hydrogen production facilities due to its comparatively higher cost when compared to other non-renewable electrolysis technologies (Verleysen et al., 2021).

The following section provides an overview of the two approaches, PEM, and alkaline electrolysis. As these technologies are both renewable if used together with renewable energy, ref Figure 2.2, and commercially available on the market today.

#### 2.2.1.1 Alkaline Electrolysis (AE)

Alkaline electrolysis (AE), also referred to as alkaline water electrolysis (AWE), is widely regarded as the most mature and well-established technology for water electrolysis (Liu et al., 2023). It is characterised by two electrodes immersed in a corrosive potash solution serving as the alkaline electrolyte (Shiva Kumar & Himabindu, 2019). As illustrated in the Figure 2.3, these electrodes are separated by a diaphragm. The process works by initiating an electric current on the cathode. Incoming water molecules $H_2O$ react with the cathode and split into two, two separate hydroxyl ions $OH^-$ and one hydrogen $H_2$ molecule (Shiva Kumar & Himabindu, 2019). The hydroxide ions ($OH^-$) are then transferred through the diaphragm (e.g., zirfon, asbestos, or microporous diaphragm) to the anode by the electric difference $V$. Here the electrons separate from the $OH^-$ and it forms half an oxygen molecule ($O_2$) and one water molecule ($H_2O$). At this point in the process, the electrons return through the power unit to the positive terminal. The diaphragm separates the $H_2$ and the $O_2$, and they are individually transported out of the electrolysis (Shiva Kumar & Himabindu, 2019).

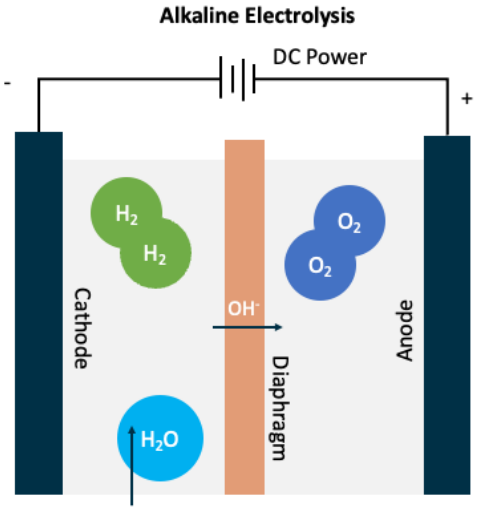


**Figure 2.3:** Illustration of the Alkaline water electrolysis (Shiva Kumar & Himabindu, 2019).

Today alkaline water electrolysis is embedded in several renewable energy systems as a method for storing energy. This as the technology is suitable for large-scale hydrogen production due to its use of non-noble metals in the catalyst and moderate temperature during production (Liu et al., 2023). Today the leading element for use in the catalyst is nickel (Ni) (Liu et al., 2023). While this element is cost-effective compared to using precious metals, it has been discovered that electrodes made of nickel degrades over time and the surface area becomes less reactive (Liu et al., 2023). This implies that the cell stack needs to be swapped more often to ensure a high degree of efficiency. While nickel has some disadvantages, it offers thermal stability for the electrolysis, an exceptional degree of conductivity, and a high degree of electrical properties (Angeles-Olvera et al., 2022).

With the relatively poor efficiency of AE, researchers have been working on enhancing it. According to Sørensen and Spazzafumo (2018) one approach that is being tested is a combination of increased temperature (above 1500 degrees), optimised design of the electrodes and the catalyst (Sørensen & Spazzafumo, 2018). There is also research being done in developing an entirely different membrane named anion exchange membrane (AEM) (Marini et al., 2012). This membrane is to be used instead of today's diaphragm and will make the system more compact (Marini et al., 2012). The membrane in the AEM consists of polymers with a negatively charged ion (Shiva Kumar & Himabindu, 2019).

#### 2.2.1.2 Polymer electrolyte membrane electrolysis (PEM)

Polymer electrolyte membrane electrolysis (PEM) is a newer approach to produce hydrogen through water electrolysis. It works by splitting water into hydrogen and oxygen, through a process named electrochemical splitting (Shiva Kumar & Himabindu, 2019). The $H_2O$ is transported to the anode, where it splits to protons $H^+$, oxygen $O_2$, and electrons $e^-$ through the use of electricity (Shiva Kumar & Himabindu, 2019). The protons $H^+$ are transported through the membrane from the anode section to the cathode section of the electrolysis. The electrons $e^-$ at the anode passes via the power source (DC Power unit in Figure 2.4) to the cathode. Electrons $e^-$ from the power source react with protons at the cathode, and hydrogen is produced (Shiva Kumar & Himabindu, 2019). The illustration of this process is presented in Figure 2.4.

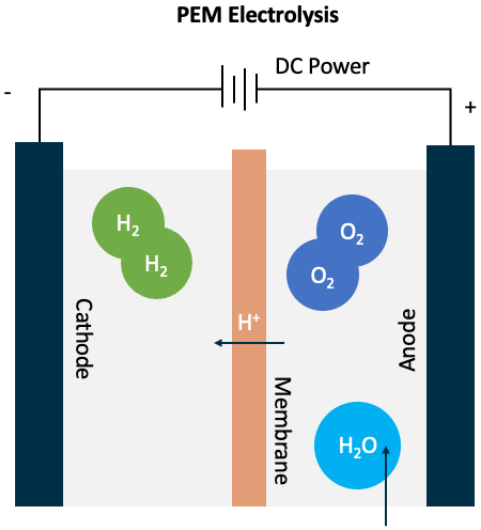


**Figure 2.4:** Illustration of the PEM water electrolysis (Shiva Kumar & Himabindu, 2019).

The PEM technology was developed in the fifties and sixties to overcome the challenges with Alkaline technology (Shiva Kumar & Himabindu, 2019). This makes PEM, relative to other technologies, a newer approach to conduct water splitting electrolysis. Carmo et al. (2013) did a comprehensive review of PEM water electrolysis. Their review found that PEM with its use of a solid polymer membrane is able to utilise a thinner electrolyte, resulting in a more compact design, higher capacity and current density (Carmo et al., 2013). It can operate with a broad selection of electricity inputs due to its ability to hinder gas transfer between the cathode and anode. This further provides the production of pure hydrogen (Carmo et al., 2013). PEM is also suitable for use in volatile energy conditions,

as it is able to execute quick responses and increase or decrease production rapidly.

While there are many notable positive aspects to the PEM technology, many of these advantages also serves as its challenges. The operational setup of PEM provides a corrosive environment, with high component costs due to its complex structure and the use of precious metals (Shiva Kumar & Himabindu, 2019). The harsh environment inside the electrolysis requires the use of distinct materials, which further increases the operational cost compared to AE (Carmo et al., 2013). Since the invention of PEM there has been little research done before the shift to this millennium, leaving its drawbacks unsolved. The introduction of renewable energy resources has seen a spike in PEM research, as their adaptability is an important aspect for renewable energy utilisation (Carmo et al., 2013). As there have not been discovered methods to decrease costs related to PEM, the majority of developers therefore build using the more known and less expensive alkaline technology. If manufacturers are able to decrease the cost of PEM, it is likely that it will emerge as the preferred choice.

### 2.2.2 Intermediate Hydrogen Storage

Due to the scope of this thesis, long-term hydrogen storage is not seen as relevant. Therefore, this paper only focuses on intermediate hydrogen storage as a step in the ammonia production process. The justification for the implementation of intermediate storage between the hydrogen and the ammonia production process derives from the difference in flexibility between them given today's technology. Hydrogen production can transition from full production to a complete stop in about half an hour, while the HB uses a day or more to achieve the same, given the correct temperature (Armijo & Philibert, 2020). Since the objective of this paper is to utilise energy price fluctuations, the added flexibility of hydrogen production might have an impact on our results.

Hydrogen storage can be categorised into two groups, either material-based or physical-based (EERE, n.d.). Physical-based hydrogen storage can further be divided into three primary storage options, compressed gas ($CH_2$), cold compressed, or liquid ($LH_2$) (EERE, n.d.). Frequently, large-scale ammonia production facilities with a constant output only have a pipeline between the hydrogen and the ammonia production facility. With the development of a remote renewable energy ecosystem, Armijo and Philibert (2020) find

that buffer-based ammonia production with the use of steel tanks is suitable due to the volatility of available energy (Armijo & Philibert, 2020). While such a buffer introduces flexibility, it also adds challenges. Firstly, hydrogen, with its low molecular weight and size, has the ability to leak through seals or materials, making it costly to store (Dawood et al., 2020). Secondly, hydrogen holds the greatest energy density per unit mass, while at the same time having some of the lowest volumetric density among all fuel sources (Juangsa et al., 2021). This makes it challenging to store large quantities of hydrogen in rationally sized spaces. Hence, compression or a low temperature is required to store adequate amounts (EERE, n.d.). For the purpose of this thesis, we intend to use the same pressurize steel tanks and associated costs as Armijo and Philibert (2020), as they are mature and provides a high degree of flexibility to the solution.

## 2.3 Air Separator Unit (ASU)

Today, the only large-scale commercially available technology for use in air separator devices is the cryogenic distillation (Ikäheimo et al., 2018). Although it possesses remarkable thermodynamic properties, its complicated architecture makes it challenging to operate (Fu & Gundersen, 2013). To gain a better understanding of the ASU, a simplified visual flowchart is presented in Figure 2.5.

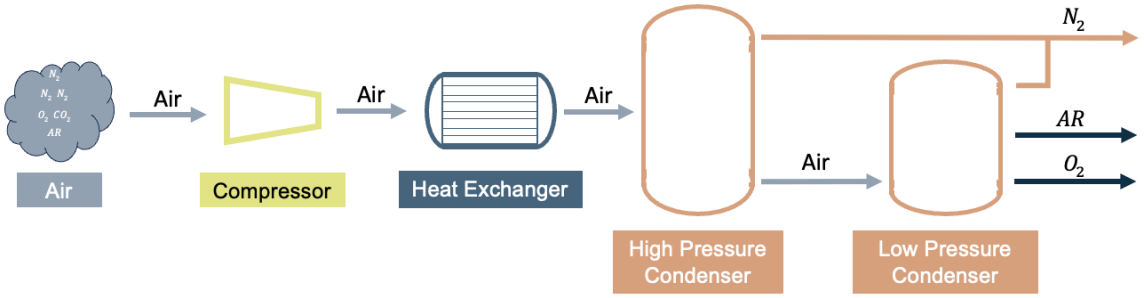


**Figure 2.5:** ASU flowchart (Gomez et al., 2020)

Air is gathered from the atmosphere, which mainly contains nitrogen ($N_2$), oxygen ($O_2$) and argon (AR)[11](UCAR, n.d.). Then the air is compressed (which generates heat) before it is cooled using a heat exchanger in the following step (Gomez et al., 2020). The air continues to the first condenser, a High-Pressure Condenser, which performs the first separation. In this condenser, only a portion of the air's nitrogen is filtered out.

[11]Air contains 78 percent nitrogen, 21 percent oxygen, 0.93 percent argon, and others constitute less than 0.1 percent (carbon dioxide, neon, helium, methane, and more) (UCAR, n.d.).

Therefore, the remaining air passes through the low-pressure condenser to extract more of the nitrogen from the air. In this condenser, the majority of nitrogen is filtered out, and the final product is >99 percent clean nitrogen (Gomez et al., 2020). Additionally, filtered oxygen and argon are available for use in other applications if needed. After the last filtering process, the gases stays cooled and depending on the application, reheating might be appropriate for further use (Gomez et al., 2020).

## 2.4 Ammonia Synthesis

There is a broad selection of ammonia production methods available, as presented in Figure 2.6. The various technologies used for ammonia synthesis can be divided into four main categories: thermochemical, electrochemical, photochemical, and plasma-assisted (Juangsa et al., 2021). Although some of these technologies are still in the development phase, such as various types of plasma-assisted processes, others are experiencing limitations in terms of efficiency, like photocatalytic processes (Juangsa et al., 2021). This narrows the viable technologies down to only including thermochemical and electrochemical production.

This thesis aims to study available ammonia synthesis technologies, therefore limiting the research to thermochemical and electrochemical production. Given that these two categories constitute all ammonia synthesis, with thermochemical and Haber-Bosch accounting for more than 96 percent (Juangsa et al., 2021). Figure 2.6 provides an overview of the different approaches to ammonia synthesis.

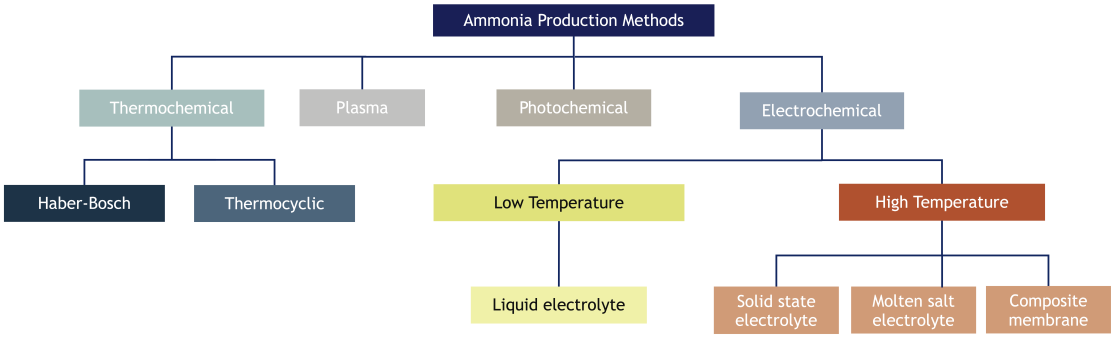


**Figure 2.6:** Overview of ammonia production approaches (Juangsa et al., 2021).

Based on the different production methods presented in Figure2.6, there are two types of thermochemical and electrochemical production. Thermochemical production of

$NH_3$ distinguishes between Haber-Bosch (HB) and thermocyclic, while electrochemical distinguishes between high and low temperature $NH_3$ production (Juangsa et al., 2021). In the following section the different electrochemical synthesis methods are to be addressed, followed by the thermochemical HB process as this is the most widely chosen thermochemical synthesis (Juangsa et al., 2021).

### 2.4.1 Electrochemical synthesis

Electrochemical $NH_3$ synthesis is a process that is divided into high or low temperatures based on the electrolyte that are utilised (Juangsa et al., 2021). This process is considered a promising solution for the integration of renewable energy in the synthesis of $NH_3$, as its energy consumption is low, requires no fossil fuel, and utilise water to obtain hydrogen (Juangsa et al., 2021).

An electrochemical ammonia synthesis utilises many of the same processes as in earlier studied hydrogen production. While it does not operate like an electrolysis in splitting a compound, it uses many of the same components, like an electrolyte, a separator, a cathode, and an anode with a separated electricity supplier. The complete flowchart with an overview of the electrolysis is presented in Figure 2.7.

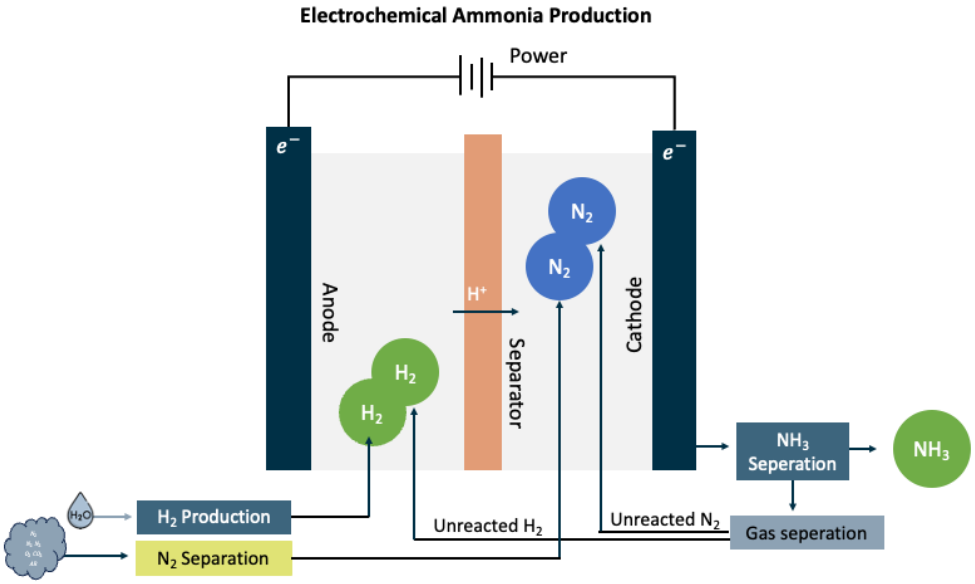


**Figure 2.7:** Flowchart and electrolysis of electrochemical ammonia production (Juangsa et al., 2021).

The electrochemical process presented in Figure 2.7 utilises pure hydrogen and nitrogen produced externally through hydrogen production and nitrogen separation. These diatomic

molecules[12] are then transported to the electrochemical ammonia synthesis. Hydrogen is led to the anode section of the unit, with nitrogen led to the cathode side (Juangsa et al., 2021). When electricity is introduced, the reaction starts. Electrons $e^-$ travels from the anode side over to the cathode side of the synthesis through the power unit, while the $H^+$ travels through the separator to the cathode side (Juangsa et al., 2021). At this stage, $H^+$ and $N_2$ react and form $NH_3$ at the cathode. After the reaction at the cathode, all substances are led out of the unit and into the $NH_3$ separator, which separates the $NH_3$ from the unreacted nitrogen $N_2$ and hydrogen $H_2$. From this separator, ammonia is transported out of the process, while hydrogen and nitrogen are led further to the gas separator, which separates $H_2$ from $N_2$. The separated diatomic molecules are transported back into the electrochemical ammonia synthesis Figure 2.7.(Juangsa et al., 2021).

Electrochemical synthesis has been presented as an alternative to the thermochemical process of Haber-Bosch (HB), and research finds that it is more energy-effective than the HB process (Juangsa et al., 2021). While electrochemical synthesis has a lot of potential, it is only regarded as a viable option under moderate conditions. The main challenge with electrochemical synthesis is its durability, costly electrical system, and operation as a result of elevated temperatures (Juangsa et al., 2021). Electrochemical synthesis at high temperature has been proven to work with solid electrolytes, molten salt electrolytes and composite membrane electrolytes (Juangsa et al., 2021). The low temperature electrochemical production works in an integrated system with PEM, and uses biological catalysts, heterogeneous catalysts, and homogeneous catalysts (Juangsa et al., 2021). The low temperature electrochemical production removes the challenge with high temperature, but its low temperature introduces new challenges and sets the stage for a slow reaction which further results in a process with low energy efficiency (Juangsa et al., 2021). The challenges with electrochemical ammonia synthesis can be compared to those of PEM for hydrogen. Both technologies are innovative and cost-effective solutions but are currently facing challenges that makes scaling them difficult, maintaining satisfactory reliability, and uses costly components.

[12]Any chemical compound consisting of just two atoms is a diatomic molecule, e.g., $N_2$ (Stewart, n.d.).

### 2.4.2 Haber-Bosch synthesis (HB)

Fritz Haber discovered, in 1908, how to produce ammonia using a catalyst (Flavell-While, 2010). This method has been known as the Haber-Bosch synthesis or process (Wang et al., 2023). Although the production of ammonia can be achieved through several different methods, the Haber-Bosch (HB) process is the most widely used method today. The method is utilised in more than 96 percent of all global ammonia production (Juangsa et al., 2021). Even though the process has been improved upon throughout the last century, no fundamental changes has been made and the basic chemical formula have stayed the same (Wang et al., 2023). The formula is presented in Formula 2.2.

$$3H_2 + N_2 \rightarrow 2NH_3 \tag{2.2}$$

The chemical formula points out that the HB process uses three hydrogen ($H_2$) and one nitrogen ($N_2$) atoms to produce two ammonia molecules ($NH_3$). This chemical process takes place inside the reactor, where the atoms are converted from nitrogen and hydrogen gases into ammonia (Verleysen et al., 2021). The HB process utilises pure hydrogen from a separate hydrogen production facility (Section 2.2) and nitrogen collected from the air through an air separator unit ASU (Section 2.3). These gases are fed into the HB process through the feeders, and at this stage the HB process starts (Verleysen et al., 2021). The entire HB synthesis process is illustrated in the flowchart presented in Figure 2.8.

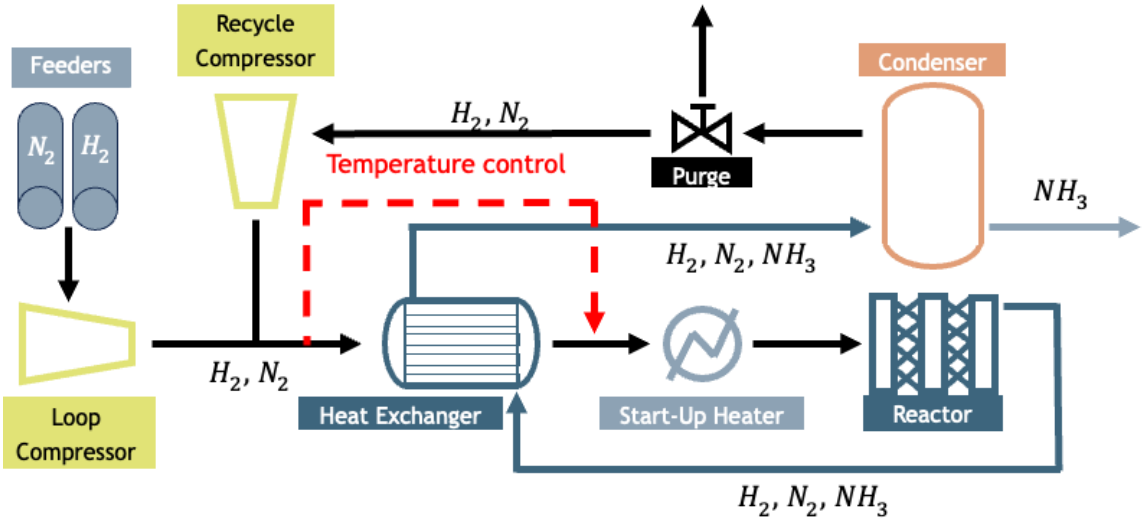


**Figure 2.8:** Flowchart of the HB synthesis loop (Verleysen et al., 2021).

The flowchart representing the HB process is a bit complicated, but the structure primarily consists of four components: a compressor, a heat exchanger, a reactor, and a condenser (Verleysen et al., 2021).

The HB process works in the following manner. Hydrogen and nitrogen are fed to the compressor, where they are pressurised (normally 100-250 bar) before continuing to the heat exchanger (Verleysen et al., 2021). On this path, the pressurised flow gets mixed together with the recycled flow coming from the condenser. The heat exchanger works by taking heat away from the outbound flow from the reactor and transferring this heat to the inbound flow. This helps to reduce the need for expensive heating and cooling systems, heats up the inlet flow, and evens out variations in the flow temperature. If the temperature increase to above a given threshold (normally 400 °C), a bypass flow is designed to decrease the inlet temperature (Verleysen et al., 2021). From this point, the gases enter the reactor, where the exothermic reaction occurs. The outbound flow is a combination of ammonia and unreacted $H_2$ and $N_2$. From this, the gases goes oppositely through the heat exchanger and get cooled down by the cooler inlet flow. In the condenser, the gases are further cooled down (normally -20°C) and ammonia is extracted, while the nitrogen and hydrogen are led back for recycling (Verleysen et al., 2021).

During a cold-start, the start-up heater heats the incoming flow, because the system lacks the thermal energy present during steady-state (Verleysen et al., 2021). This makes for a slow increase in production, as the heating process is time-consuming. However, when the HB process is in a steady state, its ability to recycle the thermodynamic energy keeps its operational cost down (Verleysen et al., 2021). It further enables the HB to sustain a high production rate, as its thermocyclic process operates at a high temperature (Juangsa et al., 2021). According to Juangsa et al. (2021) a HB process only converts around 15 percent in a single pass, which highlights the importance of operating with a recycling flow to minimise waste and utilise the majority of the hydrogen and nitrogen inserted into the process (Juangsa et al., 2021). Olabi et al. (2023) further states that green ammonia production, when utilising both high-temperature and a heat recovery system, has an efficiency of around 83 percent (Olabi et al., 2023).

# 3 Data

This chapter presents and clarifies all the required data for evaluating how increased flexibility in ammonia production can reduce costs. Section 3.1 begins by explaining how levelized cost of ammonia (LCOA) is calculated, highlighting the relevant data for this analysis. Technical and financial data for the production units are outlined in Section 3.2. The intermediate storage data are presented in section 3.3. Section 3.4 contains the electricity price data retrieved from NordPool, and the data processing. Section 3.5 determines the weighted average cost of capital (WACC).

## 3.1 Levelized cost of ammonia

In order to investigate how an increase in the production flexibility of ammonia can exploit energy price fluctuations, a clarification on how cost is measured is necessary. Levelized cost of ammonia (LCOA) is more often used with the increased interest in green ammonia, enabling comparisons between projects (Armijo & Philibert, 2020; Cesaro et al., 2021; Nayak-Luke & Bañares-Alcántara, 2020; Verleysen et al., 2023). LCOA sums up all the discounted cash flow that is divided by the discounted quantity of ammonia (Cesaro et al., 2021):

$$LCOA = \frac{\sum_{t=0}^{N} \frac{C_t + O\&M_t}{(1+r)^t}}{\sum_{t=0}^{N} \frac{A_t}{(1+r)^t}} \tag{3.1}$$

| | | | |
|---|---|---|---|
| $N$ | Economic lifetime of equipment | $t$ | is the year between 0 and $N$ |
| $C_t$ | is the CAPEX | $O\&M_t$ | operational and maintenance |
| $A_t$ | quantity ammonia produced | $r$ | is discount rate |

In addition to comparison reasons, LCOA indicates the relevant data for the analysis. These include the cost aspects of production units and intermediate storage, along with their economic life, the production capabilities, and the discount rate (Cesaro et al., 2021).

## 3.2 Production Units

From LCOA, relevant data about the AE, ASU, and HB, labelled production units, will be provided. First, the economic lifetime of the system will be presented, along with the

ratio of production capacity for each of the production units. Then the technical and economic features of production units will be described.

### 3.2.1 Lifetime

Through an extensive review, Armijo and Philibert (2020) stated the expected economic lifetime of ammonia production system to be 30 years and will be the basis for the analysis.

### 3.2.2 Process mediums

In order to facilitate ammonia production, adequate hydrogen and nitrogen supply is necessary, as highlighted in Section 2.1. Understanding the proportion hydrogen and nitrogen constitute of ammonia is therefore necessary to understand the different capacity ratios. The label process medium(s) is provided as common term for ammonia, nitrogen, and hydrogen to improve reading flow throughout.

In one tonne of ammonia, approximately 177 kg of its weight can be contributed to hydrogen and 823 kg to nitrogen.(Rivarolo et al., 2019) (Thomas & Parks, 2006). Theoretically, under low temperatures and high pressure, the conversion rate of the process mediums to ammonia can be close to 100 percent (Humphreys et al., 2021). However, these conditions are not economically viable due to their slow production rate. To improve the production rate, the HB operates at a higher temperature (Humphreys et al., 2021). At 330-550° C and 150–330 bars of pressure, the reaction rates [13] of hydrogen and nitrogen are 15–25 percent, as highlighted by Wang et al. (2023). Humphreys et al. (2021) stated a reaction rate of 10 to 15 percent at 425-450 ° C and pressure above 101 bar. However, these values are for a single pass through the HB and not the total conversion rate. The non-reacted process mediums are either recycled or purged. A portion of the process mediums are purged to avoid the accumulation of inert gases (Verleysen et al., 2021). The purged rate is approximately 4 percent of the total hydrogen and nitrogen supplied to the HB, resulting in a total cycle conversion rate of 96 percent (Verleysen et al., 2021). Similarly, Fúnez Guerra et al. (2020) and Nosherwani and Neto (2021) stated a 97 percent and 98 percent total cycle conversion rate, respectively. In the context of this thesis, a total conversion rate of 97 percent is chosen.

[13] The reaction rate is the rate at which nitrogen and hydrogen get converted to ammonia (Wang et al., 2023).

### 3.2.3 States of Operation

Given the purpose of this thesis, an examination of the production units states of operations and their limitations are necessary. This subsection is divided into three parts, one for each of the production units.

**Alkaline Electrolyser**

The first production unit to be explored is the AE. Verleysen et al. (2023) stated that approximately 92 percent of the total energy required to produce green ammonia stems from the production of hydrogen. In literature, different rates are given to produce one kilogram of hydrogen. Yates et al. (2020) declared an energy consumption of approximately 54 kWh/kg, while Matute et al. (2019) estimated 50 kWh/kg by 2025. Similarly, Buttler and Spliethoff (2018) stated that the energy consumption would be 50 kWh/kg by 2023. Hence, 50 kWh/kg is selected to produce hydrogen.

Alternatively, the AE can be put in standby mode, where it is neither producing nor idle (Varela et al., 2021). It takes approximately 20 minutes for the AE to resume production(Varela et al., 2021). This state can be advantageous in certain scenarios; however, it does consume energy. For the multi-MW AEs analysed in this thesis, it is estimated to be 2 percent of their total energy (Matute et al., 2019).

Lastly, the AE can be in an idle state. This state does not consume any energy as there is no production. A restart to make the AE able to produce again would take 30–60 minutes (Varela et al., 2021). The state of restarting a unit from an idle state is referred to as cold start in this thesis. In the literature, it is less focus on the energy consumption required for a cold start. However, 250 kWh per tonne of daily hydrogen production have been utilised (Strømholm & Rolfsen, 2021). This makes it approximately six times more energy-demanding than one hour of standby mode.

**Air Separator Unit**

The energy requirement for the ASU is significantly lower compared to the AE. The ASU accounts for approximately 2 percent of the total energy in green ammonia production (Verleysen et al., 2023). Nonetheless, to reflect the features of green ammonia production most accurately, the energy requirement for production will be provided. Depending on the variations, the energy consumption ranges between 0,12 and 0,35[14] kWh/kg nitrogen

[14]Calculated based on numbers provided by Tafone et al. (2018)

(Cesaro et al., 2021; Tafone et al., 2018). However, 0,2 kWh/kg will be utilised for this thesis.

Basán et al. (2020) demonstrated cost savings potentials using standby mode of the ASU during volatile electricity pricing. Similarly, to the AE, a two percent rate of the nominal size of the ASU is utilised.

In contrast to the AE, the ASU must be idle considerably longer to restart production. In order to reach product purity, it can range from a few hours to several days. However, a 10-hour interval indicates to be reasonable (Miller et al., 2008; Quarshie et al., 2023).

**Haber-Bosch**

Having examined the state of operation of both AE and ASU, comparable steps for HB will be carried out. Similarly to the ASU, the HB consumes significantly less energy than the AE. It accounts for approximately six percent of the energy in green ammonia production (Verleysen et al., 2023). Ikäheimo et al. (2018) used a rate of 0,64 kWh/kg but also stated that the energy requirement for production falls in the range of 0,4-0,44 kWh/kg. The reason for the discrepancy is because they modelled the HB and ASU as one entity, encapsulating the energy requirements of nitrogen and ammonia together. In this thesis the highest rate of Ikäheimo et al. (2018) is assumed.

Compared to both the AE and ASU, the HB is substantially less flexible. Firstly, it cannot be placed in standby mode due to the energy requirement of keeping the temperature stable (Armijo & Philibert, 2020). Furthermore, the machine is normally only in an idle state for maintenance purposes. Hence, it normally operates continuously (Ikäheimo et al., 2018). Armijo and Philibert (2020) incorporated greater flexibility, allowing for HB to be idle in favourable scenarios. They used an idle duration of at least 48 hours before the machine could perform a cold start.

### 3.2.4 Load and Ramp Rate

With the states of operations for the production units highlighted, the limitation during production is explored. These include the load range that the machine can produce within, in addition to their ramp rate [15].

[15]Their ability to adjust production level

**Alkaline Electrolyser**

The AE is the most flexible unit in the system of ammonia production. It can operate at a higher load rate range than the two other production units. Wang et al. (2023) argues that the minimum load rate of an AE can range from 10 to 40 percent. If operated below this range, there is a high degree of impurity in both the oxygen and hydrogen streams. Similarly, Varela et al. (2021) states that advancements in technology have made it feasible to achieve a minimum load rate of 10 percent. However, it is worth noting that manufacturers specify a minimum load requirement of 15 percent. Furthermore, Matute et al. (2019) specifies a minimum load of 10 percent based on experience from different EU projects. While it is technically feasible to operate at a minimum load of 10 percent, we have chosen to adhere to the manufacturer's recommendation of maintaining a minimum load of 15 percent in this thesis.

Additionally, the ramp rate of AE must be considered. The AE ramp rate is dependent on sufficient implementation of power electronics and proper management of the process flow (Varela et al., 2021). However, it is commonly accepted that the ramp rate is approximately 20 percent of the nominal load per second. Therefore, the AE can vary between 15 and 100 production load between hours. (Varela et al., 2021)

**Air separator unit**

The ASU is comparably more constricting than the AE. To maintain purity, the minimum load rate is approximately 30 percent (Tesch et al., 2019). Cheng et al. (2022) utilised a minimum load rate of 40 percent in order to ensure a ramp rate of 3 percent per minute. This will also be implemented for this thesis, securing a load variation between 40 and 100 percent between hours.

**Haber-Bosch**

Within the system of green ammonia production, HB is the least flexible. It can operate with a minimum load rate of 50–60 percent (Verleysen et al., 2021; Wang et al., 2023). However, a more dynamic HB seems to be within reach, having the potential to reduce the minimum load range as low as 20–30 percent (Armijo & Philibert, 2020; Ikäheimo et al., 2018). As this is not easily viable at this stage, the minimum load for HB is set at 50 percent in the context of this thesis.

The ramp rate is also significantly less flexible compared to the two other production units.

The consensus for HB states a ramp rate (up and down) of approximately 20 percent per hour of capacity per hour. Exceeding this ramp rate can result in thermal changes that cause extensive damage to the catalyst (Armijo & Philibert, 2020; Verleysen et al., 2023; Wang et al., 2023). Hence, the ramp rate will be set to 20 percent per hour.

### 3.2.5 Replaceable parts

Within all production units, there is a certain level of degradation, resulting in parts needing replacement. Although there can be numerous parts, within the context of this thesis, they are limited to parts that require significant expenditure to be replaced and have a deteriorating effect on the production capacity.

For AE and HB, these components are the cell-stack and the catalyst, respectively. Both have an estimated lifetime of 80 000 hours, or approximately 10 years with maximum load (Fúnez Guerra et al., 2020; Matute et al., 2019; Yates et al., 2020). There are no comparable parts for the ASU.

The cell-stack in the AE is normally replaced when the efficiency is reduced below 90 percent (Matute et al., 2019). Using a linear approach given its estimated lifetime, a one percent degradation can therefore be applicable, which is the estimate Buttler and Spliethoff (2018) gave. However, Yates et al. (2020) stated a 0,1-0,5 percent depending on high or low degradation. Given the disparity of the estimations, a yearly degradation of 0,75 percent is utilised.

There are some variations in the replacement cost of the cell-stack. Fúnez Guerra et al. (2020) states a 30 percent cell-stack replacement cost of the initial AE capital expenditure (CAPEX), while Yates et al. (2020) states 40 percent. Matute et al. (2019) uses a different approach by estimating the replacement cost between 270 and 380 EUR per kW. In this thesis a 30 percent replacement cost of the AE CAPEX has been assumed based on the lower end of the provided literature.

Similarly, to the cell-stack, the replacement cost of the catalyst is estimated to be 30 percent of the initial CAPEX of HB (Fúnez Guerra et al., 2020). The most common causes of depredation of the catalyst are sintering and $O_2$ & $H_20$ poisoning (Attari Moghaddam & Krewer, 2020). The degradation rate for the catalyst is set at one percent degradation of the initial capacity annually.

### 3.2.6 CAPEX

Now that the description of the technical data has been provided, focus on the financial data is necessary. This subsection focuses on the CAPEX for the different production units and devise a method to scale the CAPEX depending on their production capacities.

**Alkaline Electrolyser**

One uncertainty within the field of green hydrogen production is the estimation of AE CAPEX. Parra et al. (2019) estimated a cost between 50 and 1 200 EUR/kW, whereas Cesaro et al. (2021) estimates the cost to be between 400 and 939 USD/kW for 2020 and between 264 and 834 USD/kW for 2025. In their own model, Armijo and Philibert (2020) used a CAPEX of 600 USD/kW for an electrolyser size of 60,2 MW [16]. However, Cesaro et al. (2021) utilised a 770 USD/kW for a 313 MW AE in their paper. Hence, there is considerable uncertainty related to the cost of the electrolyser.

According to Gutiérrez-Martín et al. (2015), there is a non-linear relationship between the size of the electrolyser and the investment cost up to a production capacity of 1 tonne of hydrogen per day (≈ 2 MW) for the AE. However, bigger AEs have a nearly linear relationship between cost and capacity. The article of Proost (2019) sought to outline the CAPEX of electrolysers to create guidelines and explain the trend of the market to policymakers. He showed a non-linear relationship between cost and capacity, where a 2 MW AE is estimated at 750 EUR/kW, while a 100 MW is estimated at 400 EUR/kW. Kuckshinrichs et al. (2017) emphasises a top-down engineering approach for the cost of AE using the formula:

$$I_x = I_{base} \cdot \left( \frac{Cap_x}{Cap_{base}} \right)^{\alpha} \tag{3.2}$$

| | | | |
|---|---|---|---|
| $I$ | is the investment CAPEX | $CAP$ | is the production capacity |
| $x$ | is the new capacity | $base$ | is the previous capacity |
| $\alpha$ | is the scaling parameter | | |

This is referred to as the "six tenths rule" when $\alpha$ is set to 0,6 (Abdin et al., 2022). However, Kuckshinrichs et al. (2017) utilised a higher $\alpha$ of 0,85. Adjusting the values

[16] Calculated based on values from their research paper.

given by Proost (2019) to be in USD[17] and using the formula and $\alpha$ from Kuckshinrichs et al. (2017), the following CAPEX is derived:

$$787,5USD/kWh \cdot 2.000kW \cdot \left(\frac{100MW}{2MW}\right)^{0,85} = 43.793.000USD \Rightarrow 438USD/kWh \quad (3.3)$$

With this approach, it is within the findings of Proost (2019). Hence, the higher $\alpha$ is justified when scaling CAPEX for the AE. For the context of this thesis, 2 MW at 787,5 USD/kWh will serve as the base case.

**Air separator unit**

In Section 3.2.3, it was stated that the ASU uses a negligible amount of energy compared to the AE. Hence, there are limited cost savings opportunities by taking advantage of the ASU's excess production capacity. However, if the production capacity of ammonia is increased, there must be sufficient nitrogen supply to avoid restricting the production process. Hence, increasing the production capacity of ASU is necessary.

Similarly to the AE, Devkota et al. (2023) used the Equation 3.2 to calculate the CAPEX for ASU using an $\alpha$ of 0,67. Given that Equation 3.2 is a common method to scale chemical facilities, it will also be used in this case with an $\alpha$ of 0,67. Given the use of the method, the base case must be identified.

In their paper, Cesaro et al. (2021) developed a base case to assess the cost of green ammonia. In this base case, a production capacity of 10 metric tonnes of ammonia per hour was developed. Utilising their case and the findings from Section 3.2.2, the minimum capacity required of the ASU can be established. Given that 82,3 percent of ammonia is nitrogen, and the total conversion rate is 97 percent, the minimum required production capacity of the ASU is: $\frac{10.000kg/h \cdot 0,823}{0,97}$ ≈8 500 kg/h. Additionally, they specified the CAPEX at 1450 USD/kg nitrogen per hour. These metrics will serve as the base case for the CAPEX calculations.

[17]Exchange rate of 1.05, based on past year average(Yahoo, n.d.-c)

**Haber-Bosch**

Similarly to the ASU, the HB uses an insignificant amount of energy compared to the AE. However, the HB process influences the required level of nitrogen and hydrogen depending on the ammonia production. Hence, increasing the capacity of the HB can affect the flexibility within the system, and an approach for estimating the appropriate CAPEX is required.

For the HB synthesis loop, there seems to be a non-linear relationship between production capacity and CAPEX. Based on the available literature, the estimate of CAPEX is between 3 000 and 4 500 USD/kg of ammonia per hour (Ikäheimo et al., 2018). In order to determine the appropriate scaling properties of CAPEX for the HB process, two case studies are examined. Ikäheimo et al. (2018) utilised a CAPEX of 3 150 USD[18]/kg ammonia per hour for a system that produced 300 tonnes of ammonia per day (or 12 000 kg/h), while Cesaro et al. (2021) utilised a CAPEX of 3 300 USD/Kg ammonia per hour for a production capacity of 10,000 kg/h. By using the parameters from Cesaro et al. (2021) as the base case and the parameters from Ikäheimo et al. (2018) as the new capacity in the Equation 3.2, the following alpha is found:

$$3.300 USD/kg/h \cdot 10.000 kg/h \cdot \left(\frac{12,5}{10}\right)^{\alpha} = 3.150 USD/kg/h \cdot 12.500 kg/h \tag{3.4}$$

$$\Rightarrow \alpha \approx 0,79 \tag{3.5}$$

### 3.2.7 OPEX

Lastly, the OPEX for the production units will be explored. These include all cost related to production that has not been mentioned, such as rent, insurance, maintenance, labour etc. However, the energy cost will be excluded from OPEX, given the nature of this thesis.

**Alkaline Electrolyser**

Given the circumstances around the AE, the OPEX can range between 2 and 7 percent of CAPEX per year for AE greater than 1 MW. However, a narrower range of 2 to 5 percent is often considered as reliable. An OPEX of 3,5 percent is therefore employed (Buttler & Spliethoff, 2018; Parra et al., 2019).

[18] 3000 EUR/kg $NH_3$/h at an exchange rate of 1,05 (Yahoo, n.d.-c)

**Air Separator Unit and Haber-Bosch**

OPEX for ASU and HB are assumed to be lower compared to the ASU. Ikäheimo et al. (2018) assumed an OPEX of 2 percent of CAPEX per year for both the ASU and HB, which will also be utilised in this thesis.

## 3.3 Intermediate Storage Units

Intermediate storage units are introduced to give production units greater flexibility. With the introduction of storage units, excess production of process mediums can be stored from periods of low electricity costs to periods of high electricity costs, potentially mitigating higher production costs. Hence, technical, and financial descriptions of the intermediate storage units are necessary. Given that ammonia storage does not aid in the flexibility of ammonia production, it is exempt from this analysis.

### 3.3.1 Energy consumption

Ikäheimo et al. (2018) stated that hydrogen storage is estimated to consume 2,2–3,0 kWh/kg of hydrogen. Given the use of steel tanks as highlighted in Section 2.2.2, a value of 2,5 kWh/kg hydrogen is utilised for the work in this thesis.

Within the literature on green ammonia production, the mention of the energy requirement of storing nitrogen is limited. Both Armijo and Philibert (2020) and Ikäheimo et al. (2018) excluded it from their paper. To be comparable with the available literature, it is assumed that the energy requirement is encapsulated within the OPEX.

### 3.3.2 CAPEX and OPEX

Lastly, both the CAPEX and OPEX for the intermediate hydrogen and nitrogen storage are to be examined.

**Hydrogen**

Hydrogen storage CAPEX ranges from 200 to 1 500 USD/kg, depending on the scale and pressure. As mentioned, steel tanks are selected for intermediate hydrogen storage as they are easily available. The downside is its higher CAPEX. There is a case for salt caverns to be used, however, they are less flexible as they can only charge or discharge 0,33 percent

each hour to avoid rapid pressure change giving tension to the walls (Fasihi et al., 2021). In the model created by Armijo and Philibert (2020), 500 USD/kg was utilised for half a day's worth of hydrogen production. Given the base case of ammonia production selected in Section 3.2.6 of 10 000 kg/h, this would constitute a capacity of 21 240kg (10 000 kg/h $\cdot$ 0,177 $\cdot$ 12h).

As Equation 3.2 is established as the common way of scaling CAPEX of chemical facilities, this will be utilised for the intermediate hydrogen storage. However, a more conservative approach is considered, using a higher $\alpha$ at 0,7 instead of 0,6.

Lastly, it is assumed that storage has an OPEX of approximately one percent of CAPEX per year. (Armijo & Philibert, 2020)

**Nitrogen**

Nitrogen storage is an existing part of the ASU, with a capacity of one day's worth of production. Hence, both the CAPEX and the OPEX are encapsulated within the CAPEX and OPEX of the ASU presented in Sections 3.2.6 and 3.2.7 respectively. (Armijo & Philibert, 2020)

## 3.4 Electricity prices

According to the Section 3.2.3, significant usage of electricity is needed to produce ammonia, especially for the AE. Hence, the cost of electricity is an essential cost factor that must be considered. This section will discuss the raw data, the methods used for data aggregation, and the data that will be employed in our model.

### 3.4.1 Raw data

As highlighted, incorporating the cost of electricity is crucial due to the energy quantity necessary for ammonia production. Given the focus on Denmark, the day ahead electricity prices is gathered from Nord Pool (2023). Within Denmark, there is also two different electricity markets, DK1 (west) and DK2 (east). With the predominance of ammonia production set to be built on the west coast (Ministry of Foreign Affairs of Denmark, n.d.-b), DK1 was chosen. Additionally, determining the time period to the data set is necessary. In 2015, 89 percent of the energy was produced domestically (Danish Energy

Agency, 2017), making it a useful starting point for the data. Additionally, both 2021 and 2022 was impacted by unprecedented events, with the impact of COVID and its rapid economic recovery, and Russian withholding gas supplies from Europe months before the invasion of Ukraine (IEA, n.d.). Therefore, these years have been excluded from the data used in this thesis. The raw data structure for year 2020 is presented in table 3.1:

| **Hour** | **Day** | **Month** | **Year** | **SpotPrice €/MWh** |
|---|---|---|---|---|
| 1 | 1 | 1 | 2020 | 33,420 |
| 2 | 1 | 1 | 2020 | 31,770 |
| 3 | 1 | 1 | 2020 | 31,570 |
| ... | ... | ... | ... | ... |
| 1 | 2 | 1 | 2020 | 30,780 |
| 2 | 2 | 1 | 2020 | 30,640 |
| 3 | 2 | 1 | 2020 | 30,430 |
| ... | ... | ... | ... | ... |
| 1 | 3 | 1 | 2020 | 18,930 |
| 2 | 3 | 1 | 2020 | 9,980 |
| 3 | 3 | 1 | 2020 | 1,530 |
| ... | ... | ... | ... | ... |
| 24 | 31 | 12 | 2020 | 52,26 |

**Table 3.1:** Historical electricity price structure

These values are then first adjusted for inflation[19] and converted to USD/MWh[20]. Below are the descriptive statistics after applying the adjustments.

| Year | Min | 25% Quantile | Median | Mean | 75% Quantile | Max | St.dev |
|---|---|---|---|---|---|---|---|
| 2015 | -32.49 | 15.45 | 24.51 | 23.69 | 28.33 | 103.2 | 11.52 |
| 2016 | -55.32 | 21.81 | 25.58 | 27.55 | 33.2 | 108.29 | 10.05 |
| 2017 | -51.04 | 27.51 | 30.73 | 30.7 | 34.62 | 122.41 | 10.89 |
| 2018 | -15.18 | 36.01 | 44.72 | 44.58 | 52.89 | 146.03 | 15.25 |
| 2019 | -48.49 | 32.54 | 38.94 | 38.69 | 46.2 | 109.91 | 13.2 |
| 2020 | -58.8 | 12.38 | 23.895 | 25.04 | 35.87 | 200.04 | 17.42 |

**Table 3.2:** Summary statistics of historical electricity prices (USD/MWh)

### 3.4.2 Aggregating data

According to Teichgraeber and Brandt (2022), the increase in RE has highlighted the importance of handling time-varying data for optimisation studies in energy systems. They further elaborated that the use of representative time periods could help reduce the

[19]CPI of 100 in 2020 is used to adjust the electricity prices (Statistics Denmark, n.d.)
[20]Exchange rate of 1,05, based on past year average(Yahoo, n.d.-c)

computational requirement by upwards of two orders of magnitude. Given that there are 8 760 hours to solve for a year, totalling over 200 000 hours for multiple decades, the use of representative time periods is required.

Although they are necessary, the consequences of using representative time periods must be understood. Teichgraeber and Brandt (2022) highlighted that the aggregated data will always contain statistical errors, affecting the optimisation outcome. This will either lead to systematic bias or increased variation in the results. Therefore, an investigation into which error occurred should be performed (Teichgraeber & Brandt, 2022).

Secondly, an evaluation of the duration of the time periods must be performed. If the representative time period is too long, then it would require high amounts of computational power. Whereas if the representative time period is too small compared to the total time period, then it would lead to inaccuracies in the results. (Teichgraeber & Brandt, 2022)

The last challenge to be highlighted is how the representative time periods will be linked. Although some links may be ignored, others cannot. For example, storage will have a cumulative effect between the representative time periods; hence, appropriate modelling should be performed. (Teichgraeber & Brandt, 2022)

To determine which representative time periods will be selected, the method of Strømholm and Rolfsen (2021) will be applied. They averaged different time periods based on the hour of the day to look for trends.

#### Daily variation

The first variation to be analysed is the daily variation within a day. Hence, the entire data set is aggregated into a day based on their respective hours of the day:

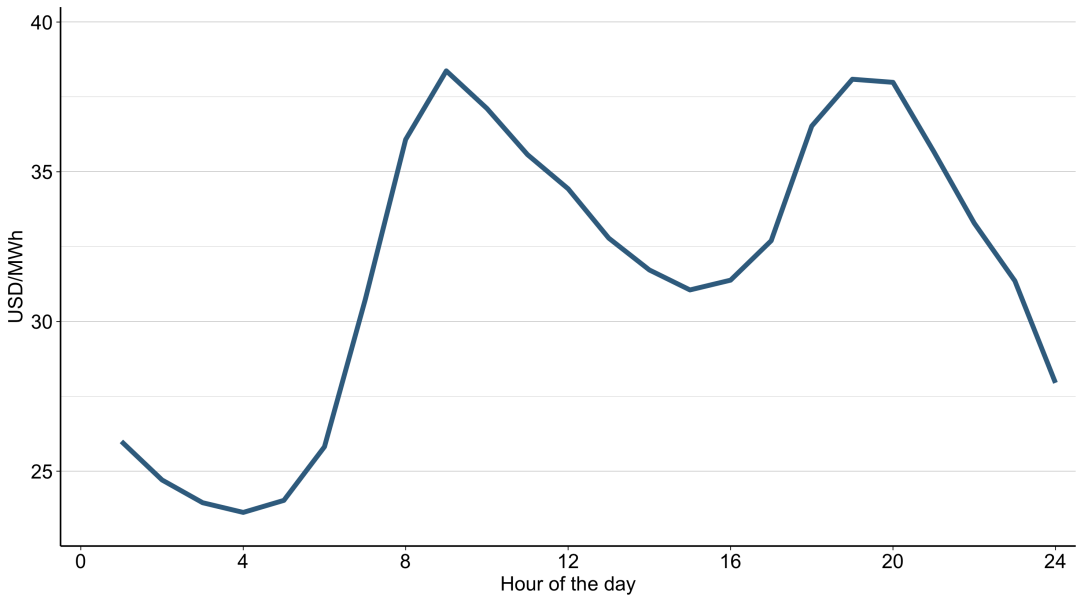


**Figure 3.1:** Average USD/MWh throughout the day (2015-2020)

The graphs illustrate variations throughout the different hours of the day. The prices are lower during the night and higher during the day. This correlates well with the routine of the general public. Hence, within the representative time period, daily variations should be included.

### Weekdays variation

The second variation to be analysed, is between weekdays and their respectable hours.

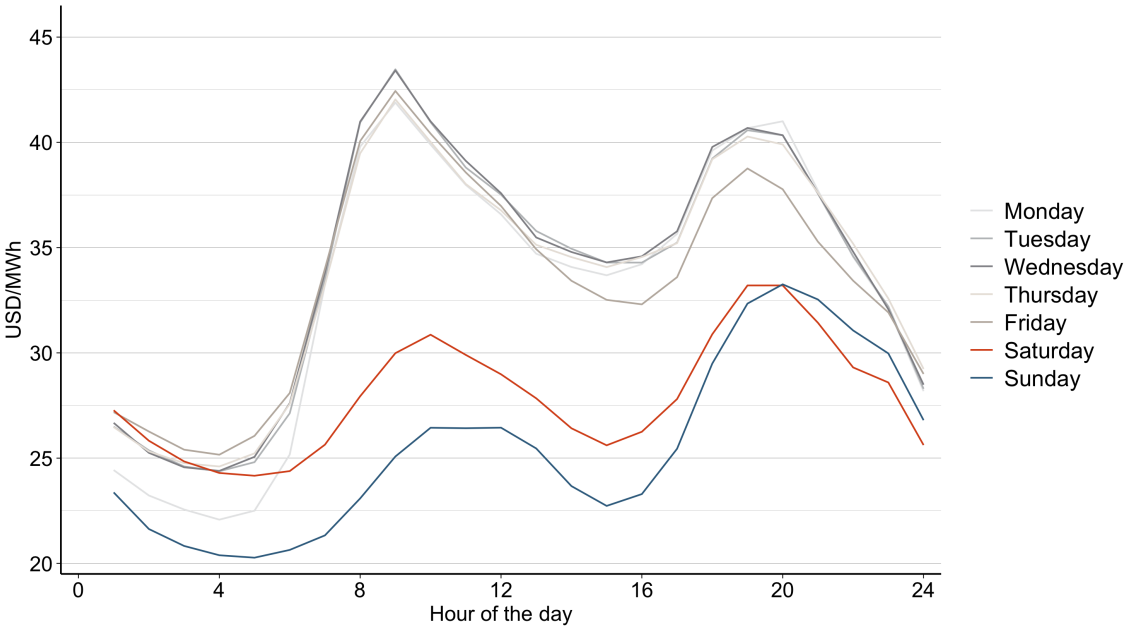


**Figure 3.2:** Average USD/MWh for each weekday (2015-2020)

The daytime differences between weekdays and weekends are evident. The weekdays

illustrate higher prices compared to weekends; however, prices tend to converge during the night. The variation between weekdays and weekends might be related to the difference in business activity. Additionally, there is also variation between Saturday and Sunday, with higher prices on Saturday during the day. Given the differences between weekdays and weekends, the variation should be included in the representative time period.

### Seasonal variation

Lastly, the difference between seasons of the year will be considered.

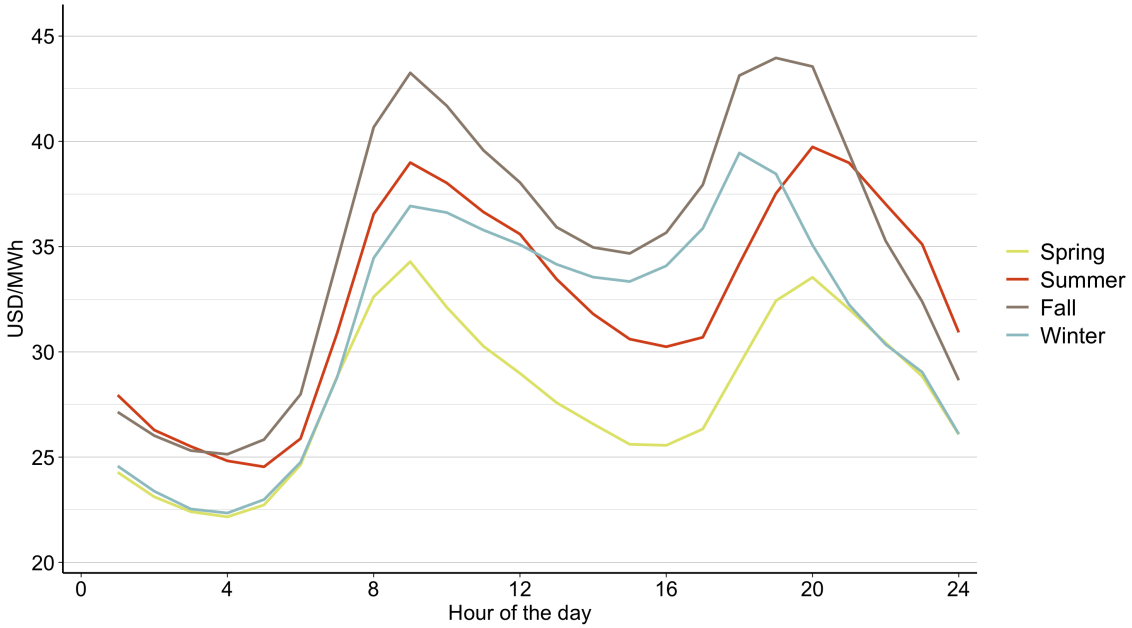


**Figure 3.3:** Average USD/MWh for average seasonal day (2015-2020)

The different seasons have similar characteristics but differ in their price levels. Prices during the winter are, on average, less expensive than in the autumn. The reasons for these findings are uncertain but will not be investigated further due to the scope of this thesis. Another observation is that spring is the cheapest of the seasons. Due to the difference illustrated, seasonal variation should be included in the representative time periods.

### Selecting representative time period

With the variation between different time periods being examined, the selection of representative time periods is feasible. From the discussion, the daily variation, the difference between weekdays and weekends, and the seasonal variation should be included.

One approach to select a representative time period is to limit each season to a single

weekday, Saturday and Sunday. Although the computational requirement is being reduced, it might be too short compared to the season it represents, reducing accuracy in the result. Another selection can be a representative week for each quarter. This includes all the aforementioned variations, and the duration appears to be appropriate, given it will represent 13 weeks within the yearly season.

To reduce model complexity, hours of the week are used instead of hours of the day. Hence, hours 1 to 24 represent Monday, 25 to 48 represent Tuesday, etc. Utilising this approach, the quantity of time periods reduces from 8 760 to 672 ($24 \cdot 7 \cdot 4$) per year. The effects of aggregating the data are illustrated in Figure 3.4.

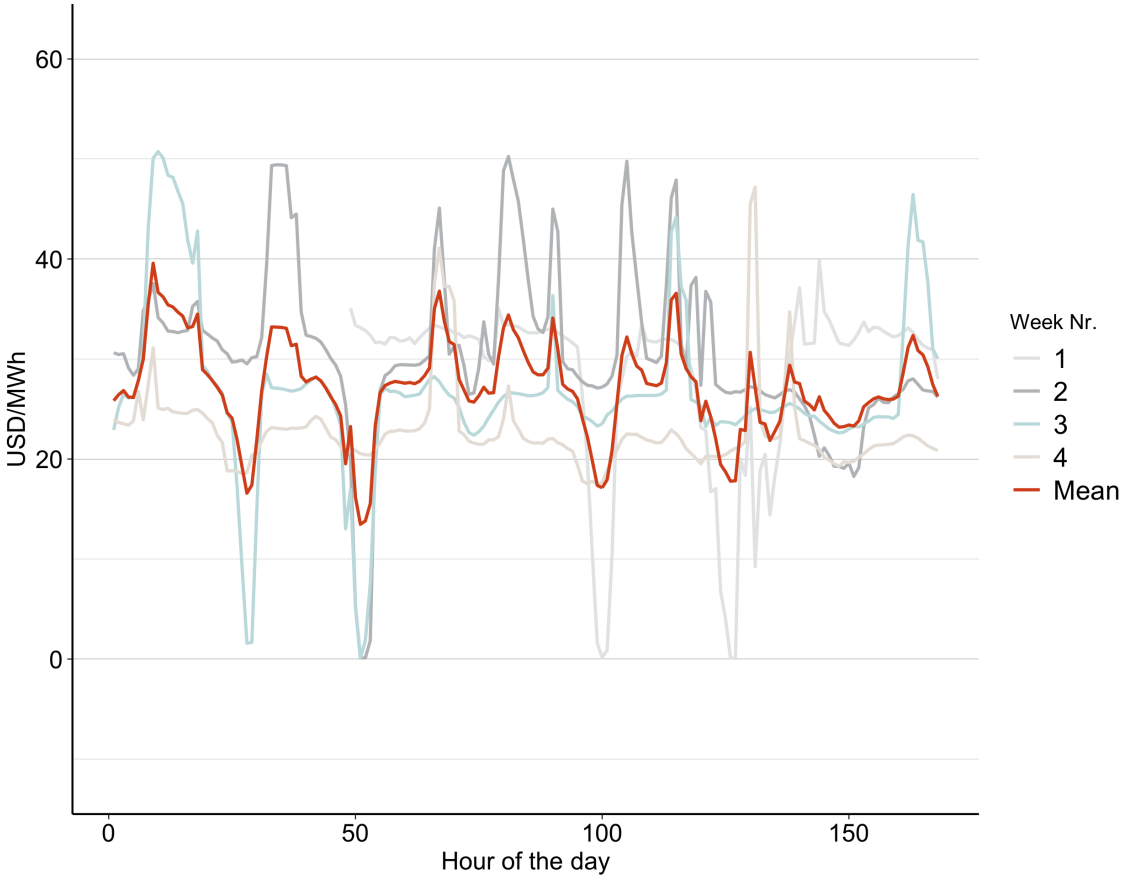


**Figure 3.4:** Aggregated data for the winter of 2020

The most evident effect is the removal of extreme prices, both high and low. Although they are removed, they also influence the aggregated data to become more volatile compared to the weeks that are not volatile. Hence the net effect of this must be explored and adjusted for.

### 3.4.3 Sampling of data

After establishing the representative time periods, the selection of future electricity prices may begin. In Section 3.2.1, the 30-year lifetime of the system was established. For sampling data, Strømholm and Rolfsen (2021) approach will be applied, where forecasted values are provided by an independent organization and the variation from the representative time period was incorporated to the forecasted values.

For this analysis, the forecasted values of electricity prices are gathered from Energistyrelsen (n.d.-a). These include a base price for the years 2030, 2040, and 2050 in addition to an hourly forecast for the year 2024[21]. To be comparable, the average of all the forecasted values for the year 2024 was selected as the base number.

For the sample, year 2024 will be the base price for the first three years; year 2027 is going to be for the next three; year 2030 will be the base price for years 6 to 12, year 2035 will work for years 13 to 21, and lastly, the forcasted values from 2045 will be the base price for the last nine years. Since these forecasted values were not provided, a linear relationship between the years Energistyrelsen (n.d.-a)[22] provided and the selected years will be utilised. Table 3.3 shows these values:

| Year | Spot Price (USD/MWh) |
|---|---|
| 2024 | 58.71 |
| 2027 | 60.86 |
| 2030 | 62.86 |
| 2035 | 57.86 |
| 2045 | 50.00 |

**Table 3.3:** Forecasted spot price

It should be noted that these forecasted values are approximately 1.8 times higher[23] compared to the historical values from NordPool. Resulting in increased cost of green ammonia production.

With the base price for all years established, variations from the representative weeks can be incorporated. This is achieved by subtracting the mean from the aggregated prices to centre them around zero, as illustrated in Figure 3.5. Then they are added to the

[21] Converted from DKK/MWh to USD/MWh based on the median exchange rate over the past year at 7 DDK per USD (Yahoo, n.d.-b)

[22] To see the linear relationship between the forecasted values, go to Appendix C: Forecasted Values

[23] The higher prices will not be explored due to the scope of this thesis

forecasted values provided in Table 3.3.

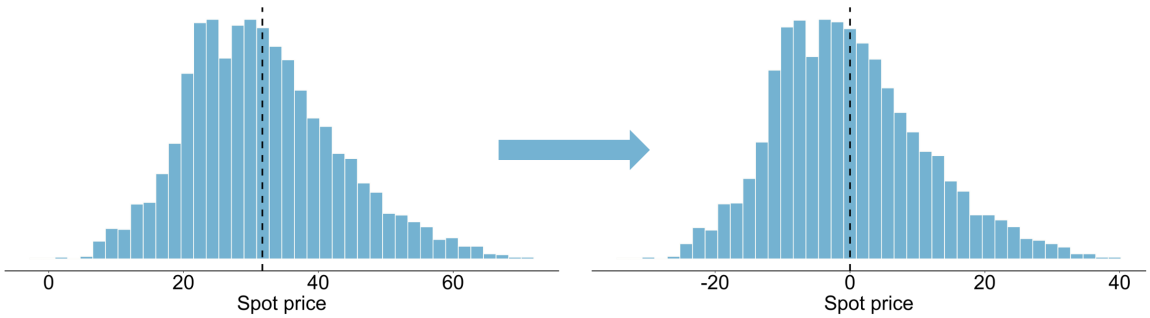


**Figure 3.5:** Centre variation around zero

To prevent selection bias, arbitrary selection using a uniform distribution is implemented. Given the limited selection of six years to cover 30 years in the model, representative years are used. This implies that for every year that is selected, they now represent three. Although each selection will have a higher impact on the result, they still cover approximately the same number of years as if they were selected 30 times. Additionally, it further reduces the computational requirement.

From the previous section, the net effect of removing extreme prices and the influence it has on periods with low volatility will be explored. The method used to find the net effect, is by comparing the Coefficient of Variation (CV) that measures the degree of variation relative to its mean (Hayes, 2023). Hence, the equation is as follows:

$$CV = \frac{\sigma}{\mu} \cdot 100 \tag{3.6}$$

The following table presents the different standard deviations, means and the CV for the historical and aggregated data set.

| Data | $\sigma$ | $\mu$ | CV |
|---|---|---|---|
| Historical | $15,944$ | $32,779$ | $48,64$ |
| Aggregated | $11,644$ | $32,764$ | $35,54$ |

**Table 3.4:** CV: Historical vs. Aggregated data

By aggregating historical data, the variation is reduced, as displayed by the CV values in Table 3.4. To adjust for the reduction, the variation centred around zero shown in Figure 3.5 is multiplied by 1,4 ($\approx \frac{48,64}{35,54}$) to resemble historical values more closely. These values are the base case for the analysis.

Although the values are adjusted, there are also other considerations to be made. Firstly, the future variations might not resemble the historical ones. Hence, different adjustments are prepared for both an increase of 20 percent and 60 percent. Additionally, the extreme values are not being reintroduced by the increase of 40 percent. Hence, one scenario of a 200 percent increase is created. It is not believed that this variation will stay this high, but the scenario was created to test what would be beneficial during longer periods of extreme variation. These other scenarios are illustrated in Figure 3.6

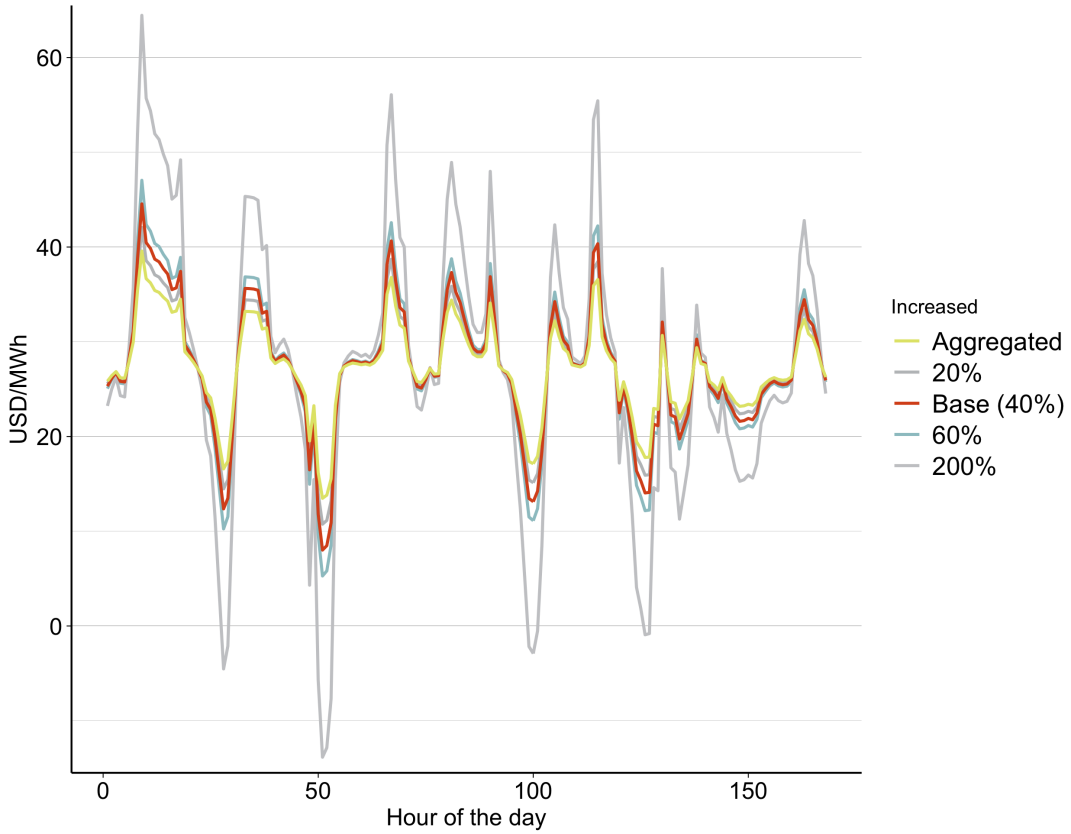


**Figure 3.6:** Volatility comparison

### 3.4.4 Grid fees

Utilising the grid incurs additional expenses, labelled grid fees. These are broken down into three categories: consumption tariffs, system tariffs, and balance tariffs(Energinet, 2022). Due to recent changes[24], these are all linear regardless of the amount of electricity used. These changes will result in consumers paying approximately 25 percent less per kWh and paying an additional annual charge of 180 DKK, which is not included due to its negligible cost. Table 3.5 breaks down the grid fees(Energinet, 2022):

[24]These changes are to be evaluated after six years to determine if they should be prolonged (Energinet, 2023)

| **Grid fees** | **USD per MHw** |
|---|---|
| Transmission grid tariff[25] | 7,00 |
| System tariffs[26] | 5,14 |
| Balance tariffs for consumption[27] | 0,33 |
| Total grid fees | 12,47 |

**Table 3.5:** Grid fees with updated system tariffs

## 3.5 Weighted Average Cost of Capital (WACC)

WACC is utilised to discount both cost and the ammonia produced. Cesaro et al. (2021) estimated it to be between 4.5-10 percent, but that the common WACC to utilize is 7,5 percent for the OECD countries. WACC is based upon the weighted cost of equity and debt (Hargrave, 2023). The cost of equity is made up of the risk-free rate, $\beta$, and the market premium (Kenton, 2023). Hence the WACC formula before tax looks like this:

$$WACC_{pre-tax} = (1 - D) \cdot (RF + \beta_e \cdot MP) + D \cdot R_D \tag{3.7}$$

| | | | |
|---|---|---|---|
| $D$ | is ration financed by debt | $\beta_e$ | is the unlevered beta |
| $RF$ | is the risk-free rate of equity | $MP$ | is the market premium |
| $R_D$ | is the cost of debt | | |

NVE (2023) establishes a basis for 60 percent debt financing, whereas Ofori-Bah and Amanor-Boadu (2023) investigated various financing schemes. They determined a financing arrangement with 25 percent debt was the most optimal given all the stakeholders involved. On the basis of this thesis, a higher debt financing rate of 30 percent is used.

For the risk-free rate, the 10-year Treasury rate will be utilised (The Investopedia Team, 2022). Yahoo (n.d.-a) monitors the yield daily, where it has fluctuated between 2,8 percent and 4,3 percent over the past year. Though volatility for the risk-free rate is recognised, a yield of 3,5 percent is chosen. For the $\beta$, the unlevered estimate of 0.83 for green and renewable energy is used (Damodaran, 2023). Regarding the market premium, PWC (2022) rate of 5 percent is selected. For the cost of debt, a rate of 6,6 percent is assumed. Given these parameters and the equation, a WACC of 7,3 percent is obtained. This is also consistent with the literature.

[25] 49 DKK/MWh
[26] 36 DKK per MWh
[27] 2,29 DKK per MWh

# 4 Mathematical Optimization Model

This chapter will first introduce an overview of the model in Section 4.1 to better understand its components and connections. Then the assumptions for the optimisation model are established in Section 4.2. Following the assumptions, the different sets, parameters, and decision variables will be described in Section 4.3, 4.4 and 4.5 respectively. The features of the ammonia process are described as constraints in Section 4.6. The objective function for this thesis combines some of the concepts used in the different constraints and is highlighted in Section 4.7. Then an outline for how LCOA is calculated based on the parameters in Section 4.8. Lastly, a clarification of why a simplification of the model was necessary is described in Section 4.9

## 4.1 Model introduction

We created a model in order to analyse how increased flexibility in the ammonia production process can exploit on the fluctuations in electricity prices. To gain meaningful results, features closely resembling those of the process must be implemented. To accomplish this objective, a multi-period, mixed integer linear programming model (MILP) were used, with the objective of minimising costs.

To understand the structure of the model, a flowchart illustrating its activities is constructed based on the information gathered. To simplify the model, the internal functions of each machine are represented as a single entity.

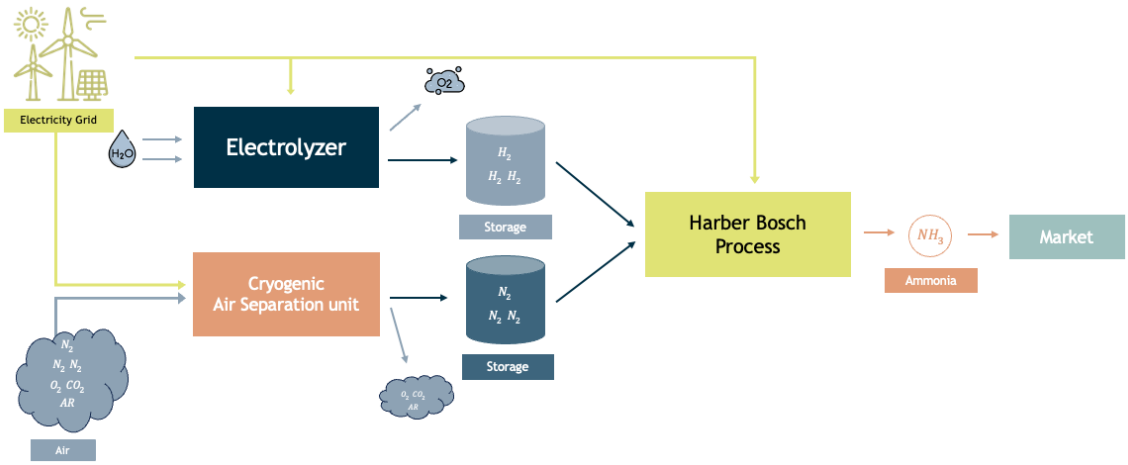


**Figure 4.1:** Model visualisation

The model consists of three machines and two intermediate storages also labelled buffers. The process begins with AE converting water into hydrogen and oxygen. The oxygen produced is disregarded, as it serves no purpose of the analysis, while the hydrogen is transported to the buffer. Parallel to the AE, the ASU separates nitrogen from the air and subsequently transport it to a buffer. The remaining gases are discarded since they do not contribute to the analysis. Hydrogen and nitrogen are then both sent from their respective buffer to the HB where ammonia synthesis takes place. The ammonia produced is then shipped to market. All machines and buffers get their energy from the electrical grid.

As previously stated in Section 3.4.2 about aggregating data, representative weeks and years are utilized. Both these initiatives are performed to reduce the computational requirement. To effectively investigate whether flexibility can utilise electricity fluctuation to reduce LCOA, production and buffer capacity are explored along with modifications to the individual machines. Consequently, the model must be executed multiple times.

## 4.2 Model assumptions

Prior to defining the model, it is essential to address the assumptions needed to be made. Each assumption will be presented, followed by an explanation for its rational.

The first assumption made is the need to fulfil a yearly demand. The motive behind an annual demand is to enhance the system's ability to leverage flexibility to take advantage of favourable electricity prices rates. The demand is based on an hourly rate and assumed to be 10 000 kg per hour, as stated in the base scenario provided in section 3.2.6. As a result, the annual demand is 87 360 000 kg ($10.000kg \cdot 24 \cdot 7 \cdot 13 \cdot 4$). Using annual demand neglect seasonality and will be seen as a limitation to the analysis.

The second assumption is that ammonia is sold directly to the market from the production process. As a result, the model determines the timing of ammonia acquisition by the market. Given the model's objective of cost reduction, these periods will be the most advantageous and not the basis of the acquirer. This reduces cost as it eliminates the need of ammonia storage capabilities. This assumption will therefore serve as a limitation for the analysis.

Another assumption is that both the HB, and ASU will operate continuously. As highlighted in Section 3.2.3, HB is only stopped for maintenance purposes. Another justification for this assumption stems from the computing resources required, as further explained in Section 4.9.

An additional assumption involves degradation of ASU. Due to the absence of a component similar to the cell restack or the catalyst, it is assumed that the degradation issue is addressed through OPEX.

## 4.3 Sets

With the introduction of the model, clarification of sets and their elements will be provided. The model works on an hourly basis, derived from the electricity price data in Section 3.4.2. Furthermore, the use of representative weeks necessitates the need for a quarterly set. To distinguish all quarters, a set of years is introduced. Section 4.1 states the use of representative years, which adds an additional time set. Since wearable parts need replacement, a set indicating the time of their replacement is necessary. Lastly, a set of process mediums differentiates the machines and buffers.

| Set | Description | Values |
|---|---|---|
| $Y$ | Set of years | (1, 4, 7, ..., 28) |
| $G$ | Replication of years | (0, 1, 2) |
| $Q$ | Set of quarters | (1, 2, 3, 4) |
| $H$ | Set of hours within a week | (1, 2, ..., 168) |
| $R$ | Replacement of wearable parts | (11, 21) |
| $K$ | Set of process mediums | ($H_2$, $N_2$, $NH_3$) |

**Table 4.1:** Model set description

Set $Y$ begins at year one and has an interval of three, demonstrating that each year is replicated three times. The cardinality of the set represents the number of representative years. This necessitates the set $G$, which states how many times each year has been replicated. Element 0 indicates the representative year; 1 is the first time the year is replicated, and 2 is the second time the year is replicated. Hence, the representative year is repeated three times. Quarters are denoted as numbers in set $Q$, where one and four correspond to spring and winter, respectively. Elements of $H$ are the hours within the representative week. The model neglects the use of days, which are incorporated

based on the hour of the week. For instance, hours 1 through 24 are Monday, hours 25 to 48 are Tuesday, and so forth. The elements within set $R$ represent the years that the wearable parts are replaced. Lastly, the set $K$ contains the chemical notation of each process medium.

## 4.4 Parameters

Having established the necessary sets for the model, the parameters established in Section 3 can be defined. Distinct categories are created due to the volume of parameters needed to comprehend their application.

**General Parameters**

These parameters can be applied to multiple optimisation models and are not specific to this thesis.

| Parameter | Description | Unit |
|---|---|---|
| $M$ | Big M parameter | Int |
| $P$ | Number of weeks within a season | Int |

**Table 4.2:** General parameters

**Production and buffer parameters**

These are the parameters associated with the technical specifications of production and buffer, which allows the model to resemble reality.

| Parameter | Description | Unit |
|---|---|---|
| $NRG_k$ | Energy consumption per kg produced | kWh/kg |
| $SNRG_k$ | Energy consumption per kg stored | kWh/kg |
| $PropSB_k$ | % of nominal energy consumption when on standby | % |
| $PropCS_k$ | Energy consumption per ton of daily production capacity | kWh |
| $MinU_k$ | Minimum utilization of equipment in % of capacity | % |
| $TotCap_k$ | Original production capacity | kg/h |
| $CapRed_{k,y}$ | Production capacity reduction due to degradation of wearable parts | % |
| $Vol_k$ | Total capacity of buffers | kg |
| $d$ | Yearly demand of $NH_3$ | kg |

**Table 4.3:** Production and buffer parameters

$CapRed_k, y$ is based on the annual degradation due to the replacement parts as highlighted in Section 3.2.5. However, annual degradation is not possible with the use of representative

years. To address this discrepancy, the three-year average represented by the corresponding representative year will be utilised. For example, in year 4 (representing year 5 and 6) the degradation equals $\frac{4\%+5\%+6\%}{3} = 5\%$.

On top of the production and buffer parameters provided, additional parameters must be supplemented. These require calculation and are therefore in its own table.

| Eq | Formula | Sets | Description |
|---|---|---|---|
| (4.4.1) | $Cap_{k,y} = TotCap_k \cdot (1 - CapRed_{k,y})$ | $\forall k \in K$ $\forall y \in Y$ | Maximum production capacity for each time period |
| (4.4.2) | $MinL_{k,y} = Cap_{k,y} \cdot MinU_k$ | $\forall k \in K$ $\forall y \in Y$ | Minimum load while producing |
| (4.4.3) | $SBNRG_k = TotCap_k \cdot NRG_K \cdot PropSB_k$ | $\forall k \in K$ | Standby energy consumption |
| (4.4.4) | $CSNRG_k = \frac{TotCap_k \cdot 24h}{1000kg} \cdot PropCS_k$ | $\forall k \in K$ | Energy consumption of cold start based on tonne production capacity per day |

**Table 4.4:** Production and buffer parameter calculations

Equation (4.4.1) introduces the parameter $CAP_{k,y}$, which closely resembles $TotCAP_k$. However, $TotCap_k$ represents the initial capacity, whereas $CAP_{k,y}$ includes degradation. $MinL_{k,y}$ in equation (4.4.2) indicates the minimum load in kilograms, whereas $MinU_k$ indicates the minimum percentage of capacity. Similarly, $SBNRG_k$ (equation (4.4.3)) displays the kWh as opposed to the percentage $PropSB_k$ signifies. Lastly, $CSNRG_k$ in equation (4.4.4) illustrates the energy consumption to perform a cold start, while $PropCS_k$ is the energy consumption per tonne of daily production.

### Haber-Bosch specific parameters

Specific technical parameters are only applicable for the HB; hence, they will not be generalised for the other machines.

| Parameter | Description | Unit |
|---|---|---|
| $Prop_k$ | Proportion of each process medium in ammonia | % |
| $Conv$ | Conversion rate of $H_2$ and $N_2$ to $NH_3$ | % |
| $MPCP$ | Maximum production change of nominal production | % |

**Table 4.5:** Haber Bosch specific parameters

Similarly to the production and buffer parameters, there are HB parameters that require calculation.

| Eq | Formula | Sets | Description |
|---|---|---|---|
| (4.6.1) | $MPC_y = Cap_{NH_3,y} \cdot MPCP$ | $\forall y \in Y$ | Maximum production change in kg for HB |

**Table 4.6:** Haber Bosch parameter calculations

Equation (4.6.1) introduces $MPC_k$, which specifies the maximum change of production in kg between production hours in contrast to $MPCP$ which is in percentage.

### Financial parameters

In addition to the technical parameters, a financial parameter is necessary to calculate the cost of ammonia production.

| Parameter | Description | Unit |
|---|---|---|
| $BSize_k$ | Base case of production capacity | kg |
| $BVol_k$ | Base case of storage capacity | kg |
| $BCAPEX_k^U$ | Base case unit CAPEX | USD |
| $BCAPEX_k^B$ | Base case buffer | USD |
| $OPEXP_k^U$ | OPEX for production units as % of CAPEX | % |
| $OPEXP_k^B$ | OPEX for buffer as % of CAPEX | % |
| $\alpha_k^U$ | Scaling parameter for production units CAPEX | Float |
| $\alpha^B$ | Scaling parameter for buffer CAPEX | Float |
| $RPRCP_k$ | Wearable parts replacement costs % of CAPEX | % |
| $ELC_{y,q,h}$ | Electricity prices | USD/kWh |
| $GF$ | Grid fees | USD/kWh |
| $WACC$ | Weighted average cost of capital | % |

**Table 4.7:** Equipment and intermediate storage cost parameters

All except $RPRCP_k$, $ELC_{y,q,h}$, $GF$ and $WACC$ are used to find the CAPEX for the different machines and buffers utilising Equation 3.2. There are different $\alpha$ for scaling the units and storage. Additionally, $\alpha$ for storage is only applicable to hydrogen buffer. Section 3.3.2 highlighted the absent of ammonia storage and that the CAPEX of the nitrogen buffer was encapsulated by the ASU CAPEX.

## 4.5 Decision variables

Following the overview of sets and parameters, the subsequent step is defining decision variables. These variables include production, storage, and extraction of buffers. To ensure continuity of storage between representative weeks, an additional variable is included. Lastly, machine states variables create more flexibility to the model.

| Parameter | Description | Unit |
|---|---|---|
| $x_{k,y,q,h}$ | Process medium produced | kg |
| $s_{k,y,q,h}$ | Process medium stored | kg |
| $z_{k,y,q,h}$ | Process medium extracted | kg |
| $\Delta s_{k,y,q}$ | End-of-week cumulative net difference between production and extraction | kg |
| $idle_{k,y,q,h}$ | Whether the machine is idle (1) or not (0) | Binary |
| $sb_{k,y,q,h}$ | Whether the machine is on standby (1) or not (0) | Binary |
| $cs_{k,y,q,h}$ | Whether the machine is doing a cold start (1) or not (0) | Binary |

**Table 4.8:** Decision variables

The time period between representative weeks is non-existent within the model, necessitating a method to ensure storage continuity. Hence, the variable $\Delta s_{k,y,q}$ is created. It's defined as the net difference between production and extraction within a week. Multiplying it $P$ times reveals the cumulative difference of the quarter, connecting subsequent representative weeks.

## 4.6 Constraints

With the definition of sets, parameters, and decision variables, the construction of constraints can commence. The objective function will be defined at a later stage, incorporating a combination of concepts defined in this subsection. Similarly to parameters, constraints are divided into the categories they represent.

### Production constraints

These constraints are associated with the technical capabilities of all units.

| Eq | Constraint | Sets | Description |
|---|---|---|---|
| (4.9.1) | $x_{k,y,q,h}, \quad s_{k,y,q,h}, \quad z_{k,y,q,h} \geq 0$ | $\forall k \in K$<br>$\forall y \in Y$<br>$\forall q \in Q$<br>$\forall h \in H$ | Non-negativity constraint |

| Eq | Constraint | Sets | Description |
|---|---|---|---|
| (4.9.2) | $x_{k,y,q,h} \leq (1 - idle_{k,y,q,h} - sb_{k,y,q,h} - cs_{k,y,k,q}) \cdot M$ | $\forall k \in K$ $\forall y \in Y$ $\forall q \in Q$ $\forall h \in H$ | No production while equipment is in no-production mode |
| (4.9.3) | $x_{k,y,q,h} \leq Cap_{k,y}$ | $\forall k \in K$ $\forall y \in Y$ $\forall q \in Q$ $\forall h \in H$ | Maximum production capacity for each time period |
| (4.9.4) | $x_{k,y,q,h} \geq MinL_k - (idle_{k,y,q,h} + sb_{k,y,q,h} + cs_{k,y,q,h}) \cdot MinL_k$ | $\forall k \in K$ $\forall y \in Y$ $\forall q \in Q$ $\forall h \in H$ | Must at least have the minimum load of nominal production while the machine is in producing mode |
| (4.9.5) | $idle_{k,y,q,h} + sb_{k,y,q,h} + cs_{k,y,q,h} \leq 1$ | $\forall k \in K$ $\forall y \in Y$ $\forall q \in Q$ $\forall h \in H$ | Equipment can only be in one state at a time |
| (4.9.6) | $cs_{H_2,y,q,h} \geq idle_{H_2,y,q,h-1} + idle_{H_2,y,q,h}$ | $\forall y \in Y$ $\forall q \in Q$ $\forall h \in H$ $h > 1$ | AE cold start will happen if the last hour was idle, and the current is not |
| (4.9.7) | $cs_{H_2,y,q,h_1} \geq idle_{H_2,y,q-1,\lvert H\rvert} + idle_{H_2,y,q,h_1}$ | $\forall y \in Y$ $\forall q \in Q$ $q > 1$ | Same as above, but between quarters |
| (4.9.8) | $cs_{H_2,y,q_1,h_1} \geq idle_{H_2,y-\lvert G\rvert,\lvert Q\rvert,\lvert H\rvert} + idle_{H_2,y,q_1,h_1}$ | $\forall y \in Y$ $y > 1$ | Same as above, but between years |
| (4.9.9) | $idle_{k,y,q,s}, \quad cs_{k,y,q,s} = 0$ | $\forall k \in K$ $\forall y \in Y$ $\forall q \in Q$ $\forall h \in H$: $k \neq H_2$ | ASU and HB cannot be deactivated |

**Table 4.9:** Production constraints

Constraints (4.9.2), (4.9.3), and (4.9.4) provide the production instructions. The first equation states whether or not the units can produce. The next two define the range it can produce within. Constraint (4.9.4) states that there is a minimum production that must occur unless the machine is in a no-production state.

Furthermore, (4.9.6), (4.9.7), and (4.9.8) highlight the mechanism for how a cold start

for the AE works. Section 3.2.3 stated a cold start for AE takes 10 to 30 minutes, but it is assumed to take one hour for this thesis. Additionally, there is a cost associated with performing a cold start. Hence, there is no incentive for the model to randomly assign a cold start to the unit. The constraint starts by verifying whether the previous hour was idle. In case it is not, then the AE is in either standby or producing mode, and a cold start is not required. If the unit was idle, then it also needs to verify whether the current hour is also idle. Given an idle state at the current hour, the cold start will not engage. In the case that the unit is not idle, it requires the AE to perform a cold start. Constraints (4.9.8) must adjust for the representative years, hence utilising the cardinality of set $G$.

Lastly, the constraint (4.9.9) demonstrates that units HB and ASU cannot be deactivated, as highlighted in Section 4.2. Initially, the model included the possibility of deactivating the units; however, this feature was eliminated due to the computational requirement to run the model. This will be furthered explained in section 4.9.

**Haber Bosch specific production constraints**

Similar to parameters, there are certain constraint that is only HB applicable.

| Eq | Constraint | Sets | Description |
|---|---|---|---|
| (4.10.1) | $\sum_{q \in Q} \sum_{h \in H} P \cdot x_{NH_3,y,q,h} \geq d$ | $\forall y \in Y$ | Annual ammonia demand must be met |
| (4.10.2) | $sb_{NH_3,y,q,h} = 0$ | $\forall y \in Y$<br>$\forall q \in Q$<br>$\forall h \in H$ | HB cannot be placed in standby |
| (4.10.3) | $z_{k,y,q,h} = \frac{x_{NH_3,y,q,h} \cdot Prop_k}{Conv}$ | $\forall k \in K$<br>$\forall y \in Y$<br>$\forall q \in Q$<br>$\forall h \in H$<br>$k \neq \mathrm{NH_3}$ | Proportion of each gas needed for ammonia production |
| (4.10.4) | $x_{NH_3,y,q,h} \geq x_{NH_3,y,q,h-1} - MPC_y$ | $\forall y \in Y$<br>$\forall q \in Q$<br>$\forall h \in H$<br>$h > 1$ | Maximum production reduction between hours within the week |
| (4.10.5) | $x_{NH_3,y,q,h_1} \geq x_{NH_3,y,q-1,\lvert H \rvert} - MPC_y$ | $\forall y \in Y$<br>$\forall q \in Q$<br>$q > 1$ | Maximum production reduction between hours of different weeks/quarters |

| Eq | Constraint | Sets | Description |
|---|---|---|---|
| (4.10.6) | $x_{NH_3,y,q_1,h_1} \geq x_{NH_3,y-\|G\|,\|Q\|,\|H\|} - MPC_y$ | $\forall y \in Y$ $y > 1$ | Maximum production reduction between hours of different years |
| (4.10.7) | $x_{NH_3,y,q,h} \leq x_{NH_3,y,q,h-1} + MPC_y$ | $\forall y \in Y$ $\forall q \in Q$ $\forall h \in H$ $h > 1$ | Maximum production increase between hours within the week |
| (4.10.8) | $x_{NH_3,y,q,h_1} \leq x_{NH_3,y,q-1,\|H\|} + MPC_y$ | $\forall y \in Y$ $\forall q \in Q$ $q > 1$ | Maximum production increase between hours of different quarters |
| (4.10.9) | $x_{NH_3,y,q_1,h_1} \leq x_{NH_3,y-\|G\|,\|Q\|,\|H\|} + MPC_y$ | $\forall y \in Y$ $y > 1$ | Maximum production increase between hours of different years |

**Table 4.10:** Production constraint: HB specific

The demand constraint (4.10.1) indicates that an annual ammonia demand must be met. To compensate for the time gaps within the model, it is necessary to multiply the ammonia produced by $P$, enabling repeated weeks to be represented within the quarter. Then, the aggregate for each year is found. Constraint (4.10.2) enforces that HB cannot be in standby mode, as stated in Section 3.2.3.

To ensure an adequate quantity of process mediums for the ammonia synthesis, constraint (4.10.3) was constructed. Section 3.2.2 stated that 83,5 percent of ammonia was nitrogen and 17,7 percent was hydrogen. Hence, the production of ammonia within the current hour multiplied by $Prop_k$ determines the quantity of process medium needed. Additionally, HB had a purge rate of three percent, leading to a conversion rate of 97 percent. Hence, excess process mediums must be supplied, resulting in the division.

Lastly, constraints (4.10.4) through (4.10.9) limit the maximum production change between hours. They all adhere to the same underlying rationale: identifying the quantity produced last hour and determining the new limit. Constraints (4.10.4) to (4.10.6) find the new minimum limit the HB is allowed to produce for the current hour, while constraints (4.10.7) through (4.10.9) find the maximum. The maximum load change is either subtracted from or added to the quantity of ammonia produced in the previous hours. Constraints (4.10.4) through (4.10.6) and (4.10.7) through (4.10.9) may allow for negative or above

100 percent production, respectively. However, constraints (4.9.3) and (4.9.4) limit unit production within the allowable range. To enhance comprehension, a visual representation is provided:

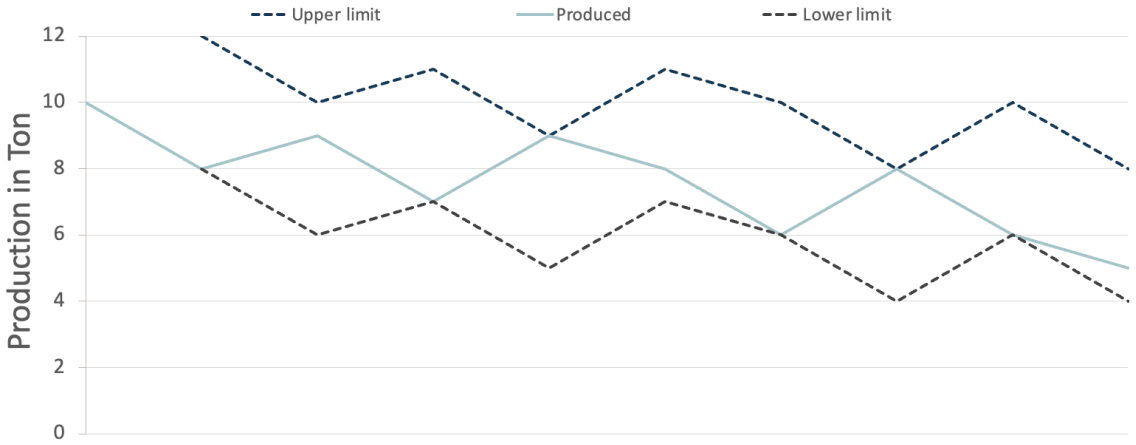


**Figure 4.2:** Maximum increase and decrease in production load

### Buffer constraints

After examining the production constrains, the buffer constraints will be addressed. Although these applies to all process mediums, ammonia does not have a storage as highlighted in section 4.2. Hence, the ammonia storage capacity equals zero.

| Eq | Constraint | Sets | Description |
|---|---|---|---|
| (4.11.1) | $s_{k,y,q,h} \leq Vol_k$ | $\forall k \in K$ | Maximum buffer capacity |
| (4.11.2) | $s_{k,y_1,q_1,h_1} = x_{k,y_1,q_1,h_1} - z_{k,y_1,q_1,h_1}$ | $\forall k \in K$ | Quantity stored at first time period |
| (4.11.3) | $s_{k,y,q,h} = s_{k,y,q,h-1} + x_{k,y,q,h} - z_{k,y,q,h}$ | $\forall k \in K$<br>$\forall y \in Y$<br>$\forall q \in Q$<br>$\forall h \in H$<br>$h > 1$ | Quantity stored each time period |
| (4.11.4) | $\Delta s_{k,y,q} = \sum_{h \in H} x_{k,y,q,h} - z_{k,y,q,h}$ | $\forall k \in K$<br>$\forall y \in Y$<br>$\forall q \in Q$ | End-of-week cumulative net difference between production and extraction |
| (4.11.5) | $s_{k,y,q,h_1} = s_{k,y,q-1,\lvert H\rvert} + (P-1) \cdot \Delta s_{k,y,q-1} + x_{k,y,q,h_1} - z_{k,y,q,h_1}$ | $\forall k \in K$<br>$\forall y \in Y$<br>$\forall q \in Q$<br>$q > 1$ | Storage continuity between hours of different quarters |

| Eq | Constraint | Sets | Description |
|---|---|---|---|
| (4.11.6) | $s_{k,y,q_1,h_1} = s_{k,y-\lvert G\rvert,\lvert Q\rvert,\lvert H\rvert} + (P-1)\cdot\Delta s_{k,y-\lvert G\rvert,\lvert Q\rvert} + x_{k,y,q_1,h_1} - z_{k,y,q_1,h_1}$ | $\forall k \in K$ $\forall y \in Y$ $y > 1$ | Storage continuity between hours of different years |
| (4.11.7) | $s_{k,y,q,\lvert H\rvert} + (P-2)\cdot\Delta s_{k,y,q} + \sum_{i=1}^{h}(x_{k,y,q,i} - z_{k,y,q,i}) \leq Vol_k$ | $\forall k \in K$ $\forall y \in Y$ $\forall q \in Q$ $\forall h \in H$ | Storage capacity constraint |
| (4.11.8) | $s_{k,y,q,\lvert H\rvert} + (P-2)\cdot\Delta s_{k,y,q} + \sum_{i=1}^{h}(x_{k,y,q,i} - z_{k,y,q,i}) \geq 0$ | $\forall k \in K$ $\forall y \in Y$ $\forall q \in Q$ $\forall h \in H$ | Non-negativity constraint |

**Table 4.11:** Buffer constraints

Constraint (4.11.1) states that the stored quantity cannot exceed the capacity of the buffer within the representative week. Quantity stored during the first time period is highlighted in constraint (4.11.2). Since there are no previous time periods, its only contingent on the process medium produced and extracted for that hour. Storage continuity during the representative weeks is ensured through in constraint (4.11.3).

Utilising representative weeks requires more complex modelling to ensure storage continuity between quarters and capacity restrictions. Representative weeks are replicated $P$ times to compose a quarter. If changes to storage quantity occur during the representative weeks, the pattern is also seen in the replicated weeks. However, the pattern is cumulative, complicating the modelling. A visual representation is provided in Figure 4.3.

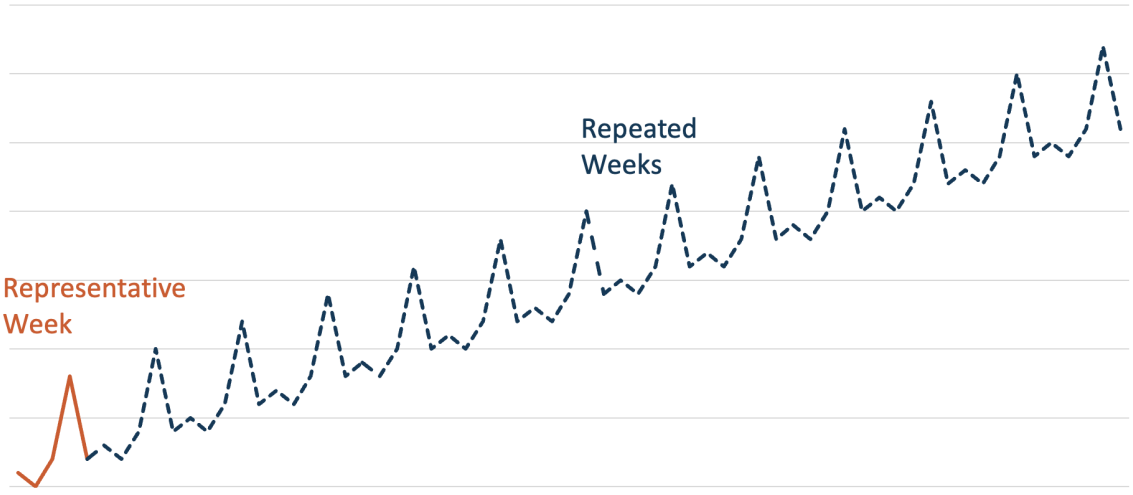


**Figure 4.3:** Storage cumulation during a quarter

Constraints (4.11.4) through (4.11.8) were created to facilitate continuity and capacity restrictions. The first step was creating the variable $\Delta s_{k,y,q}$, representing the net difference between production and extraction during the representative week for each quarter. However, the variable alone is insufficient. In the first quarter, there is no previous stored quantity to account for, and the equation $P \cdot \Delta s_{k,y,q}$ would suffice to find the end-of-quarter storage quantity. Following the first quarter, this equation would not be adequate as the stored quantity from the first quarter is not included for the next quarter. Instead, including the variable $s_{k,y,q,|H|}$ aids in resolving this discrepancy. Since this variable also includes the net difference between production and extraction, the variable $\Delta s_{k,y,q}$ must be subtracted once. The equation to find the end-of-quarter stored quantity will therefore be :

$$s_{k,y,q,|H|} + (P-1) \cdot \Delta s_{k,y,q} \tag{4.1}$$

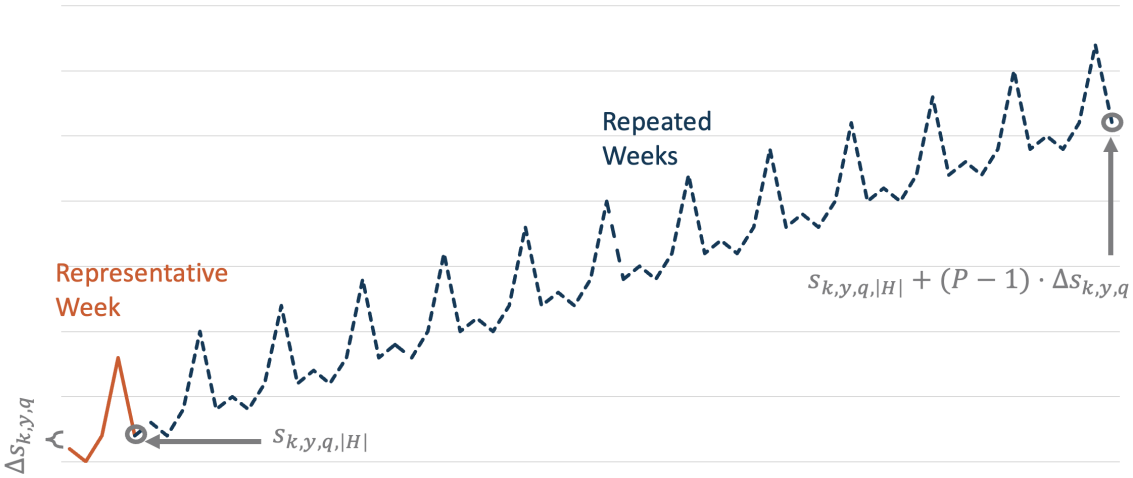


**Figure 4.4:** Storage cumulation elements

With the mechanism of finding the end-of-quarter storage quantity explained, the continuity constraints (4.11.5) and (4.11.6) can be described. They have similar functions, but constraint (4.11.5) is between hours of different quarters, while constraint (4.11.6) is between hours of different years. Though they use Equation 4.1, it is slightly modified. Instead of looking at the current end-of-quarter quantity, they looked at the previous end-of-quarter quantity. Then the production and extraction for the first hour of the current quarter are included, preserving continuity. Constraint (4.11.6) has to adjust for the use of representative years, hence including the cardinality of set $G$.

Constraints (4.11.7) and (4.11.8) provide the capacity constraints for the model. While constraint (4.11.1) restricts stored quantity within the representative week, constraints

(4.11.7) and (4.11.8) restrict between them. Due to the repetitive nature of cumulation, as shown in Figure 4.4, it is only necessary to restrict the last replicated week. Although (4.11.7) and (4.11.8) use the mechanism from Equation 4.1, alteration is needed. If the quantity stored is restricted only for the last hour of the quarter, then the quantity may exceed capacity for the earlier portion of the week. Hence, each hour of the last repeated week must be constrained. Similar to (4.11.5) and (4.11.6), $s_{k,y,q,|H|}$ is used for the continuity of the constraint. Secondly, the cumulative stored quantity of the last hour for the penultimate replicated week must be identified. By subtracting $\Delta s_{k,y,q}$ from Equation 4.1, the desired value is identified. The third concept of these constraints is to restrict all hours of the week. The variables $s_{k,y,q,h}$ are defined in constraint (4.11.3) as the continuity of the previous hour and the net difference of production and extraction for the current hour. With the continuity found in the first two concepts, the equation can be reformulated by adding the net difference between production and extraction at hour $h$. Hence, the formulation $\sum_{i=1}^{h}(x_{k,y,q,i} - z_{k,y,q,h})$ is included. The constraints are illustrated in Figure 4.5.

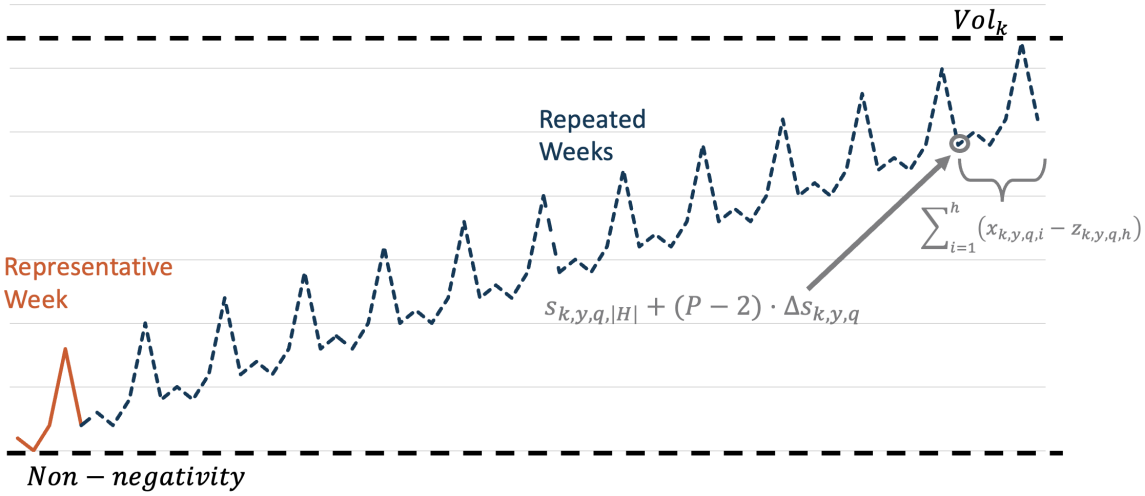


**Figure 4.5:** Storage cumulation constraints visualised

## 4.7 Objective function

The model aims to minimize cost of ammonia production. Hence the objective function is defined as

$$Minimize : TotalCost \tag{4.2}$$

In order for the objective function to reduce cost, the definition of $TotalCost$ mush be established.

| Eq | Formula | Sets | Description |
|---|---|---|---|
| (4.12.1) | $TotalCost = \sum_{k \in K} TotalCAPEX_k + TotalOPEX_k + TotalRPRC_k + TotalELC_k$ | | Total cost of ammonia production |
| (4.12.2) | $TotalCAPEX_k = CAPEX_k^U + CAPEX_k^B$ | $\forall k \in K$ | Total cost of CAPEX |
| (4.12.3) | $TotalOPEX_k = \sum_{y \in Y} \sum_{g \in G} \frac{OPEX_k^U + OPEX_k^B}{(1+WACC)^{y+g}}$ | $\forall k \in K$ | Total cost of OPEX |
| (4.12.4) | $TotalRPRC_k = \sum_{y \in R} \frac{RPRCP_k \cdot CAPEX_k^U}{(1+WACC)^y}$ | $\forall k \in K$ | Total replacement parts replacement cost |
| (4.12.5) | $TotalELC_k = TotalProdELC_k + TotalStorELC_k + TotalSBELC_k + TotalCSELC_k + TotalGridFees_k$ | $\forall k \in K$ | Total cost of electricity |

**Table 4.12:** $TotalCost$ components

Table 4.12 is used as an overview to illustrate the elements included in calculating $TotalCost$. These are CAPEX, OPEX, replacement parts replacement costs, and the cost of electricity. All these elements are further divided into more components, which will be defined at a later stage after an overview has been established.

$TotalCAPEX_k$ consists of the CAPEX of the different units and buffers. In order for production to commence in year one, it is assumed that these are bought at the end of year 0. Hence, the CAPEX will not be discounted.

Similar to $TotalCAPEX_k$, $TotalOPEX_k$ consists of the OPEX for the different units and buffers. However, these costs recur annually and must be discounted in accordance with the year of the expense. Furthermore, the use of representative years requires additional steps to calculate the cost. The OPEX for these years stays unchanged but is discounted

at different rates by the implementation of set $G$. Then all discounted expenses are added to find $TotalOPEX_k$.

$TotalRPRC_k$ differs from $TotalOPEX_k$ in that the cost reoccurs during certain years. As a result, these costs are not to be replicated for the replicated years; hence, the set $G$ is not included. Furthermore, the equation uses set $R$ instead of $Y$ to specify the distinct year of the expense.

Lastly, $TotalELC_k$ includes many more components in its calculation. To better understand the different electricity costs of production, storage, standby mode, cold start, and grid cost, they all have their own elements. A more in-depth explanation of each of these will be provided. But first, the components of $TotalCAPEX_k$, $TotalOPEX_k$ and $TotalRPRC_k$ will be defined.

| Eq | Formula | Sets | Description |
|---|---|---|---|
| (4.13.1) | $CAPEX_k^U = BCAPEX_k^U \cdot \left(\frac{TotCap_k}{BSize_k}\right)^{\alpha_k^U}$ | $\forall k \in K$ | Unit CAPEX |
| (4.13.2) | $CAPEX_k^B = BCAPEX_k^B \cdot \left(\frac{Vol_k}{BVol_k}\right)^{\alpha^B}$ | $\forall k \in K$ | Buffer CAPEX |
| (4.13.3) | $OPEX_k^U = CAPEX_k^U \cdot OPEXP_k^U$ | $\forall k \in K$ | OPEX as a % of CAPEX |
| (4.13.4) | $OPEX_k^B = CAPEX_k^B \cdot OPEXP_k^B$ | $\forall k \in K$ | OPEX as a % of CAPEX |
| (4.13.5) | $RPRC_k = CAPEX_k^B \cdot RPRCP_k$ | $\forall k \in K$ | Replacement parts cost as a % of CAPEX |

**Table 4.13:** Calculation Financial parameter of production calculation

Both $CAPEX_k^U$ and $CAPEX_k^B$ use Equation 3.2, but with different parameters from each other. As highlighted in Section 3.3.2, ammonia storage is absent from this thesis, and nitrogen buffer has its CAPEX encapsulated in the ASU CAPEX. Hence, only the expense from hydrogen buffer CAPEX is included. To not incur the expenditure of the ammonia and nitrogen buffers, their $BCAPEX_k^B$ is set to zero. Since $CAPEX_k^B$ are defined within the model, not defining them would lead to an unbounded solution as $CAPEX_k^B$ would approach infinity.

$OPEX_k^U$ and $OPEX_k^U$ are calculated based on a percentage of the CAPEX they correspond

to. Additionally, $RPRC_k$ uses the same approach.

The remaining element to define in $TotalCost$ is $TotalELC_k$. As demonstrated in Table 4.12, $TotalELC_k$ is defined by five components: $TotalProdELC_k$, $TotalStorELC_k$ $TotalSBELC_k$, $TotalCSELC_k$ and $TotalGridFees_k$. The components are kept separate in order to differentiate them in the cost analysis. The table has removed the Sets column, due to the length of the equation. However, the definition of $\forall k \in K$ is applied to them all.

| Eq | Formula | Description |
|---|---|---|
| (4.14.1) | $TotalProdELC_k = \sum_{y \in Y} \sum_{g \in G} \sum_{q \in Q} \frac{P \cdot (\sum_{h \in H} x_{k,y,q,h} \cdot NRG_k \cdot ELC_{y,q,h})}{(1 + WACC)^{y+g}}$ | Total electricity cost of production |
| (4.14.2) | $TotalSBELC_k = \sum_{y \in Y} \sum_{g \in G} \sum_{q \in Q} \frac{P \cdot (\sum_{h \in H} sb_{k,y,q,h} \cdot SBNRG_k \cdot ELC_{y,q,h})}{(1 + WACC)^{y+g}}$ | Total electricity cost of standby mode |
| (4.14.3) | $TotalCSELC_k = \sum_{y \in Y} \sum_{g \in G} \sum_{q \in Q} \frac{P \cdot (\sum_{h \in H} cs_{k,y,q,h} \cdot CSNRG_k \cdot ELC_{y,q,h})}{(1 + WACC)^{y+g}}$ | Total electricity cost of cold start |
| (4.14.4) | $TotalStoreELC_k = \sum_{y \in Y} \sum_{g \in G} \frac{TotalStoredCost_{k,y}}{(1 + WACC)^{y+g}}$ | Total electricity cost of storing |
| (4.14.5) | $TotalGridFees_k = \sum_{y \in Y} \sum_{g \in G} \frac{TotalELUsed_{k,y} \cdot GF}{(1 + WACC)^{y+g}}$ | Total grid fees cost |

**Table 4.14:** $TotalELC_k$ elements

Equation (4.14.1) through (4.14.3) have the equivalent structure. First, the decision variable is multiplied by the energy they consume and the electricity price for that specific time period. Then, the electricity cost for all hours is added together and multiplied by $P$

to capture the whole quarter. Each quarter is discounted to simplify the notation and is then added together for each representative and replicated year.

Equation (4.14.4) and (4.14.5) have another layer added to them to simplify the notation. Similar to the continuity of quantity stored in buffers, the cost aspect is also more complicated. Additionally, $TotalELU_{k,y}$ implements some of the same aspects as $TotalStoredCost_{k,y}$. Additionally, the cost is linear as shown in Section 3.4.4. The table has removed the description due to the length of the equations.

| Eq | Formula | Sets |
|---|---|---|
| (4.15.1) | $TotalStoredCost_{k,y} = \sum_{q \in Q} \sum_{h \in H} ((SRW_{k,y,q,h} + SCWk, y, q, h) \cdot ELC_{y,q,h})$ | $\forall k \in K$ $\forall y \in Y$ |
| (4.15.2) | $SRW_{k,y,q,h} = s_{k,y,q,h} \cdot SNRG_k$ | $\forall k \in K$ |
| (4.15.3) | $SCW_{k,y,q,h} = SNRG_k \cdot \sum_{p=0}^{P-2} (s_{k,y,q,\lvert H \rvert} + p \cdot \Delta s_{k,y,q} + \sum_{i=1}^{h} (x_{k,y,q,i} - z_{k,y,q,i}))$ | $\forall k \in K$ $\forall y \in Y$ $\forall q \in Q$ $\forall h \in H$ |
| (4.15.4) | $TotalELUsed_{k,y} = \sum_{\forall q \in Q} \sum_{\forall h \in H} SRW_{k,y,q,h} + \sum_{\forall q \in Q} \sum_{\forall h \in H} SCW_{k,y,q,h} + \sum_{q \in Q} \sum_{h \in H} P \cdot (x_{k,y,q,h} \cdot NRG_k + sb_{k,y,q,h} \cdot SBNRG_k + cs_{k,y,q,h} \cdot CSNRG_k)$ | $\forall k \in K$ $\forall y \in Y$ |

**Table 4.15:** Storing fees and energy usage calculations

Equation (4.15.1) specifies the electricity cost that is to be discounted in equation (4.14.4). This equation consists of three elements: the energy used to store at each hour within the representative week ($SRW_{k,y,q,h}$), the energy used to store for each hour for all repeated weeks ($SCW_{k,y,q,h}$) and the price of electricity. Equations (4.15.2) and (4.15.3) states the calculations for $SRW_{k,y,q,h}$ and $SCW_{k,y,q,h}$ respectably. The variable $SRW_{k,y,q,h}$ is calculated by multiplying the quantity stored at each hour within the representative

week by the energy required. The variable $SCW_{k,y,q,h}$ is harder to calculate due to the cumulative nature of storage illustrated in Figure 4.3. To determine the cost of electricity for repeated weeks, it is necessary to consider all hours. To find the energy requirement for all hours, a similar approach to Equation 4.1 is used. However, instead of using the equation to find the last hour of the quarter, the last hour of each repeated week must be found. Similar to constraints (4.11.7) and (4.11.8), the stored amount at each hour within the week is then calculated. Hence, the difference between constraints (4.11.7) & (4.11.8) and equation (4.15.3) is the added element of $\sum_{p=0}^{P}$. To better understand the totality of the equation, a visual representation is presented:

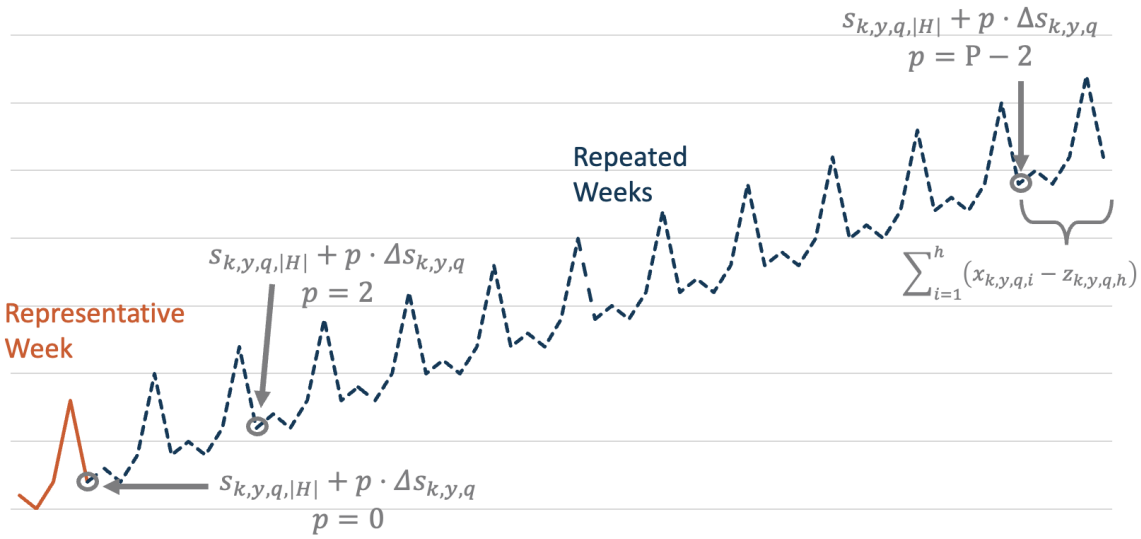


**Figure 4.6:** Storage cost calculation visualised

Lastly, $TotalELUsed_{k,y}$ is the calculation of total electricity used in order to calculate the grid fees in Equation (4.15.5). It employs the calculations of $SRW_{k,y,q,h}$ and $SCW_{k,y,q,h}$, in addition to the energy used on production, standby and cold starts as shown in Equation (4.14.1) through (4.14.3). These are all summed up for each year.

## 4.8 Levelized cost of ammonia

To maintain the linearity of the model, the objective function focused on minimising the total discounted cost. However, it did not implement the discounted ammonia produced as shown in Equation 3.1. Although it is not specified, the total can be extracted from the results of the model and used for calculation:

| Eq | Formula | Sets | Description |
|---|---|---|---|
| (4.16.1) | $A_y = \sum_{q \in Q} \sum_{h \in H} (x_{NH_3,y,q,h} \cdot P)$ | $\forall y \in Y$ | Amount of ammonia produced for each year |
| (4.16.2) | $TotalProd = \sum_{y \in Y} \sum_{g \in G} \frac{A_y}{(1+WACC)^{y+g}}$ | | Total ammonia produced discounted |

**Table 4.16:** Discounted Ammonia calculation

Similar to previously, the use of representative weeks and years complicates the calculations, but they follow the same premise. Hence, the equation for finding LCOA will be:

$$LCOA = \frac{TotalCost}{TotalProd} \tag{4.3}$$

## 4.9 Complications

Initially, the model included the possibility of having HB and ASU in idle mode in addition to all thirty years. However, this ended up being too computationally demanding. A computer with 48 logical processors and 64 GB of RAM required more than 48 000 seconds, or 13 hours, to execute some of the scenarios in the model. This made the analysis impractical as it had to run over 1 300 scenarios.

Therefore, strategies to reduce the computational requirements was implemented. First, the use of representative years was instituted. Although this reduced the computational power, it was not enough as scenarios would take multiple hours to run. Hence, a simplification of the model was required. The decision of removing the possibility of having HB and ASU in idle mode was based on two justifications. The first justification was because manufacturers normally let the HB run continuously and would only stop for maintenance purposes as highlighted in Section 3.2.3. The second justification was the computational requirement the constraints of letting HB and ASU be idle incur. To look through the constraints, view Appendix D.1.

# 5 Analysis and Results

This chapter aims to use the information gathered so far to examine the potential benefits of increased flexibility in ammonia production. Flexibility is the term used in this thesis to refer to the system's ability to take advantage of the fluctuation of electricity prices in order to mitigate the cost of ammonia production. Examples of flexibility include having excess production capacity, increased storage capacity, and modifications to systems that provide more freedom.

This section begins by providing the scope of the analysis in Section 5.1. In Section 5.2 a base case is defined to understand the functionality of the model. The analysis will begin by creating different scenarios in Section 5.3 to 5.6. Subsequently, Section 5.7 analyses the utilisation of the intermediate hydrogen storage. Lastly, Section 5.8 Section addresses the uncertainty of the data selection by rerunning the outlined scenarios.

## 5.1 Scope of analysis

Prior to the analysis, its scope will be described. This section discusses the parameters that are to be altered in order to determine if increased flexibility can reduce the cost of ammonia production.

The first parameter to be altered in this analysis is the production capacity of the AE. To find the range to be tested for, first the minimum requirement must be met. In Section 4.2, the average ammonia demand of 10 000 kg/h was assumed. Furthermore, Section 3.2.2 established that 17,7 percent of ammonia's weight is hydrogen. Additionally, the highest degradation of 6 percent and the conversion rate of 97 percent must be accounted for in order for the MILP to solve the optimisation problem. This results in the minimum production capacity being: $\frac{10.000 kg/h \cdot 17{,}7\%}{97\% \cdot (100\% - 6\%)} = 1\ 941$ kg/h. In this analysis, the minimum size that will be considered is 2 000 kg/h. To test for flexibility, a 50 percent increase seems sufficient. Hence, the production capacity of the AE will range from 2 000 to 3 000 kg/h, with increments for every 100 kg/h.

The calculation for the minimum production capacity of the ASU is similar to the calculations performed above; however, there is no degradation due to the assumptions

made in Section 4.2. In Section 3.2.2, it was stated that 82,3 percent of ammonia's weight is contributed to nitrogen. Along with the total conversion rate of 97 percent, the minimum production capacity of the ASU will be: $\frac{10.000kg/h \cdot 82{,}3\%}{97\%} = 8\ 484$ kg/h. As stated in Section 3.2.3, only two percent of the energy consumed during ammonia production is by the ASU. Hence, there are limited cost savings opportunities by increasing production capacity. However, when the HB process increases its production capacity, ASU's production capacity will be increased accordingly to prevent constraining the system.

The last production unit to be altered is the HB process. Similarly to the AE, the minimum production capacity must be able to supply the minimum required. With the highest degradation of 8 percent, the minimum production capacity is: $\frac{10.000kg/h}{100\%-8\%} = 10\ 870$ kg/h. To simplify the analysis, a 20 and 40 percent increase in HB process production capacity will be performed. Additionally, alterations to the production capacities minimum load and ramp rate will be performed.

Lastly, alterations to the intermediate storage will be performed. Given that there is no ammonia storage, it will not be considered. Similar to the ASU, nitrogen storage will not be altered due to the limited savings potentials, and it will be kept at one day's worth of nitrogen demand. Hence, only alterations for intermediate hydrogen storage will be performed. Given that its intermediate storage, the range of zero to one day's worth of necessary hydrogen supply is deemed appropriate. Hence, the capacity range will be zero and 42 480 kg, with increments of 4 hours of necessary hydrogen supply.

To better understand the scenarios described above, a summery is provided in Table 5.1. For an overview of all the data, view Appendix A

| **Scenario** | **Base** | **1** | **2** | **3** | **4** |
|---|---|---|---|---|---|
| AE: Production capacity (t/h) | 2 | $2-3$ | $2-3$ | $2-3$ | $2-3$ |
| ASU: Production capacity (t/h) | $8,5$ | $8,5$ | 8,5-12,75 | $12,75$ | $12,75$ |
| HB: Production capacity (t/h) | 10,87 | 10,87 | 10.75-15 | 15 | 15 |
| Buffer Hydrogen (t) | 0 | 0-42,48 | 0-42,48 | 0 | 0 |
| HB: Minimum Load (% of total) | 50% | 50% | 50% | $20-50\%$ | 20% |
| HB: Ramp rate (% of total) | 20% | 20% | 20% | 20% | 80% |

**Table 5.1:** Scenario overview

## 5.2 Base Case

To better understand the model's functionality, a base case is developed. This case considers the production capacity necessary to satisfy demand, as highlighted in Section 5.1. This case is where there is no excess flexibility of the system.

To demonstrate the model's functionality, a comparison between ammonia production and electricity prices is illustrated in figure 5.1. The vertical axis reflects the production of ammonia, while the horizontal axis represents hours within the first representative week of the model. The blue line describes production, while the light green line describes the cost of electricity.

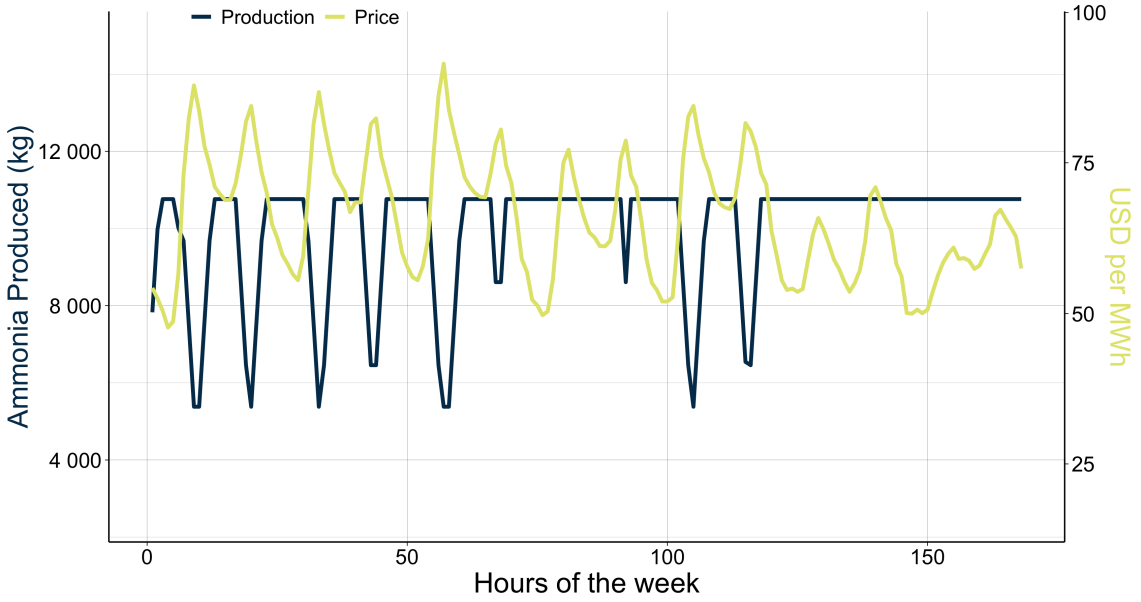


**Figure 5.1:** Production and electricity price comparison

Although this case is based on the minimum production capacity to satisfy demand, there is still variation in production. The minimum production capacity was calculated in light of the highest level of degradation. Hence, time periods with lower levels of degradation will have excess production capacity. Given that the system in the figure is new, excess production capacity exists.

The figure illustrates an inverse relationship between ammonia production and price. However, production level is not based on the electricity price for one specific time period but rather on the average price over the course of multiple time periods. This phenomenon is illustrated between the hours of 75 and 100 and can be attributed to the HB's inability

to quickly adjust. Additionally, the limitation imposed by the HB process is further evident with its minimum production constraint of 50 percent of total production capacity.

To get a holistic overview of production, the total production of ammonia for each quarter will be presented. Similar to the previous figure, the vertical axis represents production. However, the horizontal axis represents the cumulative quarters. Given the use of representative years, the number of years was reduced from 30 to 10. Hence, the total number of quarters is 40.

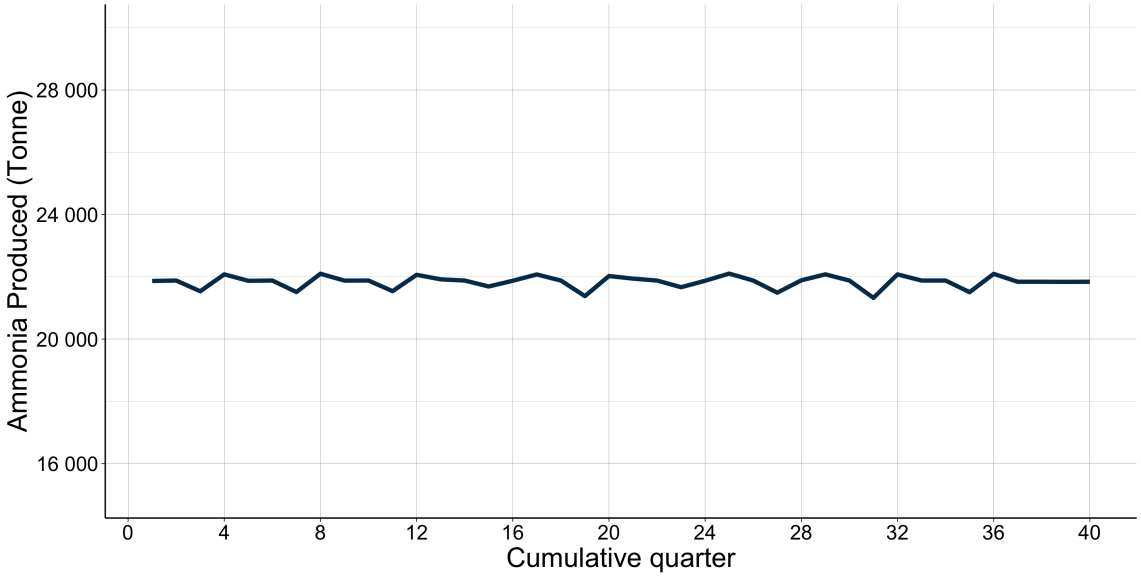


**Figure 5.2:** Quarterly ammonia production

Given the yearly demand of 87 360 tonnes, an average of 21 840 tonnes per quarter would need to be produced, which the figure illustrates with small variations. The variation exists as a result of different degradation levels, as explained earlier.

This section has demonstrated the functionality of the model by comparing electricity prices and production, along with illustrating the quarterly production of ammonia to satisfy demand.

## 5.3 Scenario 1: AE and Hydrogen Buffer

With the functionality of the model demonstrated, analysis for the first scenario can begin. As outlined in the scope of the analysis, the minimal production capacity of both the ASU and the HB process necessary will be utilised. The adjustments made in this scenario

are restricted to the AE production capacity and the hydrogen buffer capacity. Multiple combinations will be tested to determine which combination results in the lowest LCOA, labelled the optimal combination. A cost-driver analysis will be conducted on the optimal combination.

The following results are obtained by running for all the different combinations. The horizontal axis represents the production capacity of the AE, while the vertical axis represents the LCOA. Furthermore, the diverse range of colours serves as a visual representation of buffer storage capacity, measured in metric tonnes.

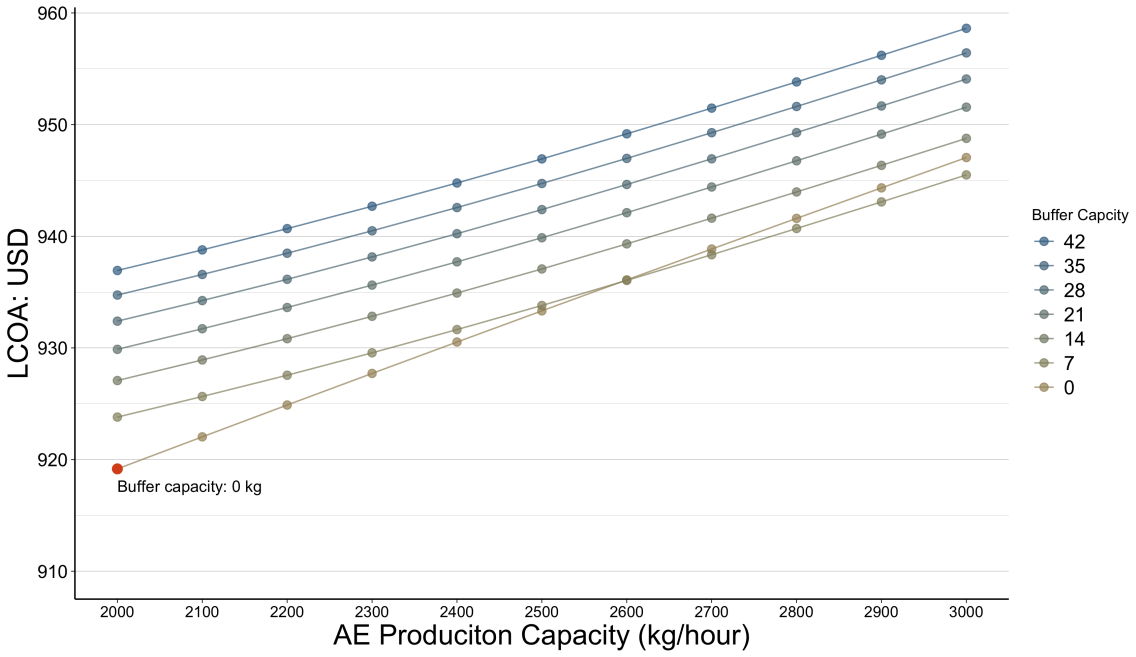


**Figure 5.3:** Scenario 1: LCOA results

The results from the model show that the LCOA ranges between 919 and 959 USD per tonne of ammonia, and the most beneficial is the combination of no excess production capacity for the AE and the absence of a buffer. Hence, the increased flexibility is not beneficial in this scenario.

One trend observed is the linear relationship between AE size when buffer capacity is kept constant. For each increase in the AE, there seems to be a linear increase in the LCOA. This suggests that the buffer is not being fully utilised. However, when there is no buffer, the excess cost is even greater, resulting in a deeper slope. Additionally, at 2 600 kg/h or greater production capacity of the AE, it becomes more advantageous to have the buffer than not as illustrated in Figure 5.3. Hence, the buffer is being utilised,

but not enough to offset the CAPEX incurred. Even though buffers are not beneficial, it might be because of how the scenario is set up. Further investigation is therefore needed.

Given the scenario of no excess production capacity, an analysis of the cost drivers should be performed. The cost drivers are categorised into four groups: electricity cost, CAPEX, OPEX, and cost or replaceable parts (RPRC), as highlighted in Section 3.2.5. Additionally, the process medium the cost is associated with is indicated through colours. Lastly, the horizontal axis describes the percentage of total cost.

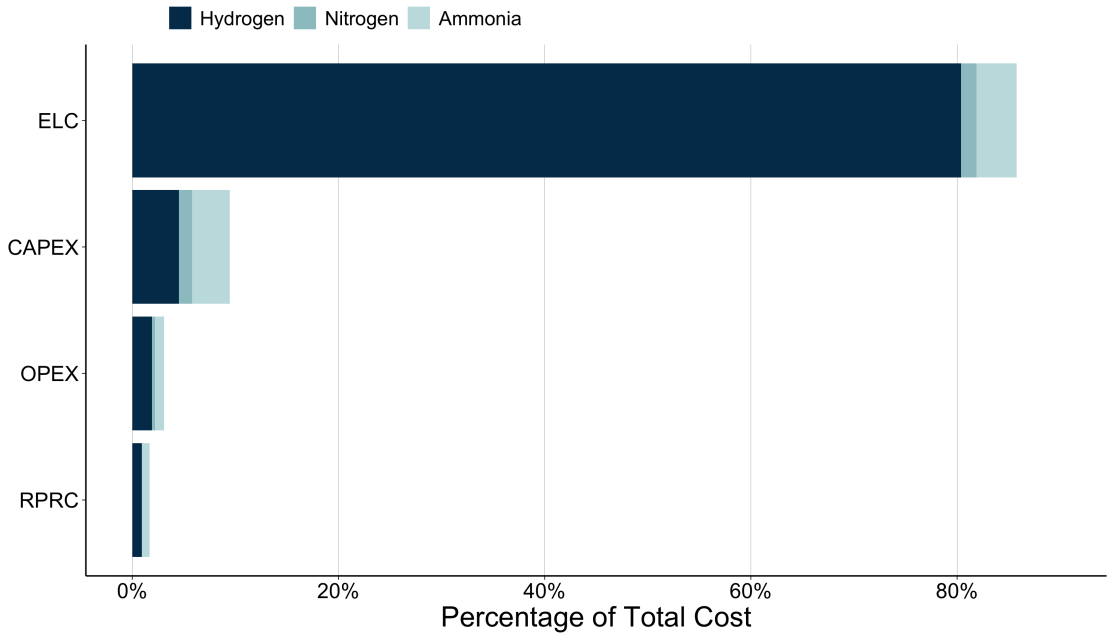


**Figure 5.4:** Cost driver of ammonia production

The figure illustrates that electricity costs are the primary expense in ammonia production, with the majority being associated with hydrogen. CAPEX, OPEX, and RPRC account for a low portion of the cost, amounting to less than 20 percent of the total lifespan cost of ammonia production. However, the CAPEX still differentiated between the different combinations. An additional feature to consider is how OPEX and RPRC are calculated, as both are a percentage of CAPEX. Hence, an increase in CAPEX will also increase both OPEX and RPRC. Nevertheless, the most influential cost driver is the electric cost, and the primary focus should be to mitigate these costs.

To better understand the cost of electricity, it is broken down into its components. A similar structure as in the previous figure will be utilised, with distinct categories and their associated process mediums.

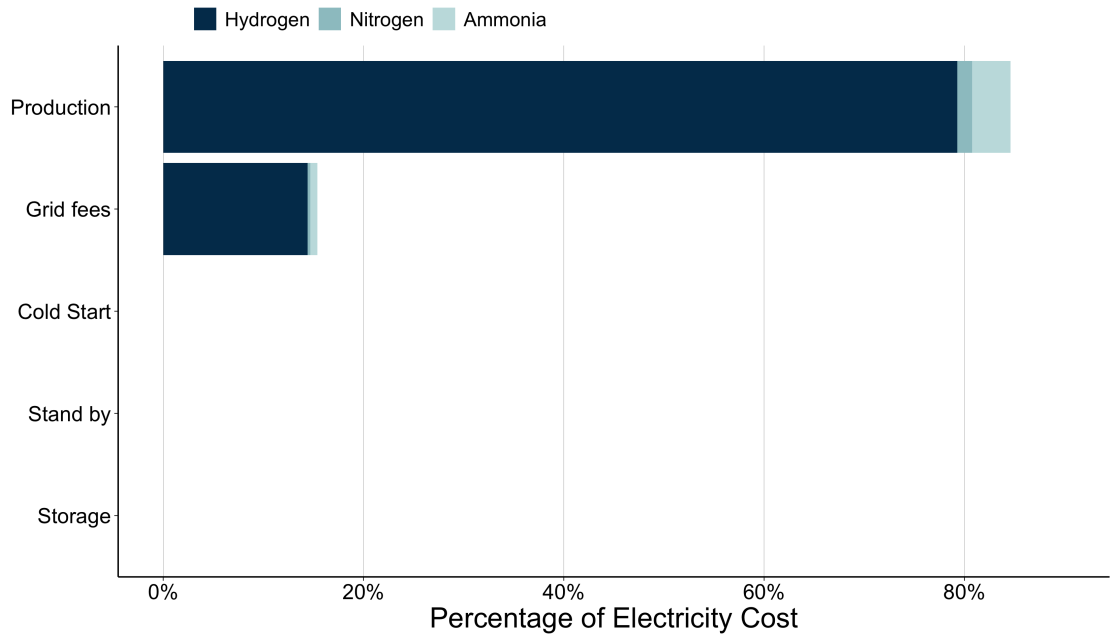


**Figure 5.5:** Breakdown of the electricity cost

The majority of electricity cost can be attributed to the production of hydrogen. Additionally, grid fees account for approximately 15 percent of the overall electricity expense. Given that the grid fees are linear, the cost will not alter if a comparable quantity of ammonia is produced. However, if there is a decrease in production costs, then grid fees will represent a greater portion of the overall costs. Since the optimal combinations did not include increased flexibility in the system to produce ammonia, it also resulted in the inability to perform a cold start and being placed in standby. Additionally, with the absence of buffers, no storage cost can occur.

In this section, the results of scenario 1 have been presented. With no excess production capacity of the HB process, the most optimal combination is the absence of the buffer in addition to no excess production capacity of the AE. This resulted in a LCOA of 919 USD per tonne of ammonia. Furthermore, an analysis of the cost drivers has been conducted. This illustrated that the majority of costs are associated with the production of hydrogen. Hence, the focus should be on mitigating this expense.

## 5.4 Scenario 2: Increased HB production capacity

As highlighted in the scope of the analysis, the production capacity of the HB process will be increased by 20 and 40 percent, with an appropriate increase in the ASU to not

constrain the system. These will be performed in separate scenarios, where the variations of buffer and AE size highlighted in Scenario 1 will be tested. Then a more detailed examination of the production trends will be conducted. Given the results of these scenarios, the relationship between the AE and HB process will be analysed.

### 5.4.1 Scenario 2.1: 20 percent increase

In this scenario, the HB process has its production capacity increased by 20 percent. Additionally, adjustments to both the AE's production capacity and the buffer size will be performed. Figure 5.3 will be repeated to identify the optimal combination with the lowest LCOA.

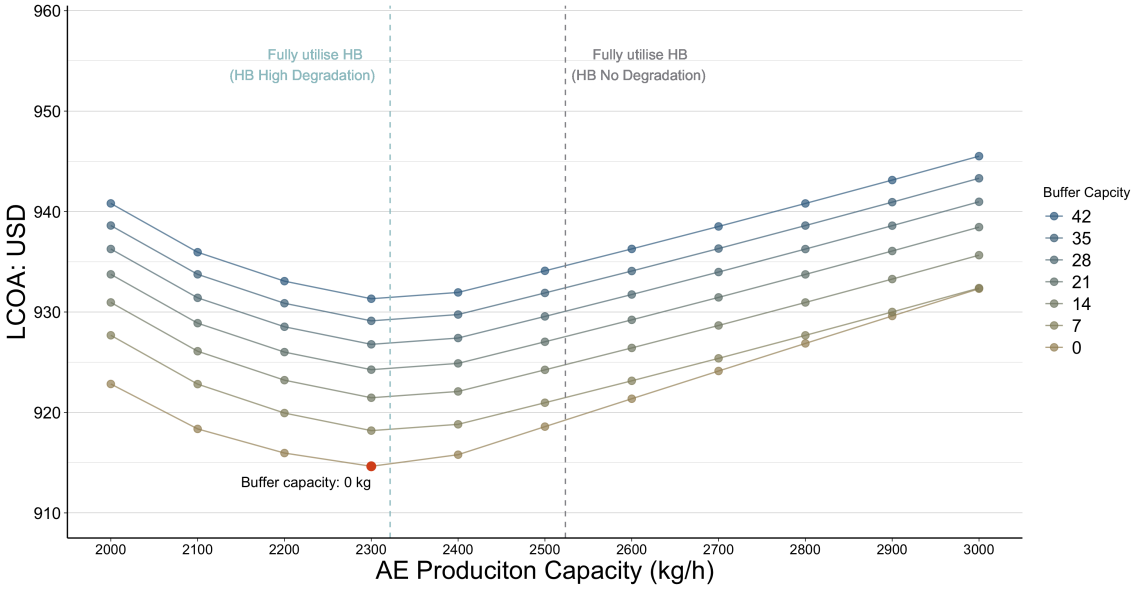


**Figure 5.6:** Scenario 2.1: LCOA results

The results show that the LCOA ranges from 915 to 946 USD per tonne of ammonia. The most optimal combination is an AE production capacity of 2 300 kg/h and the absence of a buffer. Compared to Scenario 1, the LCOA has been reduced by 0,5 percent from 919 to 915 USD per tonne of ammonia, indicating savings potential greater than the increased CAPEX.

In addition, the LCOA patterns differ from those exhibited in Scenario 1. Instead of a linear relationship when buffer capacity remained constant, it now illustrates a non-linear relationship. However, there are some similarities to Scenario 1. When AE production capacity remains constant, similar variance between the different buffer capacity, with the exception of the absent buffer. This might indicate that buffers are not being utilised.

Another observation is the correlation between the production capacity increase of the HB process and the AE. The figure highlights that the AE production capacity increase should cover the HB production capacity under high degradation and not its full capacity when the unit is new. In other words, the AE should be minimised in relation to the HB production capacity.

To better understand why LCOA has decreased, an examination of the quarterly production can be helpful. Figure 5.2 is repeated, but with the production of this scenario.

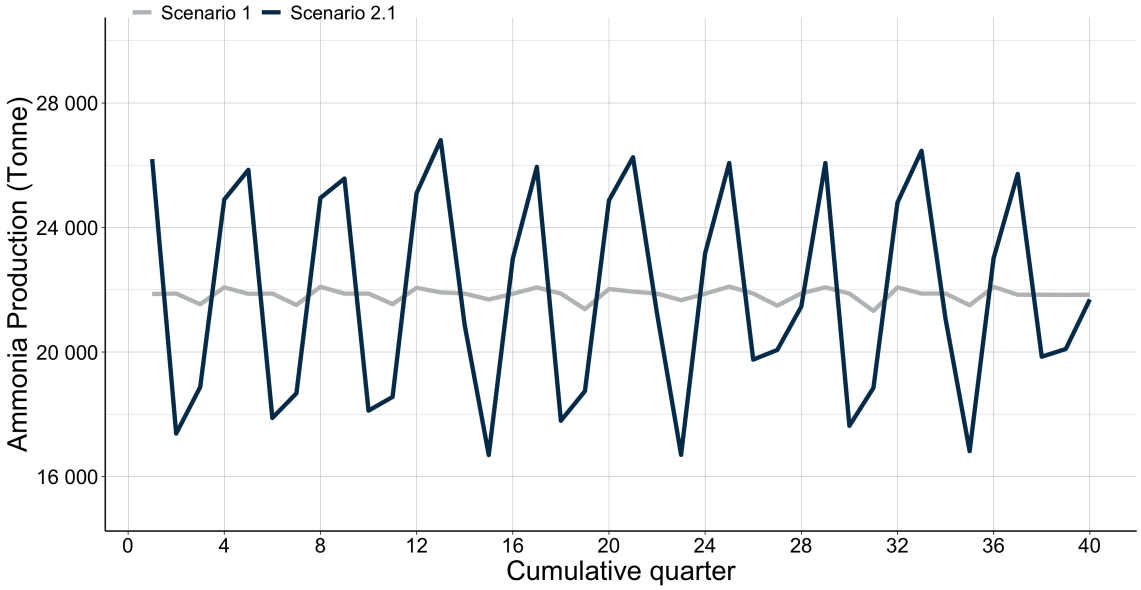


**Figure 5.7:** Scenario 2.1: Quarterly ammonia production

Ammonia production varies to a greater extent in this scenario as a result of the excess capacity. Additionally, production patterns emerge. Quarters one and four (spring and winter) consistently have the highest production, while quarters two and three (summer and fall) have the lowest production. This observation aligns with the findings shown in Figure 3.3, indicating that the average electricity prices are on average lowest during the spring and winter seasons, while they are on average highest during the summer and autumn seasons. Hence, the electricity savings offset the added CAPEX, OPEX, and RPRC incurred.

To get a better understanding of the shift on an hourly basis, a similar illustration as Figure5.1 is created for this scenario.

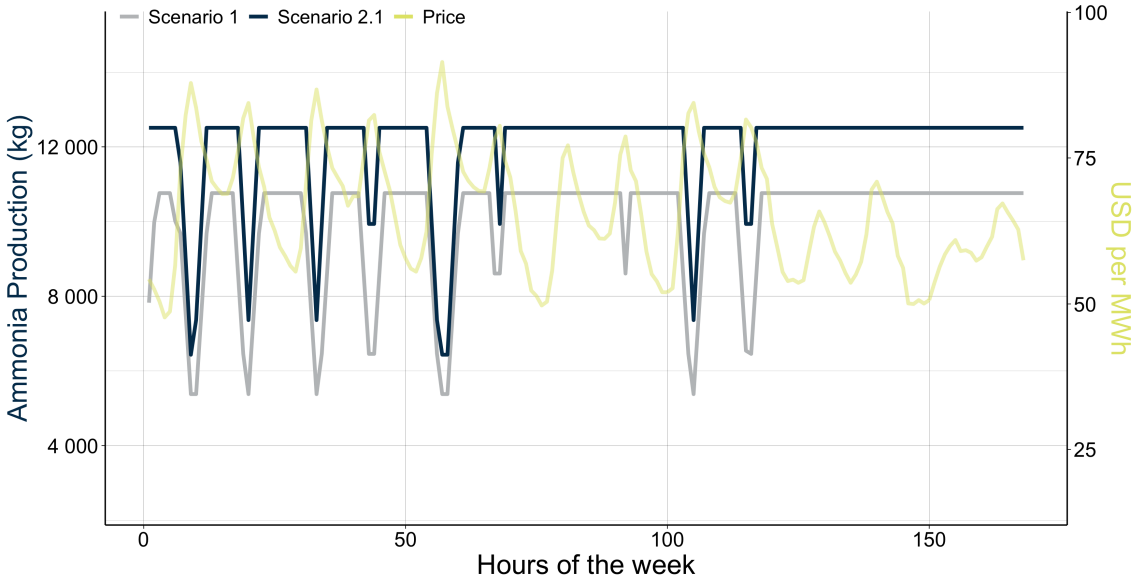


**Figure 5.8:** Production over one week with a 20 percent increase in HB capacity

Production in this scenario exhibits similarities to production shown in Scenario 1, but the production level is higher. Hence, there is still some variation within each quarter, and the production output is not maximised in these quarters.

The results show that an increase in the HB production capacity is beneficial, given the absence of a buffer and with an increase in AE's production capacity. However, AE's production capacity should not exceed that of HB's given high degradation. Furthermore, higher levels of production happen during spring and winter and lower levels during summer and fall. This allowed for savings greater than the added cost of increased flexibility.

### 5.4.2 Scenario 2.2: 40 percent increase

This section is identical to the previous scenario, except for a 40 percent increase in the HB and ASU production capacity instead of 20 percent. A similar LCOA graph as for the previous scenarios will be used.

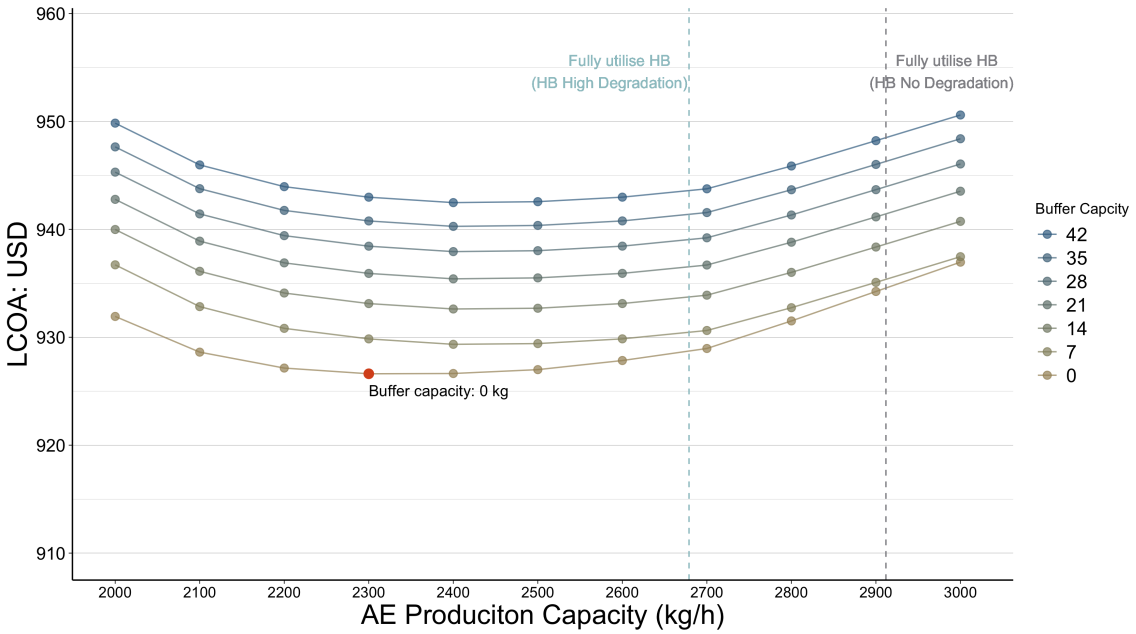


**Figure 5.9:** Scenario 2.2: LCOA results

The results in this scenario illustrate an LCOA range from 927 to 951 USD per tonne of ammonia. Similar to the previous scenario, the AE production capacity of 2 300 kg/h and the absence of buffer is the most optimal combination. Another observation is that the smallest LCOA is increased for this scenario compared to the others. Scenario 2.1 has the lowest at 915 USD per tonne, while scenario 1 has a LCOA at 919 USD per tonne. This scenario has the smallest LCOA at 927 USD per tonne of ammonia.

Another observation is that the LCOA pattern has similar characteristics to the previous scenario; however, the slope of the curve has flattened out. Thus, the consequence of selecting the wrong production capacity of AE is less influential. Similarly to the previous scenarios, there is a similar variance between the buffers when the production capacity of AE is kept constant. Hence, further investigations are required into why buffers are not utilised.

Another observation that differs, is the rate of AE size increases in relation to the size of the HB process. In the previous scenario, it was beneficial to increase AE to take full advantage of the capacity of a high degradation HB production capacity, in contrast to this scenario.

To better comprehend why LCOA increased, an illustration of its production pattern over all quarters are presented.

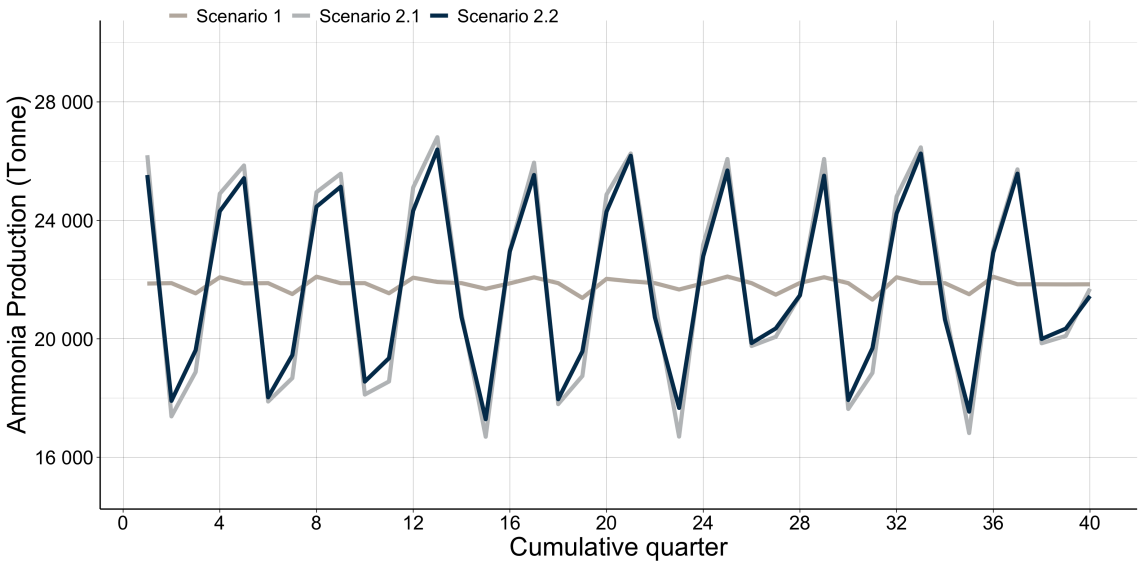


**Figure 5.10:** Scenario 2.2: Quarterly ammonia production

Compared to the previous scenario, it does follow similar production pattern. Nevertheless, there are disparities. The range between the highest and the lowest production has been contracted. This is because of the limitation the HB process introduces with its minimal load rate at 50 percent as highlighted in Section 3.2.4. The system must produce more during unfavourable time periods, and to compensate, produce less during favourable times. This results in increased cost for the system compared to Scenario 2.1. With the additional of CAPEX, OPEX and RPRC, then it becomes less favourable than Scenario 1.

Although excessive production capacity was introduced to the HB process, the results do not indicate a beneficial outcome. Additionally, the equal combination between AE and buffer size observed in Scenario 2.1 is the most optimal given the scenario. Furthermore, the increase in the AE size is less in relation to the HB process size in this scenario compared to the previous scenario. Lastly, the production pattern is comparable to the previous scenario; however, the electricity savings are not offsetting the added CAPEX, OPEX, and RPRC incurred by the increase in production capacity.

### 5.4.3 AE and HB process relation

Given that buffers are not beneficial throughout the different scenarios, the focus should be on the relationship between the AE and HB process. To explore this relation, a similar figure as the previously LCOA results will be presented. However, buffer capacity is replaced with HB production capacity.

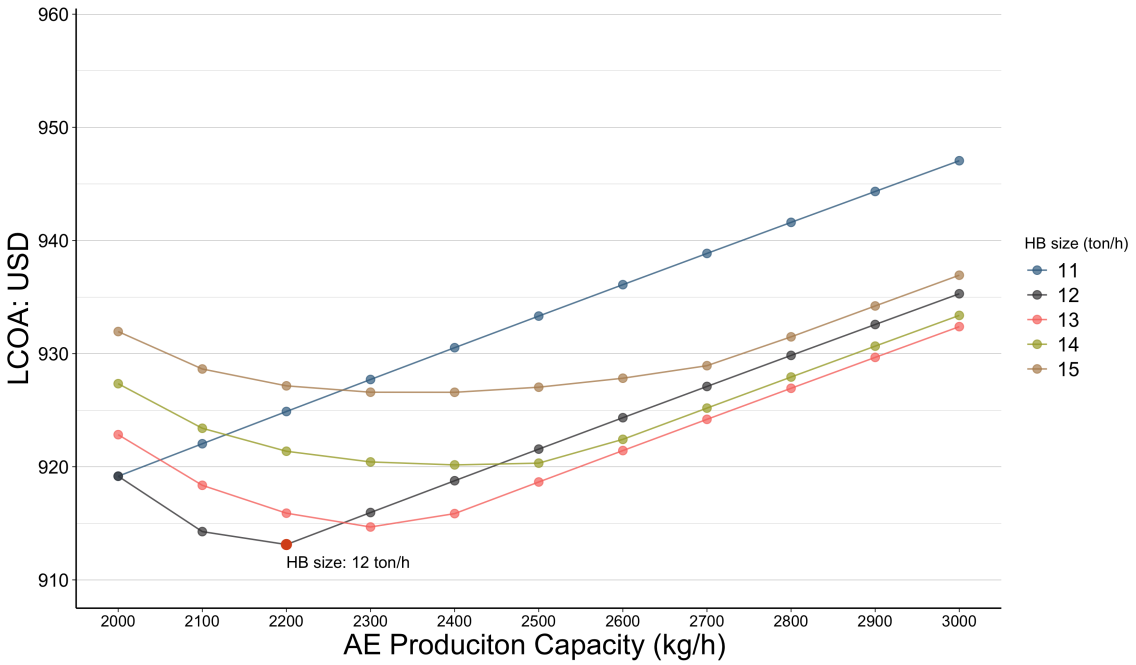


**Figure 5.11:** Relation between AE and HB process size

The results from the figure illustrate that it is beneficial to have excess production capacity to a certain degree: upwards of 20 percent (13 tonne/h) excess production capacity of the HB process. However, the results indicates that the most optimal combination is an HB process with a capacity of 12 tonnes/h combined with an AE of 2 200 kg/h. The other combinations do not yield a lower LCOA, due to the reasons highlighted in Scenario 2.2.

Additionally, there is a trend present where gradual benefits exist for each HB size (except minimum), with an increase in AE size until a threshold is met. Then there is a linear increase as the excess production capacity cannot be utilised by the HB process.

## 5.5 Scenario 3: Reducing minimal load of HB

Scenario 2.2 highlighted that the 50 percent minimal load limitation of the HB process for bigger units. This scenario will therefore focus on investigating the effect of reducing the minimal load for a production capacity of the HB process at 15 tonnes per hour. Given that the previous scenarios demonstrated that hydrogen buffer is not beneficial, the parameters that will be varied are the size of the AE and the minimal load. Additionally, the HB process and ASU will have equal production capacities to those in Scenario 2.2.

Section 3.2.4 stated that it is possible to reduce the minimal load to 20 percent; hence, the range of 20 to 50 percent with a 10 percent increment will be analysed. Given that

the lower minimal load is not widely available, its exact cost is not known. Hence, it is assumed no additional CAPEX will be incurred. Although this is unrealistic, an earlier breakdown of the cost drivers revealed that the HB CAPEX was low compared to total cost. Hence, the modification is believed to have negligible impact on the LCOA. In the figure, the horizontal axis represents the AE size, and the vertical displays LCOA. The different colours represent the different minimal loads for the HB process that is tested.

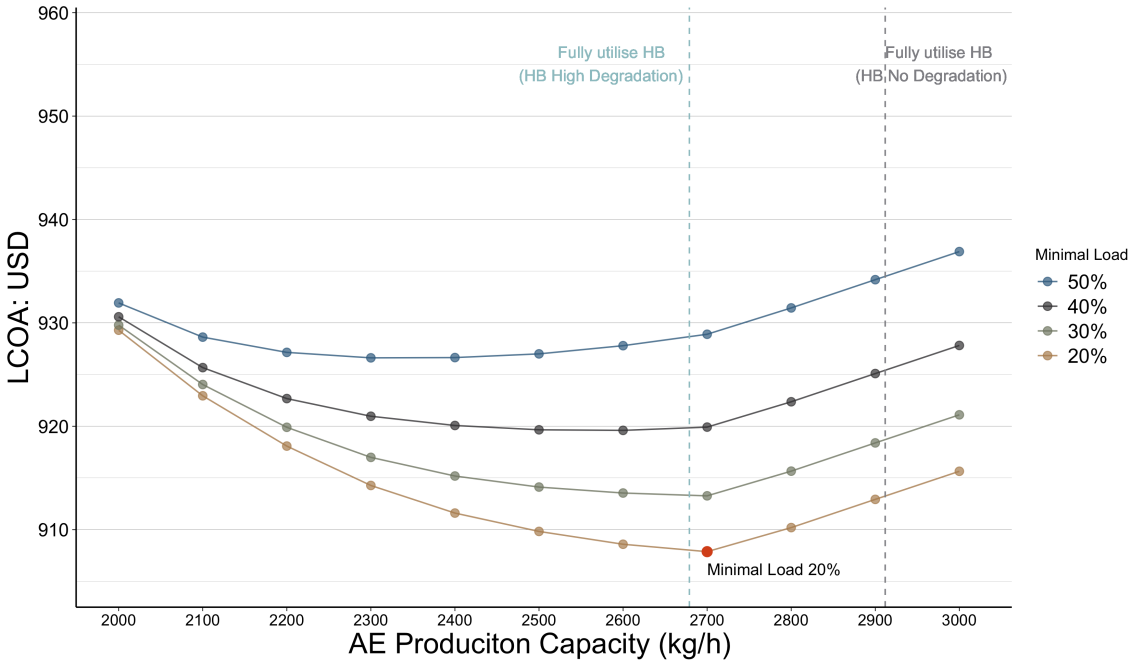


**Figure 5.12:** Scenario 3: LCOA results

The results illustrate a new optimal combination from the introduction of the minimal load. Additionally, it presents cost savings opportunities exceeding those from previous scenarios, resulting in an LCOA of 908 USD per tonne of ammonia, 1,2 percent down from Scenario 1. However, additional CAPEX as a result of the modification is not included. Hence the scenario overstates the reduction. Nevertheless, it is unlikely that all gains will be lost due to the low overall CAPEX of HB process compared to the total.

There is also a trend illustrating increased advantages for larger AE systems. However, the trend disappears after the AE is large enough to let the HB work at full capacity under high degradation. The biggest gain is experienced when the minimum load drops from 50 to 40 percent. Then the benefits become incremental smaller.

Compared to Scenario 2.1, the production capacity of the AE follows a similar ratio compared to the HB process production capacity. The size of the AE is close to the

capacity of the HB process with high degradation. In this scenario, it is slightly bigger compared to Scenario 2.1, where it was slightly smaller.

To better understand the consequences of a reduction in the minimum load, it would be beneficial to analyse the production patterns.

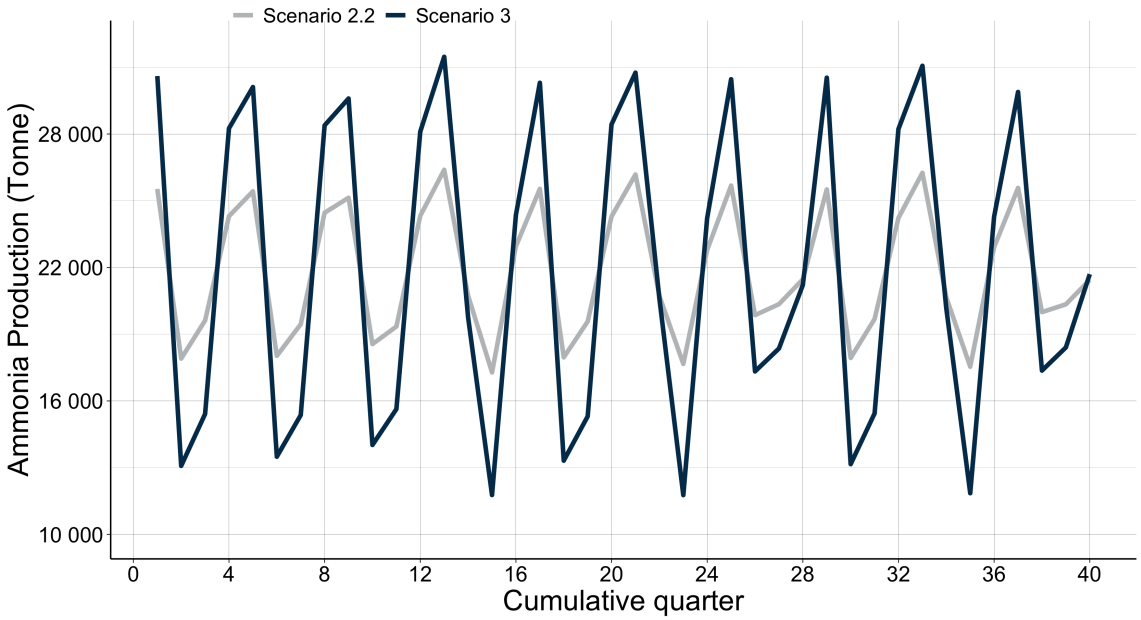


**Figure 5.13:** Scenario 3: Quarterly ammonia production

Although Scenario 2.2 and 3 have identical production capacities for the HB, the variation has expanded greatly in scenario 3 as a result of the reduction of the minimal load level. Hence, the system experience greater freedom to produce during favourable times and less during unfavourable times. These savings are sufficient to cover the added cost and reduce the LCOA to beneficial levels.

To better understand the difference between the two scenarios, analysing the hourly production can give more insights.

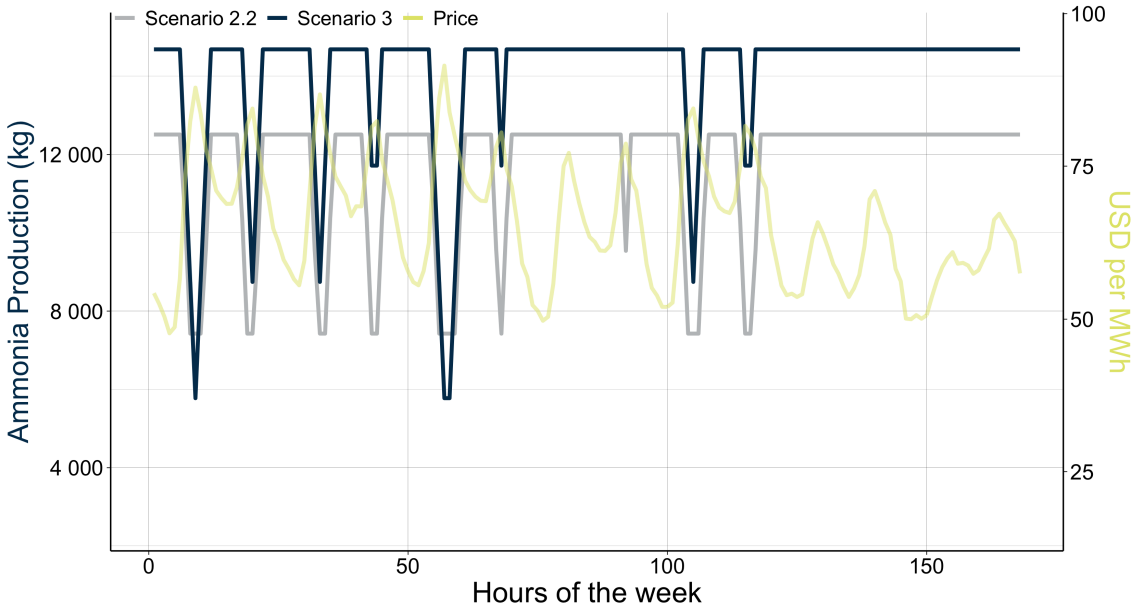


**Figure 5.14:** Production over one week with reduced minimal load

This scenario exhibits similar hourly production patterns compared to Scenario 2.2. However, production is elevated during favourable time periods and decreased during the most unfavourable time periods. This is reasonable, given that the HB process has more flexibility in determining production levels. Nevertheless, there exist other restrictions within the system. The ASU has its own minimal production load constraint of 40 percent, as highlighted in Section 3.2.4. Hence, it constricts the HB process down to around 6 000 kg of ammonia per hour, as illustrated. However, the ASU also has intermediate nitrogen storage it can utilise. Hence, under exceptional circumstances, it can allow for even lower production of the HB process as it can supply excess nitrogen. Given that an analysis of the reduction in ASU minimal load would likely result in similar outcomes, it is excluded from the analysis.

This scenario highlights the benefits of reducing HB's minimal load. This modification has increased the flexibility of the system, allowing for cost savings sufficient enough to reduce LCOA. However, the benefit is likely overstated due to the assumption of no additional CAPEX. Nevertheless, CAPEX of the HB process is a low portion of the overall cost; hence, the modification is seen as beneficial. Moreover, this analysis demonstrates that the limitation of production is not limited to the HB process but also to other units within the system.

## 5.6 Scenario 4: Increased HB ramp rate

This will be a continuation of Scenario 3, with a production capacity of 15 tonnes ammonia per hour and a minimal load of 20 percent. However, the ramp rate will be altered and analysed to determine its effect on the system. A 20 percent minimal load was chosen, as it can benefit the most by an increase ramp rate. With the modification, the system would be able to react to the volatility of electricity prices at a greater rate, introducing savings opportunities. Although there is less evidence in literature that this modification is ready for implementation, it can be educational to understand its effect on cost. It is assumed there is no additional CAPEX for the implication of this modification, similar to the previous scenario. The LCOA graph is repeated, with the modification of replacing the minimum load with the ramp rate. The different colours differentiate them.

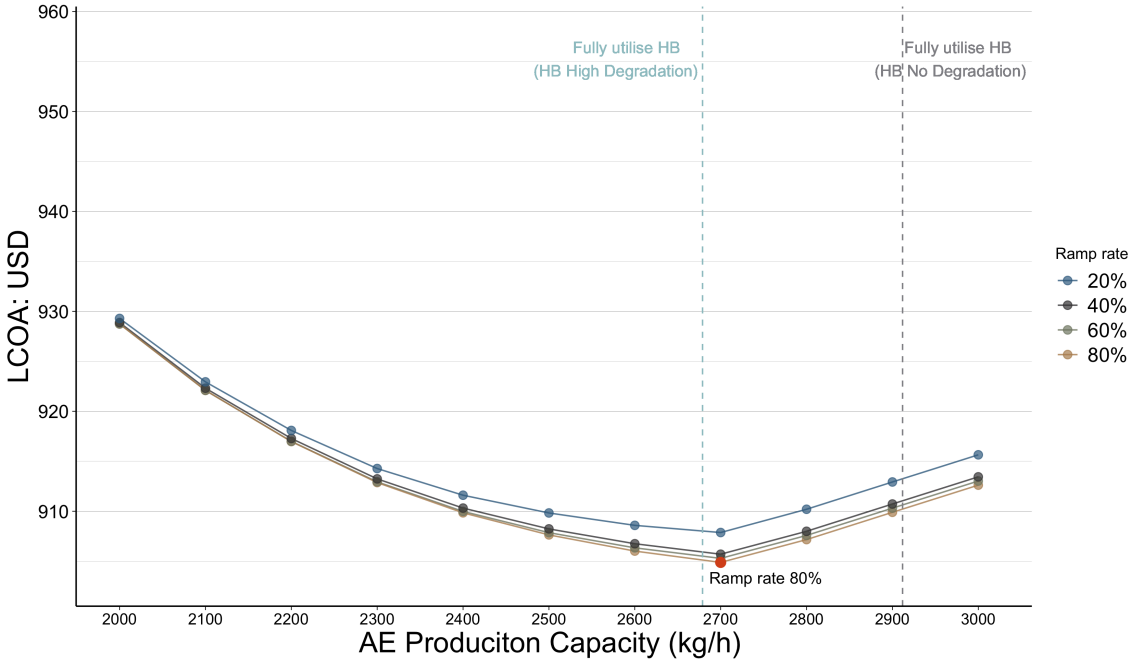


**Figure 5.15:** Scenario 4: LCOA results

The results demonstrate the equal optimal combination as Scenario 3 with a reduction in LCOA when the ramp rate is increased. The LCOA ended at 905 USD per tonne of ammonia, 1,5 percent lower compared to Scenario 1. Furthermore, the majority of reduction is gained by increasing the ramp rate from 20 to 40 percent. Considering the additional CAPEX resulting from this modification, it is uncertain whether it is beneficial to implement. Furthermore, this is based on a scenario where the minimal load is reduced. Hence, the benefit experienced under a less flexible HB process is likely to be even less.

Hence, no further investigation into ramp rates will be performed.

However, it can be beneficial to revisit the relationship between AE and HB production capacity with a reduction of the minimal load and an increased ramp rate for the HB process. Even though the ramp rate did not result in a meaningful reduction in LCOA, it can be beneficial to understand how it affects the relationship between AE production capacity.

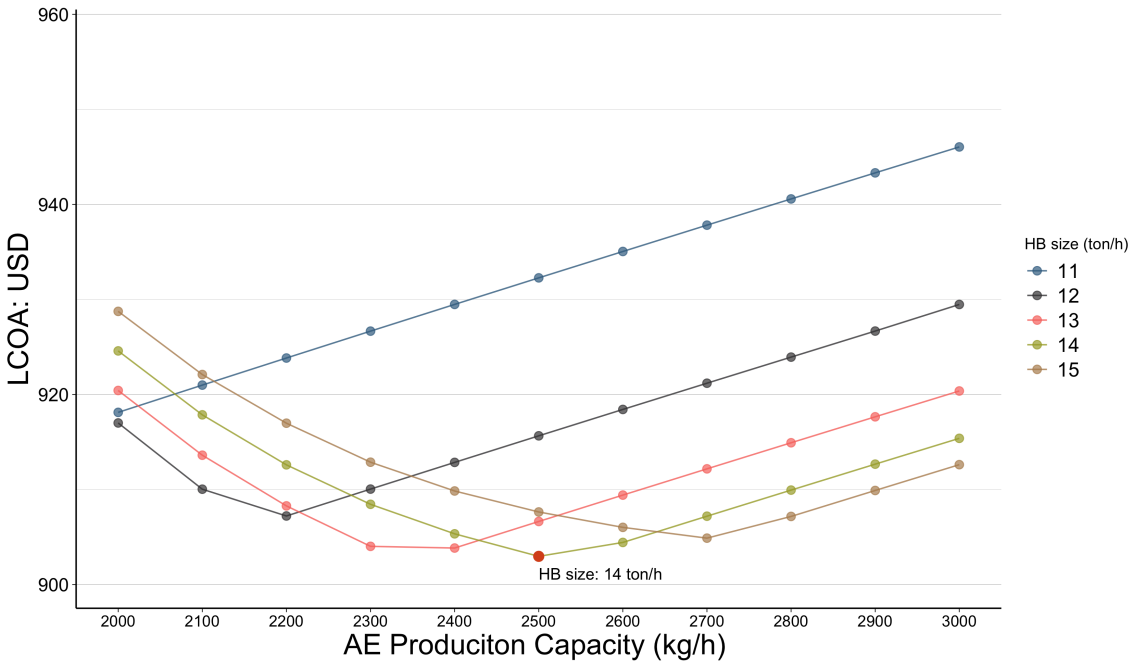


**Figure 5.16:** Relation between AE and HB revisited

The relationship displays similarities to those exhibits in Figure 5.11. However, it is now beneficial with an excess production capacity of up to 30 percent. Additionally, a new optimal combination is found, with a production capacity of 2 500 kg/h for the AE and 14 tonnes of ammonia per hour for the HB. Additionally, the LCOA is reduced from 913 to 904 USD per tonne of ammonia. However, this is likely overstated due to the additional CAPEX required to implement the modifications. Nonetheless, the results illustrate that an increase in HB process flexibility increases the excess production capacity that is beneficial for producing ammonia.

## 5.7 Why buffers are not advantageous

In Scenario 1, 2.1, and 2.2, the most advantageous combination was the absence of intermediate hydrogen storage. Hence, this section is dedicated to understanding the

rational. To make an assessment, three different conditions were created. They are all built on the specifications from Scenario 1, with the biggest AE production capacity and buffer. This combination was selected as it has the biggest potential to use the buffer. The first condition includes the energy requirement highlighted in Section 3.3.1. The second condition requires half the energy of the first condition, and the third condition has no energy requirement to store hydrogen.

The graph below illustrates the distinction between the three conditions. The horizontal axis of the graph indicates the cumulative quarters, while the vertical axis reflects the average utilisation of the storage capacity. The "Normal" line is the first condition, the "Half energy" line is the second condition, and the "No energy" line is the third condition.

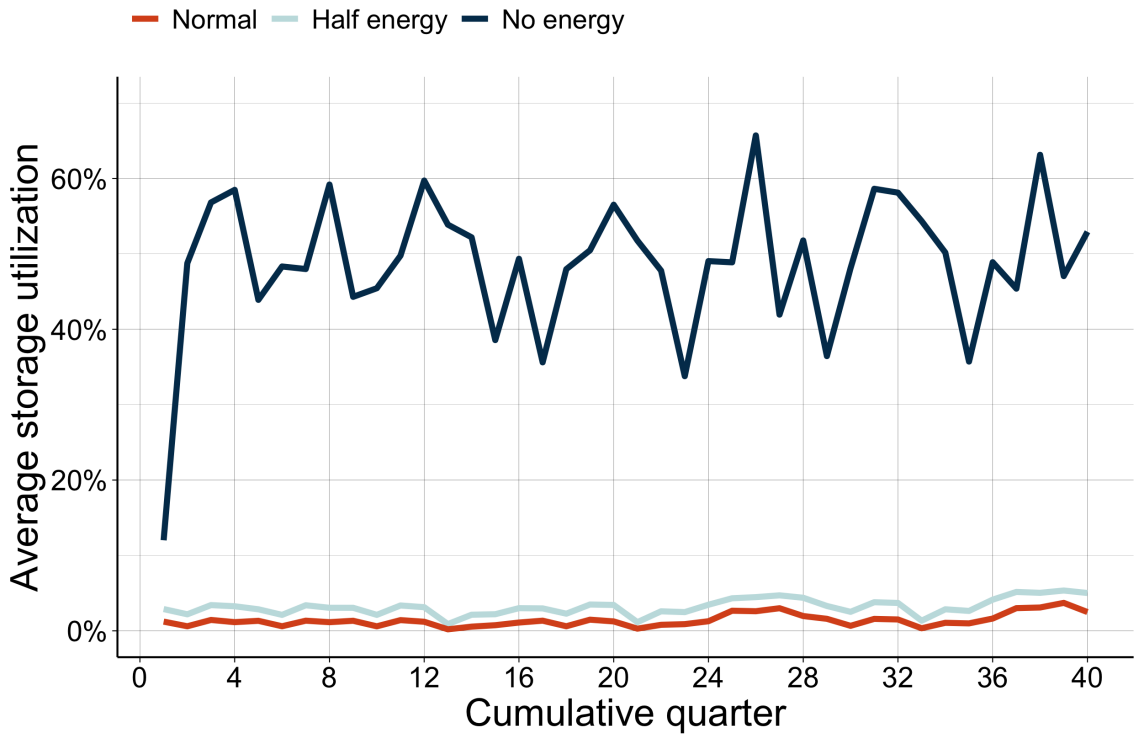


**Figure 5.17:** Storage utilisation

As seen, there exists a significant disparity in the utilisation of storage between the "Normal" and "No energy" conditions. Under normal conditions, there is little or negligible usage of the storage capacity. In comparison, the non-energy requirements condition shows a much larger utilisation of storage capacity. Furthermore, the "Half energy" line exhibits just a marginal increase in storage utilisation compared to the "Normal" line. Therefore, these findings may suggest that the expense associated with hydrogen storage is disproportionately high compared to the potential savings that might be achieved.

By examining the impacts it has on LCOA, a better understanding of the cost can be gained. Given condition one, LCOA is recorded at 958,6 USD per tonne, while given condition two, it is reduced to 951 USD per tonne. But it is not viable compared to the other combinations shown in this analysis. In contrast, under the "No energy" scenario, a significant decrease in LCOA is observed. Given this scenario, the LCOA is decreased to 919 USD per tonne, which aligns with the lowest option for Scenario 1. Therefore, it may be concluded that the energy requirement for storing hydrogen is too high, and not beneficial, resulting in insufficient savings opportunities.

However, the "Normal" condition does utilise the storage to a small degree; in some quarters, buffer utilisation averaged 3 percent. Therefore, there do exist instances within the scenario where volatility may be exploited through the use of buffers. Nevertheless, these occurrences are few and insufficient to provide significant cost reductions. If there is a rise in the frequency of these occurrences, it might be advisable to make use of buffer storage in order to exploit price volatility.

Another observation throughout the analysis is the production variation of the system. Due to degradation, some excess production capacity were implemented to account for the reduction over time. These might function as buffer without the variable cost attached. Instead of producing excess hydrogen during one time period and then add additional cost to store it for later use, the production can occur at times of the most favourable time periods.

## 5.8 Other consideration

During this thesis, some limitations have been identified. Although the effect of LCOA has been identified with the modifications to the production and hydrogen buffer, there might be bias based on the data available. Hence, modifications to these may result in different outcomes from the scenarios highlighted earlier. By altering these parameters, the reliability of the analysis may be assessed. This section will begin by describing the scenarios and then all the different adjustments that require alteration.

For this section, two scenarios will be retested: Scenario 1 and Scenario 4, hereafter referred to as the original and flexible scenarios, respectively. The original scenario served as the foundation for all subsequent assessments. If the outcomes of this sensitivity

analysis significantly deviate from those of the original scenario, it would raise concerns about the reliability of the results. Moreover, a flexibility scenario is included to assess the resilience of the optimal combination in various situations. The changes to LCOA are less important and are mostly used for the purpose of identifying the optimal combination. The parameters requiring adjustments are variations in volatility, a decrease in electricity prices, demand, and the situation of no degradation on the production units.

**Changing volatility**

In the course of the study, a 40 percent increase in volatility was applied to the aggregated data. Forecasting volatility is challenging and warrants a rundown of different volatility scenarios. In Section 3.4.3, three additional data sets of electricity prices were created, involving a 20, 60, and 200 percent increase in volatility. The 200 percent volatility is to test what transpires under extreme volatility. Though this is less realistic, an understanding of the benefit during periods of high volatility might prove useful. To view the difference between these and 40 percent volatility, refer to Figure 3.6.

**Reduced electricity prices**

In this thesis, the forecasted values shown in table 3.3 were used. They are roughly 1.8 times higher than the historical values. As with all forecasted estimations, there are inherent uncertainties in their value, particularly when considering a time frame of 30 years into the future. Therefore, these numbers are divided by 1.8 to establish comparability with historical values. It is not believed that future values will resemble historical values. However, this reduction serves as an analytical tool to examine the influence of the outcome in both scenarios. After reducing the prices, the 40 percent increase in volatility is added, as it was used throughout this analysis.

**Demand**

When designing the model, the assumption of an annual demand was created to better understand the effects of flexibility. Nevertheless, the implementation of this approach may present challenges for ammonia production businesses operating in realistic contexts. Therefore, demand on various time horizons should be included. This may include a weekly, monthly, or quarterly demand. Due to the use of representative weeks, meeting the weekly demand would also facilitate meeting the quarterly requirement. This is because

representative weeks are replicated for all weeks within the quarter. Based on the average production of 10 000 kg of ammonia per hour, as highlighted in Section 4.2, the weekly demand is calculated to be 1 680 000 kg ($10,000kg/h \cdot 24h \cdot 7$). Furthermore, it is necessary to modify the demand constraint outlined in table 4.9.

| Constraint | Sets | Description |
|---|---|---|
| $\sum_{h \in H} z_{NH_3,y,q,h} \geq d$ | $\forall y \in Y$<br>$\forall q \in Q$ | Weekly ammonia demand must be met |

**Table 5.2:** Changing demand constraint

**No degradation**

The base case highlighted the presence of a small excess production capacity in years of minimal degradation. Given the surplus production capacity, it has the potential to operate as a hydrogen buffer without incurring variable costs, thereby making hydrogen storage economically disadvantageous. Hence, it may be beneficial to examine the results in the absence of any kind of degradation. Although the scenario is not realistic, its purpose is to examine the potential consequences of operating HB at full capacity over extended periods of time. In the absence of degradation, it is necessary to reduce the production capacity of HB and ASU to meet the required level of demand. This approach enables the consistent production level of ammonia regardless of fluctuations in electricity prices. The AE will retain the same capacity range as previously. The parameters of the flexible model will remain unaltered since it has excess manufacturing capacity.

### 5.8.1 Outcomes

The outcomes from the adjustments of the highlighted are presented in two parts. First, examination of the different outcomes for the original scenario is conducted, then the flexible scenario is analysed.

**Original**

In order to facilitate an assessment of the various effects, the original scenario is presented with its outcome alongside the adjusted parameters.

| Scenario | LCOA (per Mt) | AE size kg/h | $H_2$ buffer size (kg) |
|---|---|---|---|
| **Original** | **919,165** | **2.000** | **0** |
| Volatility 20% | 905,777 | 2.000 | 0 |
| Volatility 60% | 932,551 | 2.000 | 0 |
| Extreme volatility | 1023.81 | 2 500 | 7040 |
| Reduced price | 659,147 | 2.000 | 0 |
| Weekly demand | 919,788 | 2.000 | 0 |
| No degradation | 923,395 | 2.000 | 0 |

**Table 5.3:** Sensitivity original model

All scenarios in the sensitivity analysis provide identical combinations to those in the original scenario, with the exception of the extreme volatility. The optimal combination for them is the absence of a buffer and no excess production capacity of the AE when there is no excess production capacity of the HB. One significant discovery from this thesis is therefore that the use of intermediate hydrogen storage does not provide advantageous outcomes in terms of LCOA. The exception is when there are time periods with extreme volatility. In these scenarios, it is advantageous to have a small buffer to compensate for the extreme volatility. Additionally, higher AE capacity is beneficial as well.

One observation from the table is that LCOA is reduced when volatility is reduced and increases when volatility is increased. This seems reasonable, given that the HB exhibits less flexibility and necessitates continuous production throughout all time periods. Another discovery is that a reduction in electricity prices leads to a significant decrease in the LCOA. Moreover, when the demand is changed from annual to weekly, the resulting change in LCOA is insignificant. This is reasonable due to the already limited production variation seen in the original scenario.

**Flexible**

The presented table displays the outcomes of the flexible scenario along with the adjustments present. This enables an evaluation the impacts the different scenarios have.

| Scenario | LCOA (per Mt) | AE size kg/h | $H_2$ storage size |
|---|---|---|---|
| **Flexible HB** | **904,879** | **2.700** | **0** |
| Volatility 20% | 899,088 | 2.700 | 0 |
| Volatility 60% | 910,792 | 2.700 | 0 |
| Extreme volatility | 951,796 | 2.700 | 0 |
| Reduced price | 644,824 | 2.700 | 0 |
| Weekly demand | 919,599 | 2.700 | 0 |
| No degradation | 902,236 | 2.700 | 0 |

**Table 5.4:** Sensitivity Flexible HB model

Similarly to the original scenario, it is observed that the optimal combinations remain consistent across all scenarios. Even under extreme volatility, the optimal combination didn't change as it did in the original scenario. This finding reinforces the argument that intermediate hydrogen storage is too expensive to be advantageous. The real benefit is the excess production capacity. More accurately, the presence of surplus production capacity in AE becomes advantageous when there is excess production capacity in HB and ASU.

The observed pattern of LCOA remains consistent with the findings of the original scenario. One notable pattern seen in this sensitivity analysis is the rise in LCOA when the demand is altered from an annual to a weekly basis. Nevertheless, the LCOA value remains similar to the one presented in the previous sensitivity analysis, as seen in Table 5.3. It could be argued that with similar cost, more flexibility is beneficial if there were great opportunity to exploit time periods with exceptional electricity prices. However, this scenario does not include the CAPEX of the additional modifications. Hence, it might be less beneficial if CAPEX is significant.

# 6 Discussion

Upon the completion of the analysis, discussion of the findings is necessary. This chapter starts by providing context for the results by comparing them to existing scientific literature in Section 6.1. Then the limitations and their consequences are highlighted in Section 6.2. Lastly, further studies are presented in Section 6.3.

## 6.1 Contextualise results

While the results have been described in the previous chapter, it is still essential to evaluate their alignment with the existing research.

The LCOA results highlighted in this thesis vary between 904 and 951 USD per tonne of ammonia and are on the higher end of the estimate given by Cesaro et al. (2021). In their estimations, the LCOA ranges between 500 and 1 000 USD per tonne in the year 2020, with their base case at around 780 USD per tonne of ammonia. Furthermore, they forecast that LCOA in 2025 will be within the range of 400 to 850 USD per tonne. Hence, the estimation is at the higher end of their estimation. However, they had to utilise hydrogen storage in order to mitigate the variability of solar energy. Hence, the estimations from this study are understated compared to theirs, as hydrogen storage is expensive. However, they had a different structure compared to this thesis, making a direct comparison difficult (Cesaro et al., 2021).

Bose et al. (2022) aimed to estimate the differences between two scenarios. The first scenario relied solely on RE, while the other was only connected to the grid, similar to this thesis. In their estimation, they found an LCOA of 970 to 1 200 USD per tonne of ammonia when the system relied on only RE. When the system was connected to the grid, it was within the range of 540 to 640 USD per tonne, which is significantly lower than the estimations in this thesis. However, their electricity cost was lower than the historical values provided in this thesis. Upon reducing the electricity prices to historical values, the estimates are close to their interval of 659 USD per tonne. Additionally, the cost structure from this thesis is proportional to their (Bose et al., 2022).

The findings from this thesis are that excess production capacity is beneficial, while

hydrogen storage is not. The degree of excess production depends on the flexibility of the system. For instance, when no modifications to the capabilities of the HB process were made, a 10 percent increase was the most beneficial. With the modifications, a 30 percent overcapacity was the most beneficial. Nevertheless, excess production capacity was beneficial and coincided with the findings from Armijo and Philibert (2020) that indicated an overcapacity of the HB process of 13 to 31 percent (Armijo & Philibert, 2020). Furthermore, the absence of hydrogen was the optimal choice, which is also the consensus of the literature (Armijo & Philibert, 2020; Bose et al., 2022; Cesaro et al., 2021).

## 6.2 Limitation

Throughout the thesis, certain limitations have been brought up. Though a portion has been addressed in the previous chapter, some remain overlooked. This section will present the primary elements that may operate as limitations. Each limitation will be explained, and its potential influence on the analysis will be discussed.

**Implication of data uncertainty**

All data used in this thesis exhibit some degree of uncertainty. For instance, when determining CAPEX of the AE, a broad cost estimation technique was used instead of a detailed analysis of each component. Consequently, the cost will be contingent upon the particular details of each individual project. One of the primary sources of uncertainty is in the long-term forecasting of electricity costs. Nevertheless, the optimal combination was unaltered when adjusting for the price. The significance of electricity price is therefore less than first perceived.

The volatility of electricity costs is likely the most prominent factor. If the adoption of renewable energy sources continues to grow without the availability of a cost-effective alternative for peak shaving, an increase in volatility is likely. However, in the event of a significant advancement in fusion power or a comparable technological, it is plausible that the level of volatility may diminish. Nevertheless, a different volatility scenario reveals that in all scenarios, flexibility is advantageous.

**Implication of using representative time periods**

It has been emphasised that the use of representative time periods results in statistical errors, and in our case, the volatility was reduced. To compensate for the reduction, greater volatility was implemented in the aggregated data. However, extreme volatility was still removed. To better understand how extreme volatility affects the data, a scenario was created. When tested, the optimal solution for the flexible model was not altered, but it was for the original. However, it is unlikely to have this level of volatility over a thirty-year period. Hence, the statistical errors have a low impact on the outcome of the analysis.

**Implication of ammonia sold as its produced**

In the analysis, it is assumed that ammonia is sold to consumers right after it is produced. Though this simplifies the analysis, it avoids the additional CAPEX cost of ammonia storage. However, CAPEX has a limited effect on LCOA, as shown in the breakdown of the cost drivers. Hence, it is unlikely that it would alter the results of the analysis.

**Implication of flat demand**

Another limitation is the assumption of flat demand. Though a flat demand serves to simplify the model and analysis, it can impact the results of the study. There might be seasonality across different days, weeks, months, quarters, and so forth. With significant seasonality in demand, it could alter the production pattern previously observed. Consequently, this has the potential to alter the results of the analysis. Although the sensitivity analysis altered annual to weekly demand, it did not address the issue of flat demand.

Another concern is the flat demand used for the time period of the analysis, despite projections indicating growth in the future. Nevertheless, there are uncertainties associated with forecasted values. The rate of demanded growth is dependent upon the characteristics of the current market and the adaptation of its potential. Incorporating demand growth could alter the results but also introduce more uncertainty. For analytic purposes in this thesis, it is more prudent to exclude it.

**Continuously running HB process**

Initially, deactivation of the HB was incorporated. However, the computational demand was too high. One potential outcome is that the study may provide other optimal solutions. However, findings derived from the analysis indicate advantageous outcomes when system flexibility is increased. Therefore, the incorporation of deactivation is unlikely to provide alternative discoveries.

Moreover, stops due to maintenance or the replacement of wearable components is not modelled. Although this representation does not accurately depict the system, its effects on the findings are likely to be insignificant.

**Implication of total knowledge**

Another limitation is that the electricity prices are predetermined, while this information is not easily available for management. Although the sensitivity analysis reveals comparable outcomes between the original and flexible scenarios when weekly demand is met, replicating the production pattern may still provide challenges for management. Therefore, the advantages of flexibility may be lost, resulting in increased cost.

## 6.3 Further Studies

Two limitations were identified to have the potential to impact the findings from this thesis: flat demand and total knowledge of cost. Given that management lacks knowledge of future electric prices, it might be difficult to replicate the benefits illustrated in this thesis. Additionally, fluctuating demand complicates the matter even further. Hence, future studies should focus on management's ability to utilise the added flexibility to investigate if they are able to offset the added cost of the system when demand is fluctuating.

Another study can build further upon the model to investigate how different aspects influence the optimal combination. For instance, how does the option of buying hydrogen and nitrogen affect the optimal combination? There might exist time periods where it is more expensive to produce the process mediums than to buy them. Additionally, how will the option of selling the process mediums that have been disregarded in this thesis, such as oxygen and argon, affect the optimal combination?

# 7 Conclusion

The objective of this thesis has been to study how increased flexibility can leverage energy price fluctuations in order to reduce the levelized cost of ammonia. In the context of this thesis, flexibility refers to alterations in the production capacity of the production units, their capabilities, and the utilisation of intermediate storage. In order to accomplish this objective, relevant data were gathered and implemented into a multi-period, mixed-integer linear optimisation model (MILP). Then various alterations were implemented and evaluated in order to examine their respective impact.

The findings indicates that excess production capacity proves beneficial. More precisely, with an increase in the production capacity of the HB and ASU, an increase in AE becomes beneficial. However, increasing the production capacity to excessive levels, further increases the levelized cost of ammonia. This as a consequence of the capabilities in the system, such as the minimum load. Our findings further indicate that higher excess production capacity is beneficial, if the capabilities of the system is improved. Additionally, there appears to exist a correlation between the production capacity of the HB and the AE, given a suitable increase. We find that in the optimal production state, AE should supply the HB with hydrogen equal to HB's available capacity given high degradation (the lowest capacity of its lifetime). Moreover, the use of hydrogen storage is deemed too expensive due to its high energy consumption.

We find that increased flexibility is able to offset the added cost accrued, while also reducing the LCOA by increasing production during favourable periods and decreasing it during unfavourable periods. However, this adaptability is only slightly beneficial with a limited decreased LCOA of 1,5 percent. By improving the capabilities, especially when decreasing the minimum load, we observe even more increased production during favourable periods and less during unfavourable periods.

These findings indicates that increased flexibility in the ammonia synthesis makes green ammonia a more competitive product, as it can more efficiently scale in line with the fluctuations in the electricity market. While this increased competitiveness provides only a marginal benefit of 1.5 percent. More efforts should be used in researching the possibilities of decreasing the minimum load, as this had a bigger effect on cost savings compared to

the ramp rate.

The findings of our study indicate that enhanced flexibility is beneficial for green ammonia production. However, it is important to acknowledge the limitations. Firstly, an annual demand is assumed, and seasonal variations are not accounted for. If these were to be implemented, they might potentially alter the findings of this analysis as different production outputs are needed. Furthermore, the analysis has total information on future electricity prices, which is unrealistic when management plans production. Therefore, future research should focus on these limitations.

# References

Abdin, Z., Khalilpour, K., & Catchpole, K. (2022). Projecting the levelized cost of large scale hydrogen storage for stationary applications. *Energy Conversion and Management*, *270*, 116241. https://doi.org/10.1016/j.enconman.2022.116241

Angeles-Olvera, Z., Crespo-Yapur, A., Rodríguez, O., Cholula-Díaz, J. L., Martínez, L. M., & Videa, M. (2022). Nickel-based electrocatalysts for water electrolysis. *Energies*, *15*(5). https://doi.org/10.3390/en15051609

Armijo, J., & Philibert, C. (2020). Flexible production of green hydrogen and ammonia from variable solar and wind energy: Case study of chile and argentina. *International Journal of Hydrogen Energy*, *45*(3), 1541–1558. https://doi.org/10.1016/j.ijhydene.2019.11.028

Attari Moghaddam, A., & Krewer, U. (2020). Poisoning of ammonia synthesis catalyst considering off-design feed compositions. *Catalysts*, *10*(11). https://doi.org/10.3390/catal10111225

Basán, N. P., Cóccola, M. E., Dondo, R. G., Guarnaschelli, A., Schweickardt, G. A., & Méndez, C. A. (2020). A reactive-iterative optimization algorithm for scheduling of air separation units under uncertainty in electricity prices. *Computers and Chemical Engineering*, *142*, 107050. https://doi.org/10.1016/j.compchemeng.2020.107050

Bjørnflaten, F. M. (2022). *Finland, denmark and sweden leading on the green revolution*. Retrieved July 12, 2023, from https://www.rystadenergy.com/news/finland-denmark-and-sweden-leading-on-the-green-revolution

Bose, A., Lazouski, N., Gala, M. L., Manthiram, K., & Mallapragada, D. S. (2022). Spatial variation in cost of electricity-driven continuous ammonia production in the united states. *ACS Sustainable Chemistry and Engineering*, *10*(24), 7862–7872. https://doi.org/10.1021/acssuschemeng.1c08032

Brinks, H., & Chryssakis, C. (2022). *Smells like sustainability: Harnessing ammonia as ship fuel*. Retrieved July 10, 2023, from https://www.dnv.com/expert-story/maritime-impact/Harnessing-ammonia-as-ship-fuel.html

Buttler, A., & Spliethoff, H. (2018). Current status of water electrolysis for energy storage, grid balancing and sector coupling via power-to-gas and power-to-liquids: A review. *Renewable and Sustainable Energy Reviews*, *82*, 2440–2454. https://doi.org/10.1016/j.rser.2017.09.003

Carmo, M., Fritz, D. L., Mergel, J., & Stolten, D. (2013). A comprehensive review on pem water electrolysis. *International Journal of Hydrogen Energy*, *38*(12), 4901–4934. https://doi.org/10.1016/j.ijhydene.2013.01.151

Cesaro, Z., Ives, M., Nayak-Luke, R., Mason, M., & Bañares-Alcántara, R. (2021). Ammonia to power: Forecasting the levelized cost of electricity from green ammonia in large-scale power plants. *Applied Energy*, *282*, 116009. https://doi.org/10.1016/j.apenergy.2020.116009

Cheddie, D. (2012). Ammonia as a hydrogen source for fuel cells: A review. *Centre for Energy Studies, Univerity of Trinidad and Tobago*, 333–360. https://doi.org/http://dx.doi.org/10.5772/47759

Chehade, Z., Mansilla, C., Lucchese, P., Hilliard, S., & Proost, J. (2019). Review and analysis of demonstration projects on power-to-x pathways in the world. *International Journal of Hydrogen Energy*, *44*(51), 27637–27655. https://doi.org/10.1016/j.ijhydene.2019.08.260

Cheng, M., Verma, P., Yang, Z., & Axelbaum, R. L. (2022). Flexible cryogenic air separation unit—an application for low-carbon fossil-fuel plants. *Separation and Purification Technology*, *302*, 122086. https://doi.org/10.1016/j.seppur.2022.122086

Damodaran, A. (2023). *Betas by sector (us)*. Retrieved July 4, 2023, from https://pages.stern.nyu.edu/~adamodar/New_Home_Page/datafile/Betas.html

Danish Energy Agency. (2017). *Energy statistics 2015* (tech. rep.). Danish Energy Agency.

Danish Ministry of Climate, Energy and Utilities. (2021). *The governments strategy fo power-to-x*. Retrieved June 10, 2023, from https://ens.dk/sites/ens.dk/files/ptx/strategy_ptx.pdf

Dawood, F., Anda, M., & Shafiullah, G. (2020). Hydrogen production for energy: An overview. *International Journal of Hydrogen Energy*, *45*(7), 3847–3869. https://doi.org/10.1016/j.ijhydene.2019.12.059

Devkota, S., Ban, S., Shrestha, R., & Uprety, B. (2023). Techno-economic analysis of hydropower based green ammonia plant for urea production in nepal. *International Journal of Hydrogen Energy*, *48*(58), 21933–21945. https://doi.org/10.1016/j.ijhydene.2023.03.087

Dincer, I. (2012). Green methods for hydrogen production [10th International Conference on Clean Energy 2010]. *International Journal of Hydrogen Energy*, *37*(2), 1954–1971. https://doi.org/10.1016/j.ijhydene.2011.03.173

Econnect Energy. (n.d.). *Ammonia*. Retrieved July 8, 2023, from https://www.econnectenergy.com/markets/the-ammonia-market

EERE. (n.d.). *Hydrogen storage*. Retrieved August 12, 2023, from https://www.energy.gov/eere/fuelcells/hydrogen-storage

Energinet. (2022). *Development of energinet's tariff design* (tech. rep.). Energinet.

Energinet. (2023). Forsyningstilsynet har godkendt ny model for energinets systemtarif. Retrieved July 10, 2023, from https://energinet.dk/om-nyheder/nyheder/2023/06/23/forsyningstilsynet-har-godkendt-ny-model-for-energinets-systemtarif/

Energistyrelsen. (n.d.-a). *Analyseforudsætninger til energinet*. Retrieved March 22, 2023, from https://ens.dk/service/fremskrivninger-analyser-modeller/analyseforudsaetninger-til-energinet

Energistyrelsen. (n.d.-b). *Power-to-x*. Retrieved May 19, 2023, from https://ens.dk/en/our-responsibilities/power-x

Energistyrelsen. (2021). *Denmark decides to construct the world's first windenergy hub as an artificial island in the north sea*. Retrieved June 19, 2023, from https://ens.dk/en/press/denmark-decides-construct-worlds-first-windenergy-hub-artificial-island-north-sea

Eurowind Energy. (n.d.). *Power-to-x (ptx): An enabler of the future*. Retrieved September 9, 2023, from https://eurowindenergy.com/power-to-x-ptx

Fasihi, M., Weiss, R., Savolainen, J., & Breyer, C. (2021). Global potential of green ammonia based on hybrid pv-wind power plants. *Applied Energy*, *294*, 116170. https://doi.org/10.1016/j.apenergy.2020.116170

Flavell-While, C. (2010). *Fritz haber and carl bosch – feed the world*. https://www.thechemicalengineer.com/features/cewctw-fritz-haber-and-carl-bosch-feed-the-world/

Fu, C., & Gundersen, T. (2013). Recuperative vapor recompression heat pumps in cryogenic air separation processes. *Energy*, *59*, 708–718. https://doi.org/10.1016/j.energy.2013.06.055

Fúnez Guerra, C., Reyes-Bozo, L., Vyhmeister, E., Jaén Caparrós, M., Salazar, J. L., & Clemente-Jul, C. (2020). Technical-economic analysis for a green ammonia production plant in chile and its subsequent transport to japan. *Renewable Energy*, *157*, 404–414. https://doi.org/10.1016/j.renene.2020.05.041

Ghavam Seyedehhoma, W. I. A. G., Vahdati Maria, & Peter, S. (2021). Sustainable ammonia production processes. *Frontiers in Energy Research*, *9*. https://doi.org/10.3389/fenrg.2021.580808

Givens, D. (2022). *A nasa-backed study will test ammonia as a carbon-free alternative to jet fuel*. Retrieved July 10, 2023, from https://robbreport.com/motors/aviation/nasa-ammonia-alternative-fuel-study-1234735414/

Gomez, J. R., Baca, J., & Garzon, F. (2020). Techno-economic analysis and life cycle assessment for electrochemical ammonia production using proton conducting membrane. *International Journal of Hydrogen Energy*, *45*(1), 721–737. https://doi.org/10.1016/j.ijhydene.2019.10.174

Green Hydrogen Webinars. (n.d.). *About green hydrogen*. Retrieved July 4, 2023, from https://www.sintef.no/projectweb/greenh2webinars/about-green-hydrogen/

Gutiérrez-Martín, F., Ochoa-Mendoza, A., & Rodríguez-Antón, L. (2015). Pre-investigation of water electrolysis for flexible energy storage at large scales: The case of the spanish power system. *International Journal of Hydrogen Energy*, *40*(15), 5544–5551. https://doi.org/10.1016/j.ijhydene.2015.01.184

Hargrave, M. (2023). *Weighted average cost of capital (wacc) explained with formula and example*. Retrieved July 4, 2023, from https://www.investopedia.com/terms/w/wacc.asp

Hayes, A. (2023). *Co-efficient of variation meaning and how to use it*. Retrieved July 29, 2023, from https://www.investopedia.com/terms/c/coefficientofvariation.asp

HØST PtX Esbjerg. (n.d.). *About the plant*. Retrieved July 18, 2023, from https://hoestptxesbjerg.dk/about-ptx/

Humphreys, J., Lan, R., & Tao, S. (2021). Development and recent progress on ammonia synthesis catalysts for haber–bosch process. *Advanced Energy and Sustainability Research*, *2*(1), 2000043. https://doi.org/10.1002/aesr.202000043

IEA. (n.d.). *Global energy crisis*. Retrieved July 6, 2023, from https://www.iea.org/topics/global-energy-crisis

IEA. (2021a). *Ammonia technology roadmap* (tech. rep.) [https://www.iea.org/reports/ammonia-technology-roadmap]. IEA.

IEA. (2021b). *Ammonia technology roadmap, executive summary* (tech. rep.) [https://www.iea.org/reports/ammonia-technology-roadmap/executive-summary]. IEA.

IEA. (2021c). *Danmark, country profile*. Retrieved April 12, 2023, from https://www.iea.org/countries/denmark

IEA. (2022a). *Global hydrogen review 2022* (tech. rep.) [https://www.iea.org/reports/global-hydrogen-review-2022]. IEA.

IEA. (2022b). *Wind electricity* (tech. rep.) [https://www.iea.org/reports/wind-electricity]. IEA.

Ikäheimo, J., Kiviluoma, J., Weiss, R., & Holttinen, H. (2018). Power-to-ammonia in future north european 100 % renewable power and heat system. *International Journal of Hydrogen Energy*, *43*(36), 17295–17308. https://doi.org/10.1016/j.ijhydene.2018.06.121

Juangsa, F. B., Irhamna, A. R., & Aziz, M. (2021). Production of ammonia as potential hydrogen carrier: Review on thermochemical and electrochemical processes. *International Journal of Hydrogen Energy*, *46*(27), 14455–14477. https://doi.org/10.1016/j.ijhydene.2021.01.214

Kenton, W. (2023). *Cost of equity definition, formula, and example*. Retrieved July 4, 2023, from https://www.investopedia.com/terms/c/costofequity.asp

Kuckshinrichs, W., Ketelaer, T., & Koj, J. C. (2017). Economic analysis of improved alkaline water electrolysis. *Frontiers in Energy Research*, *5*. https://doi.org/10.3389/fenrg.2017.00001

Lan, R., & Tao, S. (2014). Ammonia as a suitable fuel for fuel cells. *Frontiers in Energy Research*, *2*. https://doi.org/10.3389/fenrg.2014.00035

Liu, T., Wang, X., Jiang, X., Deng, C., Niu, S., Mao, J., Zeng, W., Liu, M., & Liao, H. (2023). Mechanism of corrosion and sedimentation of nickel electrodes for alkaline water electrolysis. *Materials Chemistry and Physics*, *303*, 127806. https://doi.org/10.1016/j.matchemphys.2023.127806

Lubitz, W., & Tumas, W. (2007). Hydrogen: An overview [PMID: 17927154]. *Chemical Reviews*, *107*(10), 3900–3903. https://doi.org/10.1021/cr050200z

Marini, S., Salvi, P., Nelli, P., Pesenti, R., Villa, M., Berrettoni, M., Zangari, G., & Kiros, Y. (2012). Advanced alkaline water electrolysis. *Electrochimica Acta*, *82*, 384–391. https://doi.org/10.1016/j.electacta.2012.05.011

Matute, G., Yusta, J., & Correas, L. (2019). Techno-economic modelling of water electrolysers in the range of several mw to provide grid services while generating hydrogen for different applications: A case study in spain applied to mobility with fcevs. *International Journal of Hydrogen Energy*, *44*(33), 17431–17442. https://doi.org/10.1016/j.ijhydene.2019.05.092

Miller, J., Luyben, W. L., Belanger, P., Blouin, S., & Megan, L. (2008). Improving agility of cryogenic air separation plants. *Industrial & Engineering Chemistry Research*, *47*(2), 394–404. https://doi.org/10.1021/ie070975t

Ministry of Foreign Affairs of Denmark. (n.d.-a). *Denmark's huge power-to-x potential*. https://investindk.com/set-up-a-business/cleantech/power-to-x

Ministry of Foreign Affairs of Denmark. (n.d.-b). *Denmark's huge power-to-x potential*. Retrieved July 5, 2023, from https://investindk.com/set-up-a-business/cleantech/power-to-x

Nayak-Luke, R. M., & Bañares-Alcántara, R. (2020). Techno-economic viability of islanded green ammonia as a carbon-free energy vector and as a substitute for conventional production. *Energy Environ. Sci.*, *13*, 2957–2966. https://doi.org/10.1039/D0EE01707H

Nord Pool. (2023). *Day-ahead prices*. Retrieved May 31, 2022, from https://www.nordpoolgroup.com/en/Market-data1/Dayahead/Area-Prices/ALL1/Hourly/?view=table

Nosherwani, S. A., & Neto, R. C. (2021). Techno-economic assessment of commercial ammonia synthesis methods in coastal areas of germany. *Journal of Energy Storage*, *34*, 102201. https://doi.org/10.1016/j.est.2020.102201

NVE. (2023). The WACC-model kernel description [Accessed: 2023-07-04]. https://www.nve.no/norwegian-energy-regulatory-authority/economic-regulation/the-wacc-model/

Ofori-Bah, C. O., & Amanor-Boadu, V. (2023). Directing the wind: Techno-economic feasibility of green ammonia for farmers and community economic viability.

*Frontiers in Environmental Science*, *10*. https://doi.org/10.3389/fenvs.2022.1070212

Okonkwo, P. C., Barhoumi, E. M., Ben Belgacem, I., Mansir, I. B., Aliyu, M., Emori, W., Uzoma, P. C., Beitelmal, W. H., Akyüz, E., Radwan, A. B., & Shakoor, R. (2023). A focused review of the hydrogen storage tank embrittlement mechanism process. *International Journal of Hydrogen Energy*, *48*(35), 12935–12948. https://doi.org/https://doi.org/10.1016/j.ijhydene.2022.12.252

Olabi, A., Abdelkareem, M. A., Al-Murisi, M., Shehata, N., Alami, A. H., Radwan, A., Wilberforce, T., Chae, K.-J., & Sayed, E. T. (2023). Recent progress in green ammonia: Production, applications, assessment; barriers, and its role in achieving the sustainable development goals. *Energy Conversion and Management*, *277*, 116594. https://doi.org/10.1016/j.enconman.2022.116594

Parra, D., Valverde, L., Pino, F. J., & Patel, M. K. (2019). A review on the role, cost and value of hydrogen energy systems for deep decarbonisation. *Renewable and Sustainable Energy Reviews*, *101*, 279–294. https://doi.org/10.1016/j.rser.2018.11.010

Pattabathhula, V., & Richardson, J. (2016). Introduction to ammonia production. *American Institute of Chemical Engineers (AIChE)*, 69–75. https://www.google.com/url?sa=t&rct=j&q=&esrc=s&source=web&cd=&ved=2ahUKEwi0tt6f-5eAAxWh_7sIHVpiASEQFnoECCcQAQ&url=https%3A%2F%2Fwww.aiche.org%2Fsites%2Fdefault%2Ffiles%2Fcep%2F20160969.pdf&usg=AOvVaw3xxxnYxp4WMOd7_kzo6twy&opi=89978449

Pedersen, O. P. (2021). *Danmark seiler opp som europas stormakt på strøm. blir norge akterutseilt?* Retrieved July 12, 2023, from https://www.tu.no/artikler/danmark-seiler-opp-som-europas-stormakt-pa-strom-blir-norge-akterutseilt/506428

Proost, J. (2019). State-of-the art capex data for water electrolysers, and their impact on renewable hydrogen price settings [European Fuel Cell Conference and Exhibition 2017]. *International Journal of Hydrogen Energy*, *44*(9), 4406–4413. https://doi.org/10.1016/j.ijhydene.2018.07.164

PWC. (2022). *Risikopremien i det norske markedet*. Retrieved July 4, 2023, from https://www.pwc.no/no/publikasjoner/risikopremien.html

Quarshie, A. W. K., Swartz, C. L. E., Madabhushi, P. B., Cao, Y., Wang, Y., & Flores-Cerrillo, J. (2023). Modeling, simulation, and optimization of multiproduct cryogenic air separation unit startup. *AIChE Journal*, *69*(2), e17953. https://doi.org/10.1002/aic.17953

Rivarolo, M., Riveros-Godoy, G., Magistri, L., & Massardo, A. F. (2019). Clean hydrogen and ammonia synthesis in paraguay from the itaipu 14 gw hydroelectric plant. *ChemEngineering*, *3*(4). https://doi.org/10.3390/chemengineering3040087

Shiva Kumar, S., & Himabindu, V. (2019). Hydrogen production by pem water electrolysis – a review. *Materials Science for Energy Technologies*, *2*(3), 442–454. https://doi.org/10.1016/j.mset.2019.03.002

Sørensen, B., & Spazzafumo, G. (2018). 2 - hydrogen. In B. Sørensen & G. Spazzafumo (Eds.), *Hydrogen and fuel cells (third edition)* (Third Edition, pp. 5–105). Academic Press. https://doi.org/10.1016/B978-0-08-100708-2.00002-3

State of Green. (2023). *This is what the world's first energy island may look like*. Retrieved June 27, 2023, from https://stateofgreen.com/en/news/this-is-what-the-worlds-first-energy-island-may-look-like/

Statista. (2023). *Ammonia production worldwide from 2010 to 2022*. Retrieved July 9, 2023, from https://www.statista.com/statistics/1266378/global-ammonia-production/

Statistics Denmark. (n.d.). *Consumer price index*. Retrieved July 5, 2023, from https://www.dst.dk/en/Statistik/emner/oekonomi/prisindeks/forbrugerprisindeks

Stewart, K. (n.d.). *Diatomic molecule*. Retrieved September 18, 2023, from https://www.britannica.com/science/diatomic-molecule

Strømholm, L. S., & Rolfsen, R. A. S. (2021). *Flexible hydrogen production*.

Tafone, A., Dal Magro, F., & Romagnoli, A. (2018). Integrating an oxygen enriched waste to energy plant with cryogenic engines and air separation unit: Technical, economic and environmental analysis. *Applied Energy*, *231*, 423–432. https://doi.org/10.1016/j.apenergy.2018.09.024

Tang, X., Pu, W., Chen, Q., Liu, R., & Yang, Y. (2023). A comprehensive study on kinetics for hydrogen generation from aquathermolysis gasification of heavy crude oil. *International Journal of Hydrogen Energy*. https://doi.org/https://doi.org/10.1016/j.ijhydene.2023.07.145

Teichgraeber, H., & Brandt, A. R. (2022). Time-series aggregation for the optimization of energy systems: Goals, challenges, approaches, and opportunities. *Renewable and Sustainable Energy Reviews*, *157*, 111984. https://doi.org/10.1016/j.rser.2021.111984

Tesch, S., Morosuk, T., & Tsatsaronis, G. (2019). Comparative evaluation of cryogenic air separation units from the exergetic and economic points of view. In T. Morosuk & M. Sultan (Eds.), *Low-temperature technologies*. IntechOpen. https://doi.org/10.5772/intechopen.85765

The Investopedia Team. (2022). *Why are t-bills used when determining risk-free rates?* Retrieved July 4, 2023, from https://www.investopedia.com/ask/answers/040915/how-riskfree-rate-determined-when-calculating-market-risk-premium.asp

Thomas, G., & Parks, G. (2006). Potential roles of ammonia in a hydrogen economy, 7.

UCAR. (n.d.). *What's in the air?* Retrieved September 13, 2023, from https://scied.ucar.edu/learning-zone/air-quality/whats-in-the-air

Varela, C., Mostafa, M., & Zondervan, E. (2021). Modeling alkaline water electrolysis for power-to-x applications: A scheduling approach. *International Journal of Hydrogen Energy*, *46*(14), 9303–9313. https://doi.org/10.1016/j.ijhydene.2020.12.111

Varney, C. (2017). *Ammonia favoured as energy storage solution*. Retrieved July 11, 2023, from https://hydrogeneast.uk/ammonia-favoured-as-energy-storage-solution/

Verleysen, K., Parente, A., & Contino, F. (2021). How sensitive is a dynamic ammonia synthesis process? global sensitivity analysis of a dynamic haber-bosch process (for flexible seasonal energy storage). *Energy*, *232*, 121016. https://doi.org/10.1016/j.energy.2021.121016

Verleysen, K., Parente, A., & Contino, F. (2023). How does a resilient, flexible ammonia process look? robust design optimization of a haber-bosch process with optimal dynamic control powered by wind. *Proceedings of the Combustion Institute*, *39*(4), 5511–5520. https://doi.org/10.1016/j.proci.2022.06.027

Wang, C., Walsh, S. D., Longden, T., Palmer, G., Lutalo, I., & Dargaville, R. (2023). Optimising renewable generation configurations of off-grid green ammonia production systems considering haber-bosch flexibility. *Energy Conversion and Management*, *280*, 116790. https://doi.org/10.1016/j.enconman.2023.116790

Yahoo. (n.d.-a). *Treasury yield 10 years (tnx)*. Retrieved July 4, 2023, from https://finance.yahoo.com/quote/%5ETNX/history?p=%5ETNX

Yahoo. (n.d.-b). *Usd/dkk (dkk=x)*. Retrieved July 6, 2023, from https://finance.yahoo.com/quote/DKK%3DX/history?p=DKK%3DX

Yahoo. (n.d.-c). *Usd/eur (eurusd=x)*. Retrieved July 5, 2023, from https://finance.yahoo.com/quote/EURUSD=X/

Yates, J., Daiyan, R., Patterson, R., Egan, R., Amal, R., Ho-Baille, A., & Chang, N. L. (2020). Techno-economic analysis of hydrogen electrolysis from off-grid stand-alone photovoltaics incorporating uncertainty analysis. *Cell Reports Physical Science*, *1*(10), 100209. https://doi.org/10.1016/j.xcrp.2020.100209

# Appendices

## A Model parameters

Some parameters have the value - and it is set to zero, either because of the findings in Chapter 3 or due to the assumptions in Section 4.2.

| Parameters | AE | ASU | HB |
|---|---|---|---|
| $NRG_k$ | 50 kWh | 0,2 kWh | 0,44 kWh |
| $SNRG_k$ | 2,5 kWh | - | - |
| $PropSB_k$ | 2% | 2% | - |
| $PropCS_k$ | 250 kWh | - | - |
| $MinU_k$ | 15% | 40% | 50% |
| $TotCap_k$ | 2 000 kg/h | 8 500 kg/h | 10 870 kg/h |
| $Vol_k$ | 21 240 kg | 204 000 kg | - |
| $Prop_k$ | 17,7% | 82,3% | - |
| $Conv$ | - | - | 97% |
| $MPCP$ | - | - | 20% |
| $BSize_k$ | 40 kg/h | 8 500 kg/h | 10 000 kg/h |
| $BCAPEX_k^U$ | 1 575 000 USD | 12 325 000 USD | 33 000 000 USD |
| $OPEXP_k^U$ | 3,5% | 2% | 2% |
| $BVol_k$ | 21 240 kg | 204 000 kg | - |
| $BCAPEX_k^B$ | 10 620 000 USD | - | - |
| $OPEXP_k^B$ | 1% | - | - |
| $\alpha^U$ | 0.85 | 0.67 | 0.79 |
| $\alpha^B$ | 0.7 | - | - |
| $RPRC_k$ | 30% | - | 30% |

**Table A.1:** Production unit and buffer parameters

The different columns represent the year of the degradation. In year 11, the replacement parts are replaced; hence, degradation is reset to zero.

| Unit | 1 | 4 | 7 | 10 | 13 | 16 | 19 | 22 | 25 | 28 |
|---|---|---|---|---|---|---|---|---|---|---|
| AE | 0,75% | 3% | 5,25% | 2,5% | 2,25% | 4,5% | 4,25% | 1,5% | 3,75% | 6,0% |
| ASU | - | - | - | - | - | - | - | - | - | - |
| HB | 1% | 4% | 7% | 3,33% | 3% | 6% | 5,67% | 2% | 5% | 8% |

**Table A.2:** Degradation: Average of their three consecutive years

| Parameters | Value |
|---|---|
| $P$ | 13 |
| $d$ | 87 360 000 kg |
| $GF$ | 0,01247 USD |
| $WACC$ | 7,3 % |

**Table A.3:** Other Parameters

# B Electricity Prices

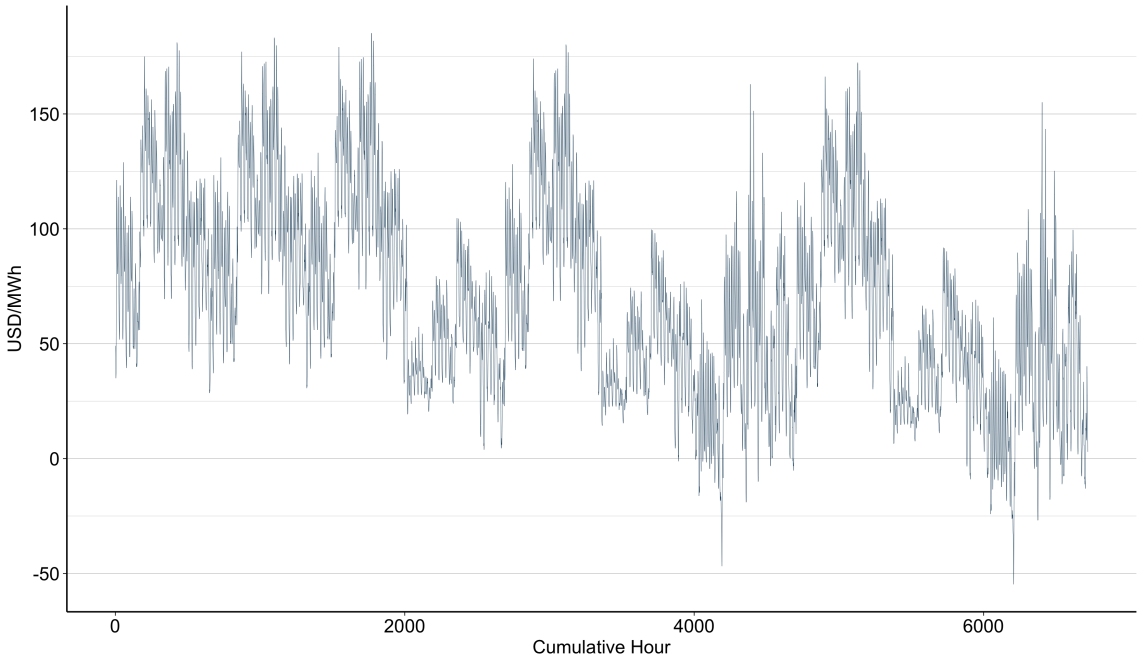


**Figure B.1:** Extreme volatility: 200 percent increased volatility

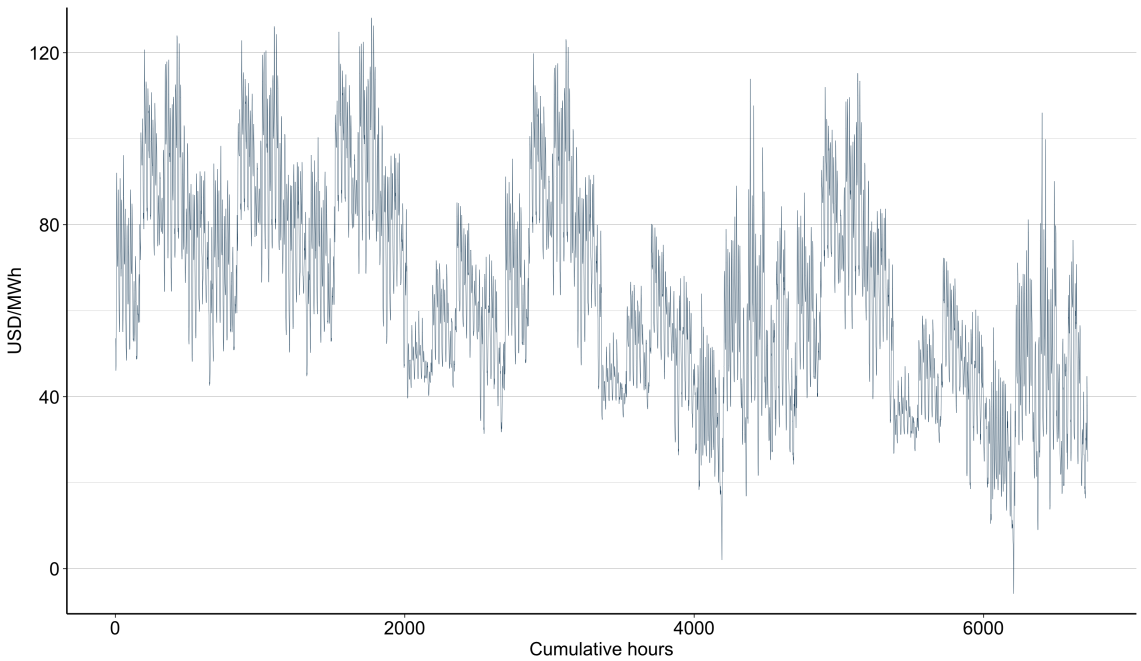


**Figure B.2:** 60 percent increased volatility

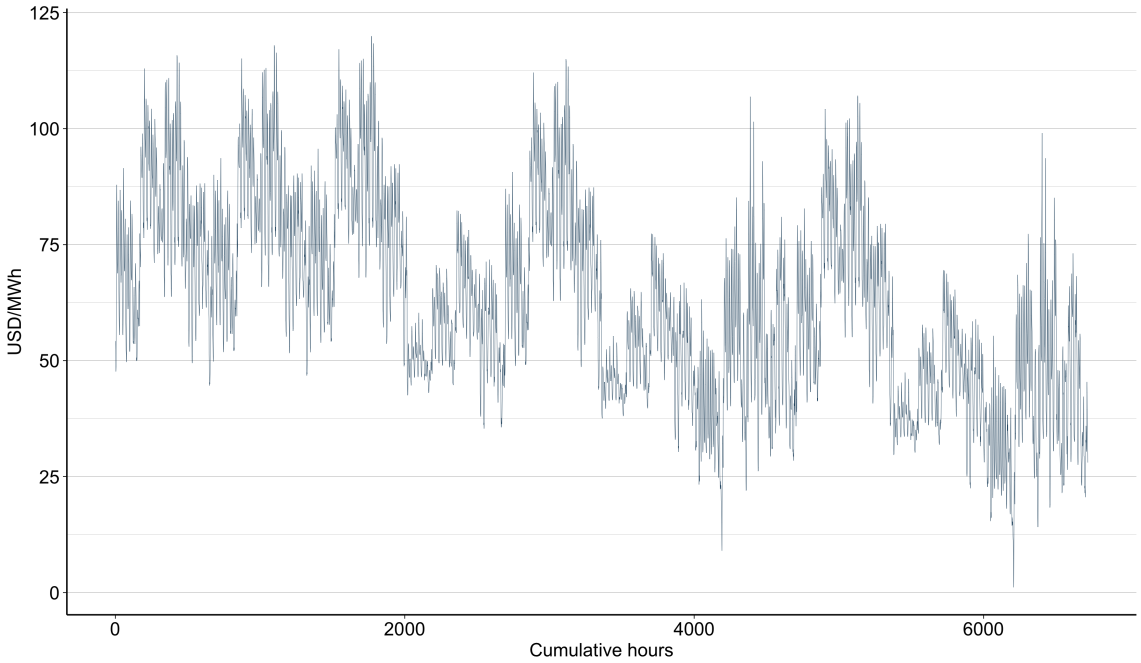


**Figure B.3:** Base case: 40 percent increased volatility


**Figure B.4:** 20 percent increased volatility

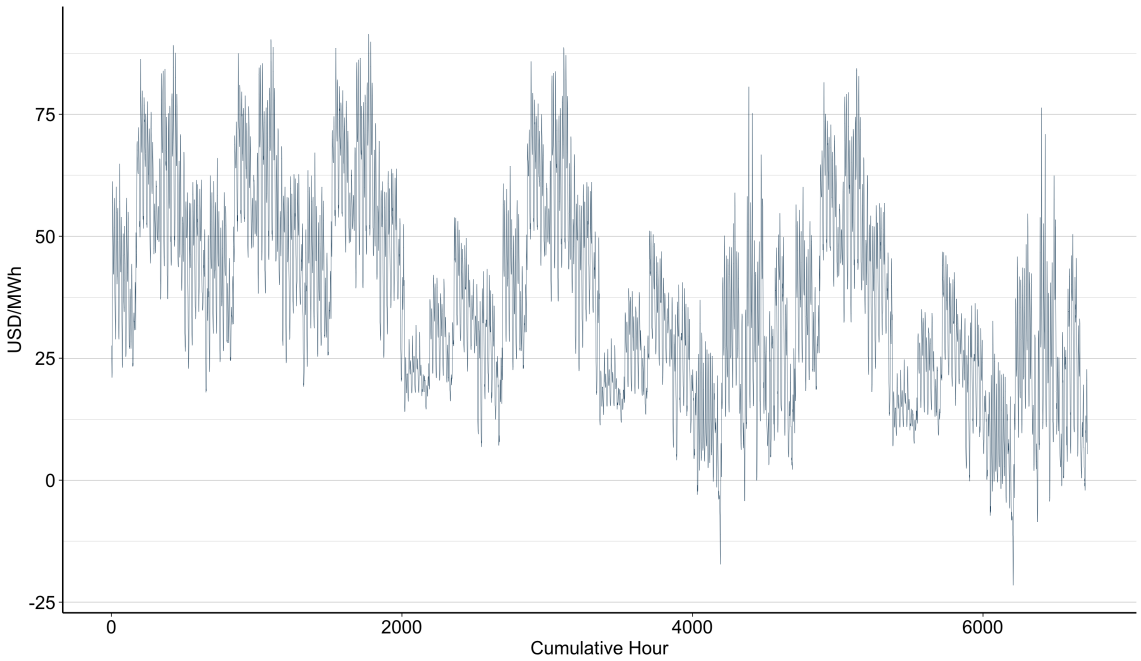


**Figure B.5:** Half price

# C Forecasted Values

The highlighted values are provided by Energistyrelsen (n.d.-a) and the rest are found based on a linear relation between the provided values:

| Year | Forecasted: DKK/MWh |
|---|---|
| **2024** | **411** |
| 2025 | 416 |
| 2026 | 421 |
| 2027 | 426 |
| 2028 | 430 |
| 2029 | 435 |
| **2030** | **440** |
| 2031 | 433 |
| 2032 | 426 |
| 2033 | 419 |
| 2034 | 412 |
| 2035 | 405 |
| 2036 | 398 |
| 2037 | 391 |
| 2038 | 384 |
| 2039 | 377 |
| **2040** | **370** |
| 2041 | 366 |
| 2042 | 362 |
| 2043 | 358 |
| 2044 | 354 |
| 2045 | 350 |
| 2046 | 346 |
| 2047 | 342 |
| 2048 | 338 |
| 2049 | 334 |
| **2050** | **330** |

**Table C.1:** Forecasted Values

# D Not Utilised Constraints

## D.1 Removed constraints

This demonstrates the constraint if HB and ASU were allowed to be placed in idle state. When these models were implemented, cold start was not a component.

| Constraint | Sets | Description |
|---|---|---|
| $idle_{k,y,q,h} \cdot ID_k \geq idle_{k,y,q,h-1} \cdot ID_k - \sum_{i=h-ID_k}^{h-1} idle_{k,y,q,i}$ | $\forall k \in K$ $\forall y \in Y$ $\forall q \in Q$ $\forall h \in H$ $h > ID_k$ | Minimum duration needed between production after the machine goes idle |
| $idle_{k,y,q,h} \cdot ID_k \geq idle_{k,y,q,h-1} \cdot ID_k - \sum_{i=1}^{h} idle_{k,y,q,i}$ | $\forall k \in K$ $\forall y \in Y$ $\forall q \in Q$ $\forall h \in H$ $h > 1$ $h \leq ID_k$ | Same as above, but for the first to hour $ID_k$ |
| $idle_{k,y,q,\lvert H\rvert} \cdot ID_k \leq \sum_{i=\lvert H\rvert-ID_k+1}^{\lvert H\rvert} idle_{k,y,q,i}$ | $\forall k \in K$ $\forall y \in Y$ $\forall q \in Q$ | If last hour in the representative week is idle, then the previous $ID_k$ hours must also be idle |

**Table D.1:** Non Used constraints

$ID_k$ represents the minimum amount of time required in the idle state before it can be turned on again. In the original model, these were used instead of the cold start constraint that is presently implemented in the thesis model.

The first of the three constraints is the primary, with the other two serving as supplementary measures for what it cannot constrain. It applies to all time periods within the representative week, with the exception of the first $ID_k$ hours. The right side of the equation determines whether there have been sufficient hours of inactivity for the machine to start up again. If the right side does not equal zero, indicating that there have not been enough idle hours, the present hour will have to be idle. This will also permit the machine to be inactive for additional hours if cost savings are realized. This constraint's flaw is

that it omits the first $ID_k$ hours. With this constraint alone, the first $ID_k - 1$ hours may be idle while hour $ID_k$ can be idle and still follow the constraint if hour $ID_k + 1$ is not idle. This breaks with reality and thus, the second constraint is needed. It follows the same logic as the first one, only for the firs $ID_k$ hours.

The final constraint controls whether the previous $ID_k$ must also be idle if the last hour of the representative week is idle, which is not checked by the primary constraint. In practice, the machine may be idle at the last hour of the week, but then it must also be idle at the start of the following week. Due to the fact that we utilise representative weeks, such a feat is not possible without some consequence. This would imply, for instance, that the representative week will begin and conclude in a idle state. This does not seem to be realistic, as the sate of the machine should be reliant on the previous hours and not by the future hours. In addition, the following quarter or year will be required to be inactive, complicating the model even further. Due to these reasons, we assume that the idle time cannot go over different weeks, quarters or years but must stay within the representative week. This will reduce the model's flexibility, thereby limiting our analysis.

This constraint operates differently than the previous two. It will examine whether the last hour multiplied by $ID_k$ is less or equal than the previous $ID_k - 1$ hours plus the last hour; if not, it cannot be idle. If it is, then the previous $ID_k - 1$ hours must also be idle.

## D.2 Constraint Requiring adjustments

Additionally, the some HB constraints would need to be changed:

| Constraint | Sets | Description |
|---|---|---|
| $x_{NH_3,y,q,h} \geq x_{NH_3,y,q,h-1} - MPC_y - Cap_{NH_3,y} \cdot idle_{NH_3,y,q,h}$ | $\forall y \in Y$ $\forall q \in Q$ $\forall h \in H$ $h > 1$ | Maximum production reduction between hours within the week |
| $x_{NH_3,y,q,h} \leq x_{NH_3,y,q,h-1} + MPC_y - MPC_y \cdot idle_{NH_3,y,q,h-1} + MinL_{NH_3,y} \cdot idle_{NH_3,y,q,h-1}$ | $\forall y \in Y$ $\forall q \in Q$ $\forall h \in H$ $h > 1$ | Maximum production increase between hours within the week |
| $x_{NH_3,y,q,h_1} \geq x_{NH_3,y,q-1,\lvert H\rvert} - MPC_y - Cap_{NH_3,y} \cdot idle_{NH_3,y,q,h_1}$ | $\forall y \in Y$ $\forall q \in Q$ $q > 1$ | Maximum production reduction between hours of different weeks/quarters |
| $x_{NH_3,y,q,h_1} \leq x_{NH_3,y,q-1,\lvert H\rvert} + MPC_y - MCP_y \cdot idle_{NH_3,y,q-1,\lvert H\rvert} + MinL_{NH_3,y} \cdot idle_{NH_3,y,q-1,\lvert H\rvert}$ | $\forall y \in Y$ $\forall q \in Q$ $q > 1$ | Maximum production increase between hours of different quarters |
| $x_{NH_3,y,q_1,h_1} \geq x_{NH_3,y-\lvert G\rvert,\lvert Q\rvert,\lvert H\rvert} - MPC_y - Cap_{NH_3,y} \cdot idle_{NH_3,y,q_1,h_1}$ | $\forall y \in Y$ $y > 1$ | Maximum production reduction between hours of different years |
| $x_{NH_3,y,q_1,h_1} \leq x_{NH_3,y-\lvert G\rvert,\lvert Q\rvert,\lvert H\rvert} + MPC_y - MCP_y \cdot idle_{NH_3,y-\lvert G\rvert,\lvert Q\rvert,\lvert H\rvert} + MinL_{NH_3,y} \cdot idle_{NH_3,y-\lvert G\rvert,\lvert Q\rvert,\lvert H\rvert}$ | $\forall y \in Y$ $y > 1$ | Maximum production increase between hours of different years |

**Table D.2:** Haber-Bosch specific constraints

All constraints except the standby constraint will require a more thorough explanation. The proportion constraint is used to ensure continuity between the ammonia produced and the required $H_2$ and $N_2$. This means that in order to produce ammonia, the $H_2$ and $N_2$ must be removed from the buffers and added to the ammonia synthesis. Since the proportion is known from section 3.2.2, it is multiplied by the ammonia produced for that hour. Additionally, we must divide it by the conversion rate, as the purge rate is 3% in our case. Therefore, not all $H_2$ and $N_2$ will be utilised in the ammonia synthesis, necessitating a higher volume of the process mediums.

Additionally, there is the constraint of decreasing and increasing production load, which are visualized below:

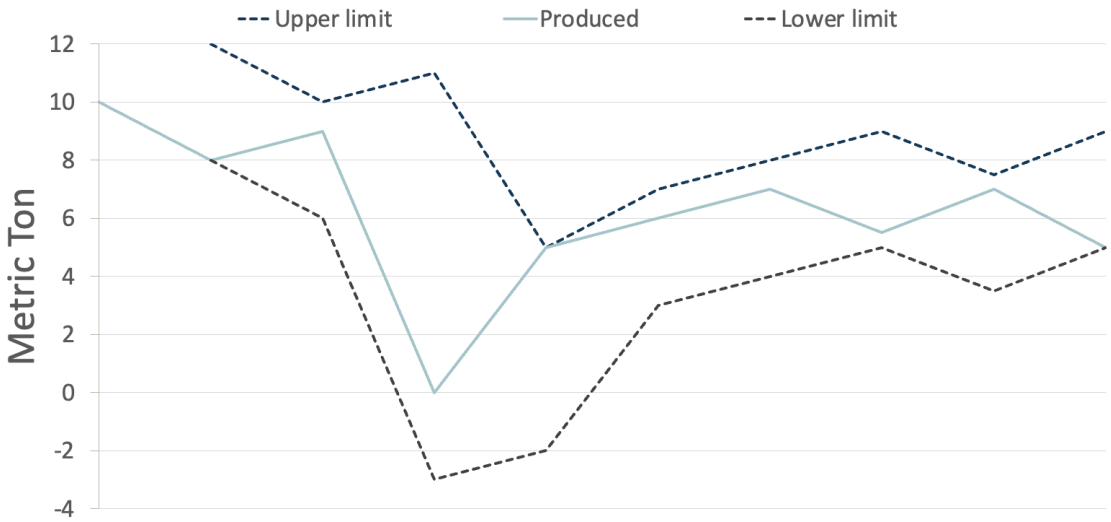


**Figure D.1:** Maximum increase and decrease in production load altered constraint

The reduction is calculated by subtracting the maximal load difference in kilograms from the amount of ammonia produced in the previous hour. In order for the HB to be placed in idle, it must allow production to fall below the maximum load change. Therefore, if the machine is inactive, the capacity will be subtracted from the previous hours production. The right side of the equation can be below 0 if the machine is not producing. However, this constraint is irrelevant in these situations because of the non negativity constraints in table 4.9. The same logic is applied to the other maximum production decrease constraints, but it applies to hours in different quarters/weeks or years.

Then there is the constraint for maximum increase, which is somewhat more complex. Using the same logic as the decrease percentage, this function examines the previous

hour and adds the maximum allowed load change in kilograms. The capacity on the right side of the equation can exceed 100 percent. However, the maximal production constraint in table 4.9 restricts to the capacity of the HB. The most complicated aspect of the constraint, is when the previous hour did not produce and the current hour will produce. In this case, we must subtract the maximum load change $MCP_k$ and add the allowed minimum load. This is because if $MCP_k$ is not subtracted, the first producing hour will have a utilization load of $MinU_k + MPCP$ percent, which is not realistic for the first producing hour after idle state. Hence, it must be subtracted and the allowed minimum load is then added. During idle periods, the right side of the equation will indicate that the system can produce at minimum load. However, the model is constrained from producing due to the no producing constraint in table 4.9.

To maintain the model's consistency, these constraints are then replicated between hours of various weeks, quarters, and years.

# E Results

The results show the production capacity of the AE in the left column. The other column represents the buffer size in tonnes.

## E.1 Original Volatility

### Original Volatility 20%

| AE | 0 | 7 | 14 | 21 | 28 | 35 | 42 |
|---|---|---|---|---|---|---|---|
| 2000 | 905, 77 | 910, 60 | 913, 87 | 916, 67 | 919, 19 | 921, 53 | 923, 73 |
| 2100 | 908, 64 | 912, 77 | 916, 04 | 918, 84 | 921, 36 | 923, 70 | 925, 90 |
| 2200 | 911, 49 | 914, 97 | 918, 24 | 921, 04 | 923, 56 | 925, 90 | 928, 10 |
| 2300 | 914, 32 | 917, 23 | 920, 50 | 923, 30 | 925, 82 | 928, 16 | 930, 36 |
| 2400 | 917, 13 | 919, 54 | 922, 81 | 925, 61 | 928, 13 | 930, 47 | 932, 67 |
| 2500 | 919, 93 | 921, 89 | 925, 16 | 927, 96 | 930, 48 | 932, 82 | 935, 02 |
| 2600 | 922, 70 | 924, 29 | 927, 57 | 930, 36 | 932, 88 | 935, 22 | 937, 42 |
| 2700 | 925, 46 | 926, 73 | 930, 01 | 932, 80 | 935, 33 | 937, 66 | 939, 87 |
| 2800 | 928, 21 | 929, 21 | 932, 48 | 935, 28 | 937, 80 | 940, 14 | 942, 34 |
| 2900 | 930, 94 | 931, 70 | 934, 98 | 937, 77 | 940, 29 | 942, 63 | 944, 83 |
| 3000 | 933, 66 | 934, 21 | 937, 48 | 940, 28 | 942, 80 | 945, 14 | 947, 34 |

### Original Volatility 60%

| AE | 0 | 7 | 14 | 21 | 28 | 35 | 42 |
|---|---|---|---|---|---|---|---|
| 2000 | 932, 55 | 936, 97 | 940, 24 | 943, 04 | 945, 56 | 947, 90 | 950, 10 |
| 2100 | 935, 42 | 938, 44 | 941, 72 | 944, 51 | 947, 03 | 949, 37 | 951, 57 |
| 2200 | 938, 26 | 940, 02 | 943, 29 | 946, 08 | 948, 61 | 950, 95 | 953, 15 |
| 2300 | 941, 09 | 941, 73 | 945, 00 | 947, 80 | 950, 32 | 952, 66 | 954, 86 |
| 2400 | 943, 91 | 943, 55 | 946, 82 | 949, 62 | 952, 14 | 954, 48 | 956, 68 |
| 2500 | 946, 70 | 945, 50 | 948, 77 | 951, 56 | 954, 09 | 956, 43 | 958, 63 |
| 2600 | 949, 48 | 947, 57 | 950, 84 | 953, 64 | 956, 16 | 958, 50 | 960, 70 |
| 2700 | 952, 24 | 949, 71 | 952, 99 | 955, 78 | 958, 31 | 960, 64 | 962, 85 |
| 2800 | 954, 98 | 951, 93 | 955, 20 | 957, 99 | 960, 52 | 962, 86 | 965, 06 |
| 2900 | 957, 71 | 954, 19 | 957, 46 | 960, 26 | 962, 78 | 965, 12 | 967, 32 |
| 3000 | 960, 43 | 956, 51 | 959, 78 | 962, 58 | 965, 10 | 967, 44 | 969, 64 |

### Original Volatility 200%

| AE | 0 | 7 | 14 | 21 | 28 | 35 | 42 |
|---|---|---|---|---|---|---|---|
| 2000 | 1026, 26 | 1028, 82 | 1032, 09 | 1034, 89 | 1037, 41 | 1039, 75 | 1041, 95 |
| 2100 | 1029, 13 | 1026, 92 | 1030, 19 | 1032, 99 | 1035, 51 | 1037, 85 | 1040, 05 |
| 2200 | 1031, 98 | 1025, 45 | 1028, 73 | 1031, 52 | 1034, 04 | 1036, 38 | 1038, 58 |
| 2300 | 1034, 81 | 1024, 44 | 1027, 71 | 1030, 51 | 1033, 03 | 1035, 37 | 1037, 57 |
| 2400 | 1037, 62 | 1023, 94 | 1027, 21 | 1030 | 1032, 53 | 1034, 87 | 1037, 07 |
| 2500 | 1040, 41 | 1023, 81 | 1027, 04 | 1029, 84 | 1032, 36 | 1034, 70 | 1036, 90 |
| 2600 | 1043, 19 | 1024, 05 | 1027, 27 | 1030, 07 | 1032, 59 | 1034, 93 | 1037, 13 |
| 2700 | 1045, 95 | 1024, 58 | 1027, 78 | 1030, 58 | 1033, 10 | 1035, 44 | 1037, 64 |
| 2800 | 1048, 70 | 1025, 39 | 1028, 58 | 1031, 37 | 1033, 90 | 1036, 24 | 1038, 44 |
| 2900 | 1051, 43 | 1026, 39 | 1029, 47 | 1032, 26 | 1034, 79 | 1037, 12 | 1039, 33 |
| 3000 | 1054, 15 | 1027, 55 | 1030, 57 | 1033, 37 | 1035, 89 | 1038, 23 | 1040, 43 |

### Original Half Price

| AE | 0 | 7 | 14 | 21 | 28 | 35 | 42 |
|---|---|---|---|---|---|---|---|
| 2000 | 659, 14 | 663, 38 | 666, 66 | 669, 45 | 671, 97 | 674, 31 | 676, 51 |
| 2100 | 662, 01 | 664, 50 | 667, 77 | 670, 57 | 673, 09 | 675, 43 | 677, 63 |
| 2200 | 664, 86 | 665, 76 | 669, 04 | 671, 83 | 674, 35 | 676, 69 | 678, 89 |
| 2300 | 667, 69 | 667, 19 | 670, 46 | 673, 25 | 675, 78 | 678, 12 | 680, 32 |
| 2400 | 670, 50 | 668, 78 | 672, 05 | 674, 84 | 677, 37 | 679, 70 | 681, 91 |
| 2500 | 673, 29 | 670, 55 | 673, 82 | 676, 62 | 679, 14 | 681, 48 | 683, 68 |
| 2600 | 676, 07 | 672, 44 | 675, 71 | 678, 51 | 681, 03 | 683, 37 | 685, 57 |
| 2700 | 678, 83 | 674, 36 | 677, 62 | 680, 42 | 682, 94 | 685, 28 | 687, 48 |
| 2800 | 681, 58 | 676, 41 | 679, 67 | 682, 47 | 684, 99 | 687, 33 | 689, 53 |
| 2900 | 684, 31 | 678, 53 | 681, 79 | 684, 59 | 687, 11 | 689, 45 | 691, 65 |
| 3000 | 687, 03 | 680, 71 | 683, 96 | 686, 76 | 689, 28 | 691, 62 | 693, 82 |

### Original Weekly Demand

| AE | 0 | 7 | 14 | 21 | 28 | 35 | 42 |
|---|---|---|---|---|---|---|---|
| 2000 | 919, 78 | 924, 43 | 927, 70 | 930, 50 | 933, 02 | 935, 36 | 937, 56 |
| 2100 | 922, 65 | 926, 27 | 929, 54 | 932, 34 | 934, 86 | 937, 20 | 939, 40 |
| 2200 | 925, 50 | 928, 17 | 931, 44 | 934, 23 | 936, 76 | 939, 10 | 941, 30 |
| 2300 | 928, 33 | 930, 16 | 933, 44 | 936, 23 | 938, 75 | 941, 09 | 943, 29 |
| 2400 | 931, 14 | 932, 24 | 935, 51 | 938, 31 | 940, 83 | 943, 17 | 945, 37 |
| 2500 | 933, 94 | 934, 40 | 937, 67 | 940, 47 | 942, 99 | 945, 33 | 947, 53 |
| 2600 | 936, 71 | 936, 65 | 939, 92 | 942, 72 | 945, 24 | 947, 58 | 949, 78 |
| 2700 | 939, 47 | 938, 95 | 942, 22 | 945, 02 | 947, 54 | 949, 88 | 952, 08 |
| 2800 | 942, 22 | 941, 30 | 944, 57 | 947, 37 | 949, 89 | 952, 23 | 954, 43 |
| 2900 | 944, 95 | 943, 67 | 946, 95 | 949, 74 | 952, 26 | 954, 60 | 956, 80 |
| 3000 | 947, 67 | 946, 09 | 949, 36 | 952, 15 | 954, 68 | 957, 01 | 959, 22 |

**Original No degradation**

| AE | 0 | 7 | 14 | 21 | 28 | 35 | 42 |
|---|---|---|---|---|---|---|---|
| 2000 | 923, 39 | 926, 67 | 929, 94 | 932, 74 | 935, 26 | 937, 60 | 939, 80 |
| 2100 | 926, 26 | 928, 51 | 931, 78 | 934, 58 | 937, 10 | 939, 44 | 941, 64 |
| 2200 | 929, 11 | 930, 43 | 933, 70 | 936, 50 | 939, 02 | 941, 36 | 943, 56 |
| 2300 | 931, 94 | 932, 42 | 935, 69 | 938, 49 | 941, 01 | 943, 35 | 945, 55 |
| 2400 | 934, 75 | 934, 55 | 937, 82 | 940, 61 | 943, 14 | 945, 48 | 947, 68 |
| 2500 | 937, 54 | 936, 77 | 940, 04 | 942, 84 | 945, 36 | 947, 70 | 949, 90 |
| 2600 | 940, 32 | 939, 04 | 942, 32 | 945, 11 | 947, 63 | 949, 97 | 952, 17 |
| 2700 | 943, 08 | 941, 36 | 944, 63 | 947, 43 | 949, 95 | 952, 29 | 954, 49 |
| 2800 | 945, 83 | 943, 74 | 947, 01 | 949, 80 | 952, 33 | 954, 66 | 956, 87 |
| 2900 | 948, 56 | 946, 16 | 949, 43 | 952, 23 | 954, 75 | 957, 09 | 959, 29 |
| 3000 | 951, 27 | 948, 64 | 951, 92 | 954, 71 | 957, 23 | 959, 57 | 961, 77 |

## E.2 Flexible Volatility

**Flexible Volatility 20%**

| AE | 0 | 7 | 14 | 21 | 28 | 35 | 42 |
|---|---|---|---|---|---|---|---|
| 2000 | 916, 65 | 921, 85 | 925, 12 | 927, 91 | 930, 44 | 932, 77 | 934, 98 |
| 2100 | 911, 36 | 916, 52 | 919, 79 | 922, 59 | 925, 11 | 927, 45 | 929, 65 |
| 2200 | 907, 36 | 912, 49 | 915, 76 | 918, 56 | 921, 08 | 923, 42 | 925, 62 |
| 2300 | 904, 27 | 909, 36 | 912, 63 | 915, 43 | 917, 95 | 920, 29 | 922, 49 |
| 2400 | 902, 07 | 907, 13 | 910, 40 | 913, 20 | 915, 72 | 918, 06 | 920, 26 |
| 2500 | 900, 57 | 905, 61 | 908, 88 | 911, 67 | 914, 20 | 916, 53 | 918, 73 |
| 2600 | 899, 58 | 904, 60 | 907, 88 | 910, 67 | 913, 19 | 915, 53 | 917, 73 |
| 2700 | 899, 08 | 904, 08 | 907, 35 | 910, 15 | 912, 67 | 915, 01 | 917, 21 |
| 2800 | 901, 44 | 906, 05 | 909, 32 | 912, 12 | 914, 64 | 916, 98 | 919, 18 |
| 2900 | 904, 09 | 908, 51 | 911, 78 | 914, 58 | 917, 10 | 919, 44 | 921, 64 |
| 3000 | 906, 81 | 910, 97 | 914, 25 | 917, 04 | 919, 56 | 921, 90 | 924, 10 |

**Flexible Volatility 60%**

| AE | 0 | 7 | 14 | 21 | 28 | 35 | 42 |
|---|---|---|---|---|---|---|---|
| 2000 | 940, 82 | 945, 98 | 949, 25 | 952, 05 | 954, 57 | 956, 91 | 959, 11 |
| 2100 | 932, 82 | 937, 91 | 941, 18 | 943, 97 | 946, 50 | 948, 84 | 951, 04 |
| 2200 | 926, 49 | 931, 52 | 934, 80 | 937, 59 | 940, 11 | 942, 45 | 944, 65 |
| 2300 | 921, 47 | 926, 43 | 929, 70 | 932, 50 | 935, 02 | 937, 36 | 939, 56 |
| 2400 | 917, 69 | 922, 47 | 925, 75 | 928, 54 | 931, 069 | 933, 40 | 935, 60 |
| 2500 | 914, 66 | 919, 51 | 922, 79 | 925, 55 | 928, 10 | 930, 42 | 932, 62 |
| 2600 | 912, 38 | 917, 21 | 920, 48 | 923, 27 | 925, 80 | 928, 14 | 930, 34 |
| 2700 | 910, 79 | 915, 44 | 918, 71 | 921, 51 | 924, 03 | 926, 37 | 928, 57 |
| 2800 | 912, 96 | 917, 13 | 920, 40 | 923, 19 | 925, 72 | 928, 06 | 930, 26 |
| 2900 | 915, 69 | 919, 15 | 922, 43 | 925, 22 | 927, 74 | 930, 08 | 932, 28 |
| 3000 | 918, 40 | 921, 29 | 924, 56 | 927, 36 | 929, 88 | 932, 22 | 934, 42 |

### Flexible Volatility 200%

| AE | 0 | 7 | 14 | 21 | 28 | 35 | 42 |
|---|---|---|---|---|---|---|---|
| 2000 | 1025, 43 | 1030, 37 | 1033, 63 | 1036, 43 | 1038, 95 | 1041, 29 | 1043, 49 |
| 2100 | 1007, 90 | 1012, 62 | 1015, 89 | 1018, 68 | 1021, 20 | 1023, 54 | 1025, 74 |
| 2200 | 993, 55 | 998, 09 | 1001, 36 | 1004, 16 | 1006, 68 | 1009, 02 | 1011, 22 |
| 2300 | 981, 73 | 985, 80 | 989, 07 | 991, 86 | 994, 39 | 996, 73 | 998, 93 |
| 2400 | 971, 97 | 975, 78 | 979, 06 | 981, 85 | 984, 37 | 986, 71 | 988, 91 |
| 2500 | 963, 99 | 967, 51 | 970, 79 | 973, 51 | 976, 10 | 978, 37 | 980, 57 |
| 2600 | 957, 26 | 960, 55 | 963, 82 | 966, 61 | 969, 14 | 971, 48 | 973, 68 |
| 2700 | 951, 79 | 954, 73 | 958, 01 | 960, 80 | 963, 33 | 965, 66 | 967, 86 |
| 2800 | 953, 54 | 954, 08 | 957, 35 | 960, 14 | 962, 67 | 965, 01 | 967, 21 |
| 2900 | 956, 27 | 954, 37 | 957, 64 | 960, 44 | 962, 96 | 965, 30 | 967, 50 |
| 3000 | 958, 99 | 954, 74 | 958, 01 | 960, 80 | 963, 33 | 965, 67 | 967, 87 |

### Flexible Half Price

| AE | 0 | 7 | 14 | 21 | 28 | 35 | 42 |
|---|---|---|---|---|---|---|---|
| 2000 | 668, 68 | 673, 82 | 677, 10 | 679, 89 | 682, 41 | 684, 75 | 686, 95 |
| 2100 | 662, 04 | 667, 10 | 670, 37 | 673, 17 | 675, 69 | 678, 03 | 680, 23 |
| 2200 | 656, 86 | 661, 85 | 665, 12 | 667, 91 | 670, 44 | 672, 77 | 674, 98 |
| 2300 | 652, 82 | 657, 73 | 661, 00 | 663, 80 | 666, 32 | 668, 66 | 670, 86 |
| 2400 | 649, 78 | 654, 55 | 657, 82 | 660, 62 | 663, 14 | 665, 48 | 667, 68 |
| 2500 | 647, 56 | 652, 22 | 655, 50 | 658, 27 | 660, 81 | 663, 13 | 665, 33 |
| 2600 | 645, 90 | 650, 49 | 653, 76 | 656, 56 | 659, 08 | 661, 42 | 663, 62 |
| 2700 | 644, 82 | 649, 29 | 652, 56 | 655, 36 | 657, 88 | 660, 22 | 662, 42 |
| 2800 | 647, 10 | 650, 75 | 654, 02 | 656, 82 | 659, 34 | 661, 68 | 663, 88 |
| 2900 | 649, 83 | 652, 66 | 655, 93 | 658, 73 | 661, 25 | 663, 59 | 665, 79 |
| 3000 | 652, 55 | 654, 56 | 657, 83 | 660, 62 | 663, 15 | 665, 48 | 667, 69 |

### Flexible Weekly Demand

| AE | 0 | 7 | 14 | 21 | 28 | 35 | 42 |
|---|---|---|---|---|---|---|---|
| 2000 | 933, 58 | 938, 80 | 942, 07 | 944, 87 | 947, 39 | 949, 73 | 951, 93 |
| 2100 | 929, 51 | 934, 69 | 937, 97 | 940, 76 | 943, 29 | 945, 62 | 947, 83 |
| 2200 | 926, 50 | 931, 64 | 934, 91 | 937, 70 | 940, 23 | 942, 57 | 944, 77 |
| 2300 | 924, 24 | 929, 33 | 932, 61 | 935, 40 | 937, 93 | 940, 26 | 942, 47 |
| 2400 | 922, 50 | 927, 57 | 930, 84 | 933, 63 | 936, 16 | 938, 49 | 940, 70 |
| 2500 | 921, 18 | 926, 22 | 929, 49 | 932, 28 | 934, 81 | 937, 14 | 939, 34 |
| 2600 | 920, 20 | 925, 22 | 928, 50 | 931, 29 | 933, 82 | 936, 15 | 938, 36 |
| 2700 | 919, 59 | 924, 59 | 927, 87 | 930, 66 | 933, 18 | 935, 52 | 937, 72 |
| 2800 | 921, 92 | 926, 48 | 929, 75 | 932, 54 | 935, 07 | 937, 40 | 939, 61 |
| 290 | 924, 65 | 928, 84 | 932, 11 | 934, 91 | 937, 43 | 939, 77 | 941, 97 |
| 3000 | 927, 37 | 931, 21 | 934, 48 | 937, 28 | 939, 80 | 942, 14 | 944, 34 |

**Flexible No degradation**

| AE | 0 | 7 | 14 | 21 | 28 | 35 | 42 |
|---|---|---|---|---|---|---|---|
| 2000 | 922, 77 | 927, 89 | 931, 17 | 933, 96 | 936, 49 | 938, 82 | 941, 03 |
| 2100 | 916, 95 | 922, 02 | 925, 30 | 928, 09 | 930, 61 | 932, 95 | 935, 15 |
| 2200 | 912, 43 | 917, 45 | 920, 72 | 923, 52 | 926, 04 | 928, 38 | 930, 58 |
| 2300 | 908, 92 | 913, 88 | 917, 15 | 919, 94 | 922, 47 | 924, 80 | 927, 01 |
| 2400 | 906, 41 | 911, 33 | 914, 60 | 917, 39 | 919, 92 | 922, 26 | 924, 46 |
| 2500 | 904, 58 | 909, 46 | 912, 74 | 915, 52 | 918, 05 | 920, 38 | 922, 58 |
| 2600 | 903, 24 | 908, 10 | 911, 38 | 914, 17 | 916, 69 | 919, 03 | 921, 23 |
| 2700 | 902, 23 | 907, 08 | 910, 36 | 913, 15 | 915, 67 | 918, 01 | 920, 21 |
| 2800 | 903, 67 | 908, 22 | 911, 49 | 914, 29 | 916, 81 | 919, 15 | 921, 35 |
| 2900 | 906, 40 | 910, 56 | 913, 84 | 916, 63 | 919, 15 | 921, 49 | 923, 69 |
| 3000 | 909, 12 | 912, 84 | 916, 11 | 918, 90 | 921, 43 | 923, 77 | 925, 97 |